Response to Referee 1

The authors would like to thank the Referee #1 for her/his valuable comments and suggestions to improve the manuscript. They have been taken into account in the revised manuscript, as follows (original referee's comments in bold):

General comments

This paper introduces the isotopic tracking of the ecohydrological model EcH2O. The new model development is evaluated using isotope time series from a montane, low-energy catchment in Scotland. The isotope tracking addition to the model is interesting for the GMD readership and the approach is in general well-documented. The availability of isotope time series in different parts of the study catchment is also very useful for gaining scientific insights. However, . . .

1. the paper lacks a clear focus at times, and the writing varies between being very detailed to very general. The authors know the topics very well, and occasionally make jumps or sweeping descriptions that easily lose the reader. (Examples in specific comments.)

We thank the referee for this comment. In general, we have tried to make the narrative more consistent as specified in the corresponding specific comments below.

2. Also, the model development rationale is not entirely clear, which makes it difficult to understand whether the evaluation procedure and criteria are sound, well defined, and in proportion to the goals the model are set to achieve.

The objective of the paper is to describe and demonstrate the development of a flux/age tracking component built on an existing ecohydrological model. The rationale for this new development is twofold. First, the tracking component is added to a spatially-distributed energy and water balance model with a strong physical base that explicitly simulates the spatio-temporal heterogeneity of the water mixing processes. Then, we evaluate how this ecohydrological model calibrated solely on hydrometric/energy balance data could simulate spatio-temporal isotope variations without any additional calibration of the tracking and fractionation components. Because of the diversity of fluxes and storage dynamics tracked in the model, we put the emphasis on testing the new model with a wide range of isotopic datasets, and use visual inspection and generic quantitative metrics (such as mean absolute error and model-data correlation, see response to the corresponding specific comment) for a generic evaluation and further discussion. In the future, when moving towards more operational purposes, specific calibrations of the isotopic component using metrics such as KGE or NSE may be beneficial. Note that specific aspects of this discussion relevant to the model development rationale, and the evaluation metrics are further addressed below in Specific Comments.

3. The authors also do not test the sensitivity of neither parameters, mixing assumptions, nor isotope model structure, which limit the insights that could have been generated in the subsequent evaluation process.

A comprehensive sensitivity analysis of parameters was already performed by Kuppel et al. (2018), along with a description of the ensemble of parameters used in this paper, which were derived from a multi-objective calibration method conducted using constraints from hydrometric and energy balance observations (see Sect. 3.3).
Additional parameter sensitivity analysis and calibration using isotopes datasets would provide complementary information to further constrain parameter uncertainty. However, by doing so we would lose an opportunity to assess how the original EcH_2O structure performs against a dataset that is truly independent form the standard hydrometric information typically used in model calibration/validation exercises.
A comparison of the performance of different mixing models is beyond the scope of the paper. The presented model simulates isotope tracking using a simple full mixing assumption, which avoids hard-to-test partial or incomplete mixing hypotheses and therefore permits an in-depth discussion of model strengths and weaknesses for potential applications and hypothesis-driven model developments.

4. The authors repeatedly refer to Kuppel et al. (2018) and at times assume the reader to have taken part of it. This is a bit unfortunate, as Kuppel et al. (2018) is not open access (and also was not accessible for me during my review). Please consider including key information, if only in Supplementary information.

It is difficult not to refer extensively to Kuppel et al. (2018) because it gives key details such as a description of improvements to the original EcH_2O model, a quantification of the model performance on the study site and also describes the basic configuration used to evaluate EcH2O-iso. While it is not possible to reproduce all this information in the paper, we strived to include the information relevant for the interpretation of the results of the present study. Nevertheless, we recognize this can be frustrating. To ameliorate this problem we revised the manuscript to add further details regarding model development rationale, key features and limitations, and the range of environments on which the model has been successfully applied. We have also added a figure to the Supplementary Information that indicates the time spans used for calibration and evaluation (Fig. S1) and the list and description of the calibrated parameters (Table S1, adapted from Kuppel et al., 2018):

Table S1. Calibrated parameters used in this study, grouped according to their four components: soil units or vegetation types.

Name	Description
	Soil-distributed (Peat, Gley, Podzol, Ranker)
D_{soil}	Total soil depth (m)
D_{L1}	Depth of the 1st hydrological layer (m)
D_{L2}	Depth of the 2nd hydrological layer (m)
η	Porosity ($m^3.m^{-3}$)
K_{hx}	Saturated horizontal hydraulic conductivity ($m.s^{-1}$) ǂ
K_{hratio}	Ratio of vertical-to-horizontal hydraulic conductivity (–) ǂ
λ_{BC}	Brooks-Corey exponent parameter (–)
ψ_{ae}	Air-entry pressure head (m)
θ_r	Residual soil moisture

k_{root}	Exponential root profile (m^{-1})
	Vegetation-distributed (Pine, Heather, Peat Moss, Grass)
gs_{max}	Maximal stomatal conductance ($m.s^{-1}$) ǂ
CWS_{max}	Maximum interception storage per unit LAI (m) ǂ
T_{opt}	Optimal photosynthesis temperature (°C)
ψ_d	Soil water potential halving stomatal conductance (-m)
c	Sensitivity of stomatal conductance to soil water potential (–)
K_{beer}	Light attenuation coefficient (–)

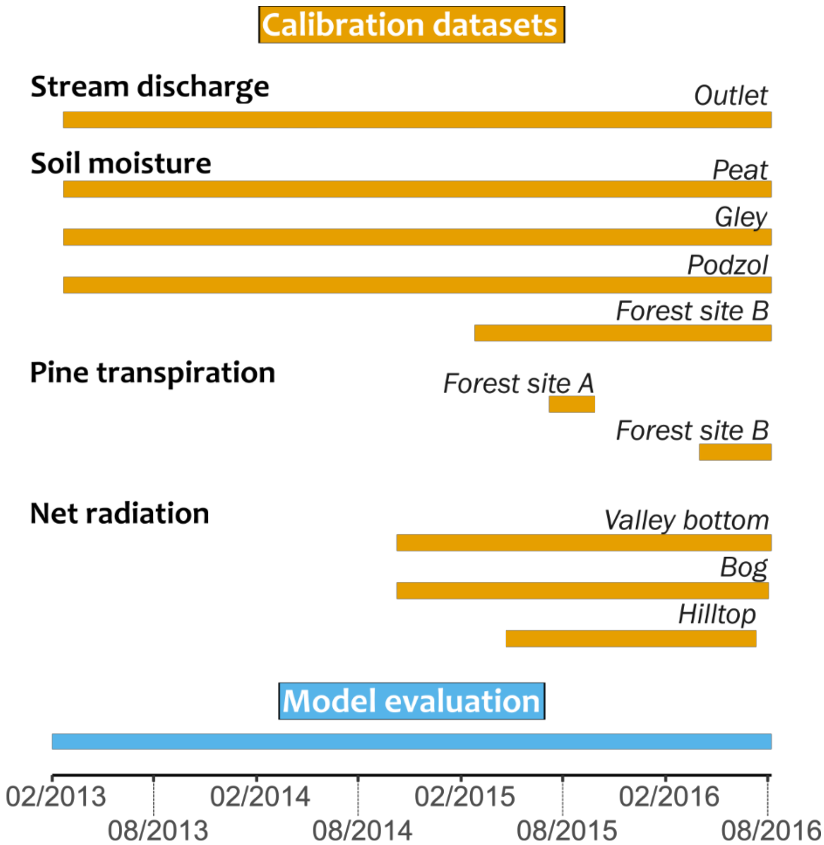

Figure S1. Temporal windows –at daily resolution– covered by each of the datasets (orange) at the different sites (italic font) grouped by observation type (bold font) used to calibrate the EcH_2O-iso model, while the full simulation period (blue) is used for evaluating the isotopes and age tracking module.

5. The paper is lengthy and readability could be improved by e.g., summarising tables and more condensed graphs that can act as reference, or point the reader to the key results (e.g., notations table, definitions table, and scatterplots etc., more figures like Fig 8).

Striking a balance between providing sufficient detail while keeping the paper concise is challenging. We moved away much of the methodological details to Supplementary Materials or to Kuppel et al (2018) and much of the bulk of the paper describes and discusses results on the temporal and spatial patterns of water compositions and age, which are key foci of our study. Nonetheless, we have edited the manuscript to reduce verbosity and have moved the section and figures on lc-excess (Fig. 11) to Supplementary Information, as they offered similar information to Fig. 10.

6. The authors mention in their literature review and discussions other models ranging from local to global scale, but it's not clear if the authors mean that their modelling procedure can be scaled up.

The review was meant to contextualize the model within the state of the art, and to indicate that other similar models with different strengths and weaknesses exist. However, one of the features of the EcH2O model is that it can be run at a wide range of spatial scales, provided that the necessary inputs are available. Indeed, its spatial domain is constructed and determined by a regular-gridded digital elevation model (DEM) map that defines the topography and the drainage network, and establishes the finite-differences grid on which the governing equations are solved (Maneta & Silverman, 2013). Currently applications have been conducted at the plot scale (Maneta & Silverman, 2013; Douinot et al., *Plot scale modelling to asses forest effects on water partitioning and flux ages*, in prep.), in small catchments (1-10 km^2) (Kuppel et al., 2018; Lozano-Parra et al., 2014), in larger watersheds and small regions (10^2-10^3 km^2) (Maneta & Silverman, 2013; Simeone, 2018). While these studies obviously did not include isotopic tracking, the hydrologic core is the same. In the revised manuscript, we added the following sentence in the model description (sect. 2.1) in order to emphasize this multi-scaling potential:

"*[…] relative humidity, and wind speed). In addition, the flexible definition of the spatial domain in EcH$_2$O allows for applications at a range of scales: from the plot (Maneta and Silverman, 2013), to small catchments (1-10 km^2 – Lozano-Parra et al., 2014; Kuppel et al., 2018), to larger watersheds (10^2-10^3 km^2 – Maneta and Silverman, 2013; Simeone, 2018).*"

7. In the abstract and conclusions, the authors claim that the framework is useful beyond the type of low energy catchment simulated here. However, I feel this statement is misleading and goes well beyond the evidence provided in the paper, and would require e.g. validation in other types of catchments.

The abstract has been edited to avoid making such claim (see the first Specific Comment below). In the conclusions however, we argue that the EcH2O-iso was not specifically designed for simulating the kind of catchment here studied and that it has applicability to other regions. In addition, at present the implementation of isotope and age tracking also avoids any location-specific parameterization. From a methodological viewpoint, the specificity of our site lies not so much in its environmental conditions but rather in the richness of available datasets. As a result, there is no reason to think that our methodology (including the EcH2O-iso model) could not perform well in other environments. The conclusions have been modified in the revised manuscript to emphasize this aspect (P30L14):

"Despite some limitations, this isotope-based evaluation suggests a reasonable capture of the velocity fields (i.e., how fast water parcels move) across the catchment, and complements a previous calibration and evaluation mostly using hydrometric observations (water fluxes and storage dynamics) which indicated a good simulation of catchment functioning from a celerity viewpoint (i.e., how fast energy propagates via the hydraulic gradient) (Kuppel et al., 2018). Satisfying this dual velocity-celerity perspective is key to characterising water pathways and quantifying the associated travel times in different ecohydrological compartments of

headwater landscapes. Complementing more conceptual approaches, the physical basis of the EcH_2O-iso model further provides the potential to extrapolate these insights beyond recorded conditions and scales, and to notably project the reciprocal feedbacks between plant water use, hydrological pathways and potential environmental changes. The relatively simple conceptualisation of compartment-scale velocities, e.g. assuming complete mixing and without site-specific parameterization, and the absence of isotopic calibration, already make the current results particularly encouraging. It also provides a useful framework for hierarchising model development and benchmarking needs. For example, some of the model-data discrepancies in our results stress the necessary incorporation of partial mixing hypotheses, likely to be critical in drier and/or flatter landscapes where diffusive water movement prevails. Second, our model-data analysis of isotope dynamics strongly reflects fractionation effects, be it via soil evaporation or species-specific plant water use. Finally, the versatility of climatic settings in which the original EcH_2O model has already been evaluated facilitates applying the presented methodology beyond the specifics of a high-latitude, low-energy, wet and steep headwater catchment such as the one simulated here. Further, the flexible spatial domain used by the model will help providing a process-based modelling framework for plot-to-catchment-scale hypothesis testing. This is timely for current challenges in critical zone science, such as exploring the occurrence and mechanisms behind the postulated ecohydrological separation of water fluxes (Berry et al., 2017).”

8. Equations: subscripts and superscript should be in upright font when constituting a describing word (e.g., out, in, snow etc.) and only in cursive for variables (e.g., t). Function names such as “max” and “min” should also be in upright font.

We thank the referee for this suggestion. All subscript and superscript notations, as well as function names, have been formatted accordingly in the revised manuscript.

<u>**Specific comments**</u>

Abstract: Very sweeping and general, and raises many questions. Please consider to be more specific. E.g., what is meant by “good [. . .] match in most cases”, “powerful tool”, “some model development”? What kind of cases, why is it powerful, what kind of model development? And what is the model development rationale? What can the model be used for? “Celerity” – a term used in the abstract, introduction, discussion and conclusion, but not clearly explained in the analyses and results sections.

We thank the Referee for this. We have edited the abstract to add precision, as well as to add specificity to the rationale and potential model applications. We also addressed the issue of making “celerity” easier to understand / redefined when used here and in other parts of the manuscripts (see other corresponding comments). In the revised manuscript, the abstract now reads as follows:

“We introduce EcH_2O-iso, a new development of the physically-based, fully-distributed ecohydrological model EcH_2O where the tracking of water isotopic tracers (^2H and ^{18}O) and age has been incorporated. EcH_2O-iso is evaluated at a montane, low-energy experimental catchment in northern Scotland using 16 independent isotope time series from various landscape positions and compartments; encompassing soil water, groundwater, stream water, and plant xylem. The results show consistent isotopic ranges and temporal variability (seasonal and higher-frequency) in across the soil profile at most sites (especially on hillslopes), a broad model-data agreement in heather xylems, and consistent deuterium

dynamics in stream water and in groundwater. Since EcH_2O-iso was calibrated only using hydrometric and energy flux datasets, tracking water composition provides a truly independent validation of the physical basis of the model for successfully capturing catchment hydrological functioning, both in terms of celerity of energy propagation shaping the hydrological response (e.g. runoff generation under prevailing hydraulic gradients), and of flow velocities of water molecules (e.g., in consistent tracer concentrations at given locations and times). Additionally, we also show that the spatially-distributed formulation of EcH_2O-iso provides the possibility to quantitatively link water stores and fluxes with spatio-temporal patterns of isotopes ratios and water ages. However, our study case also highlights model-data discrepancies in some compartments, such as an over-dampened variability in groundwater and stream water lc-excess, and over-fractionated riparian topsoils. The adopted minimalistic framework, without site-specific parameterization of isotopes and age tracking, facilitates the interpretation of these mismatches into model development and benchmarking needs, while taking into account the idiosyncracies of our study catchment. Notably, we suggest that more advanced conceptualisation of soil water mixing and of plant water use would be needed to reproduce some of the observed patterns. Balancing the need for basic hypothesis testing with that of improved simulations of catchment dynamics for a range of applications (e.g., plant water use under changing environmental conditions, water quality issues, and calibration-derived estimates of landscape characteristics), further works could also benefit from including isotope-based calibration."

Introduction: It could be useful for the authors to explain how such their study is linked to practical and societal meaningful issues. For example, the authors explains many times how isotopic characterisation could "provide insights into water pathways", linked to "water flux partitioning", and understanding "catchment functioning", but the reader is left to figure out on her own if these topics are interesting and important also in a broader context. E.g., could improving our understanding of catchment functioning also for example be directly linked to our capacity to design models capable of forecasting floods, and works well under a rapidly changing climate? No need to be lengthy, but just to provide a context. Some interesting debates about evaporation partitioning is also not included, among others: (Coenders-Gerrits et al., 2014; Evaristo et al., 2015; Jasechko et al., 2013; Schlesinger and Jasechko, 2014; Wei et al., 2017).

We thank the Referee for bringing this perspective. In the revised manuscript, the end of the first paragraph of the Introduction has been modified in this regard (P2L6):

"[…] water pathways at scales ranging from the pedon (Sprenger et al., 2018) to the catchment landscape (McGuire and McDonnell, 2006; Birkel and Soulsby, 2015). At larger scales, such approaches can yield global estimates of terrestrial water flux partitioning (Good et al., 2015), where recent scrutiny has been brought upon separating plant transpiration from other source of evaporative losses (e.g., Jasechko et al., 2013; Coenders-Gerrits et al., 2014; Schlesinger and Jasechko, 2014; Wei et al., 2017). At catchment and watershed scales, an understanding of landscape functioning in turn helps designing robust models to predicts the impact of climate extremes and environmental changes in society-relevant issues such as water resources management, flood forecasting, and impact assessment of land cover – land use change (e.g., Troy et al., 2015; Zhang et al., 2017)."

P2L10: What do the authors mean when writing that the "hydrology has remained simplistic" in land surface models? Please specify. And why are dynamic vegetation models and global hydrological models not mentioned?

Given the scope of the paper, we only refer to land surface models on which (to our knowledge) isotopes tracking have been implemented: JSBACH (Haese et al., 2013), ORCHIDEE (Risi et al., 2016) and CLM (Wong et al., 2017). These land surface model have simplified descriptions of the hydrologic system that do not include explicit laterals water transfers (or is represented using a calibrated residence time for linear storage decrease), shallow and deeper subsurface flows, or channel routing. This is made clearer in the revised manuscript. Some of these models also include vegetation dynamics, and this will be mentioned. To our knowledge, no global hydrological model integrates isotope tracking. The revised manuscript has been modified as follows:

"[...] While the simulation of energy budgets and biogeochemical cycles is increasingly detailed in these land surface models -sometimes including vegetation dynamics- the hydrology has, however, remained somewhat simplistic (or even absent) regarding lateral transfers as overland flow, shallow and deeper subsurface flows and channel routing (Fan, 2015). This makes it difficult to take advantage of isotopes tracking to characterise the role of cascading downstream water redistribution in the spatial patterns of catchment functioning. [...]"

P3L9: "evaporative losses in ET". Please consider "terrestrial evaporation".

It has been modified to "terrestrial evaporation" in the revised manuscript. In addition, we now use "E" instead of "Et" to refer to evapotranspiration.

P3L11: "transpiration (T)". Please consider using "Et " for transpiration, to avoid the confusion with temperature T.

"T" has now been replaced by "E_t" throughout the revised manuscript.

P3L19: Key features are described, but the rationale is not explained. E.g., why the model developed is the described way? What are the authors hoping to achieve?

We have modified the introduction so that the rationale of the original EcH_2O development explains our choice for developing an isotopes and age tracking module (P3L20):

" Here, we implement isotope and age tracking in the physically-based, fully-distributed model EcH_2O (Maneta and Silverman, 2013). This model was chosen because of it provides a physically-based, yet computationally-efficient representation of energy-water-ecosystem couplings where intra-catchment connectivity (both vertical and lateral) can be explicitly resolved. In addition, EcH_2O separately solves the energy balance at the top of the canopy and at the soil surface, allowing a process-based separation of E_s, E_t, and E_c. The novel isotopic and age [...]"

P3L28: Please consider new paragraph for the research questions.

P3L30: The research questions could be formulated in a more specifically way. E.g., What are "physics"? Are "mixing assumptions" really investigated in this paper? What kind of "implications and opportunities" do the authors have in mind?

We answer to these two comments jointly. These are good suggestions, and the research questions are now shown as a list in the revised manuscript, for further clarity. In addition, these questions have been modified as follows:

"We ask the following questions:
• To what extent can a hydrometrically-calibrated, physically-based hydrologic model correctly reproduce internal catchment dynamics of isotopes?
• What are the limitations of these isotopic simulations? Do they relate to the underlying model physics and/or to the tracking approach adopted?
• How useful and transferrable is this model framework for simulating spatio-temporal patterns of isotopes and water ages?"

P4 Sect 2.1: Please describe the key features and main limitations of the EcH2O model. Including examples of where and for what kind of purposes the model has been used would also be useful.

We have extended the first paragraph of Sect. 2.1 to include a further description of EcH_2O and examples of past applications:

"[…] *relative humidity, and wind speed). In addition, the flexible definition of the spatial domain in EcH_2O allows for applications at a range of scales: from the plot (Maneta and Silverman, 2013), to small catchments (1-10 km^2 – Lozano-Parra et al., 2014; Kuppel et al., 2018), to larger watersheds (10^2-10^3 km^2 – Maneta and Silverman, 2013; Simeone, 2018). Despite some potential limitations due to the absence of diffusion-driven water redistribution or an explicit biogeochemical cycle providing ecosystem respiration, to date the model yielded satisfactory results and insights across the diversity of climatic settings (semiarid to humid/energy-limited) and scientific focuses (e.g., water balance, energy balance, or plant hydraulics) covered by the aforementioned studies. A comprehensive description of EcH_2O can be found […]"*

P5 Fig 1: Please consider illustrating the isotope tracking assumptions within the model chart, e.g., transpiration is not considered fractioning, throughfall is not aging etc.

This a good suggestion, we have modified Fig. 1 and its caption, so that fractionating processes appears more explicitly but we kept the throughfall assumptions in the main text in order not overload the figure:

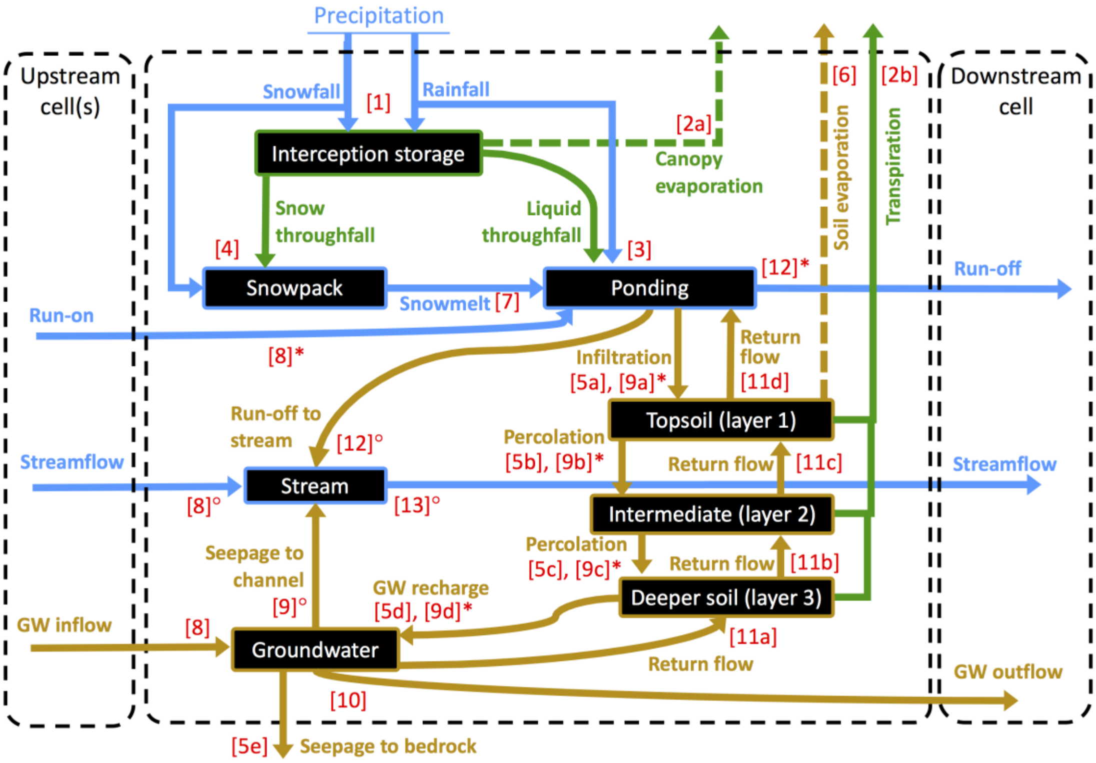

*“**Figure 1.** Water compartments (black rectangles) and fluxes (coloured arrows) as represented in EcH$_2$O, with the dashed arrows indicating processes where isotopic fractionation is simulated. The numbers between brackets reflect the sequence of calculation within a time step. Note that water routing (steps [8] to [13]) differs between cells where a stream is present (◦) or not (∗).”*

P6L9: “One exception. . .” Perhaps new paragraph?

It has been amended in the revised manuscript.

P6L14 “No spill-over”. Not sure what is meant. There is throughfall, right?

By “no spill-over”, we meant that since in the EcH2O model “canopy drainage occurs at the rate at which precipitation increases above the maximum canopy storage” (Maneta & Silverman, 2013), and because maximum canopy storage is constant in our simulations, only the precipitation from the current time step can contribute to throughfall. This is the reason why throughfall does not age, as correctly pointed out by Referee#1 a few paragraphs above. We made this clearer in the revised manuscript:

“[…]. Only the same-time-step precipitation can contribute to throughfall in the EcH$_2$O model, whenever the resulting canopy storage would exceed the maximum canopy storage capacity (Maneta & Silverman, 2013), the latter being constant in our simulations. As a result, intercepted water eventually evaporates from the canopy and does not interact with the surface/subsurface. […]”

P8L13 "PET" Please consider using Epot, as PET could also be precipitation, evaporation, and temperature.

We realized that this acronym is not used anywhere else in the manuscript, so was removed from the revised manuscript.

P11L3-4 "Autumn" Lowercase letters

It has been corrected in the revised manuscript.

P13L26-27 "model-to-data ratio of standard deviation and model-data Pearson's correlation factor". Please consider discussion the merits and pitfalls of using these evaluation metrics. See for example (Biondi et al., 2012) for review of different validation procedures that might be of relevance.

We thank the Referee for this suggestion. As stated in our reply to General Comment 2, our approach consists in a generic evaluation of the new model using an ensemble of diverse isotopic datasets across ecohydrological compartments. This is why we rely on visual inspection (recommended in Biondi et al., 2012) as well as on generic metrics of model skill. The mean absolute error gives a generic quantification model-data fit across different type with lower sensitivity to high values within time series, contrary to metrics based on squared differences (such as RMSE or NSE; Krause et al., 2005; Legates and McCabe, 1999) and, to a lesser extent the Kling-Gupta Efficiency (KGE, Kling et al., 2012). In addition, NSE and KGE have been developed primarily for extracting information (and scores) from stream hydrograph for time series with a large number of points and pronounced variability, which is not the case for most isotopic datasets used here. Following the Referee's comment, in the revised manuscript we have used the mean absolute error (MAE) and Pearson's correlation factor as reference metrics. First, model-data MAE is shown for all relevant time series (displayed the ensemble median so as not to overload the figures). Second, Fig. 8 has been modified in order to display the normalized MAE (using the range of values of observations) against the Pearson's correlation factor:

Figure 8. *Summary of model performance in the dual space of mean absolute error (normalized by the observed range of values) and Pearson's correlation factor between*

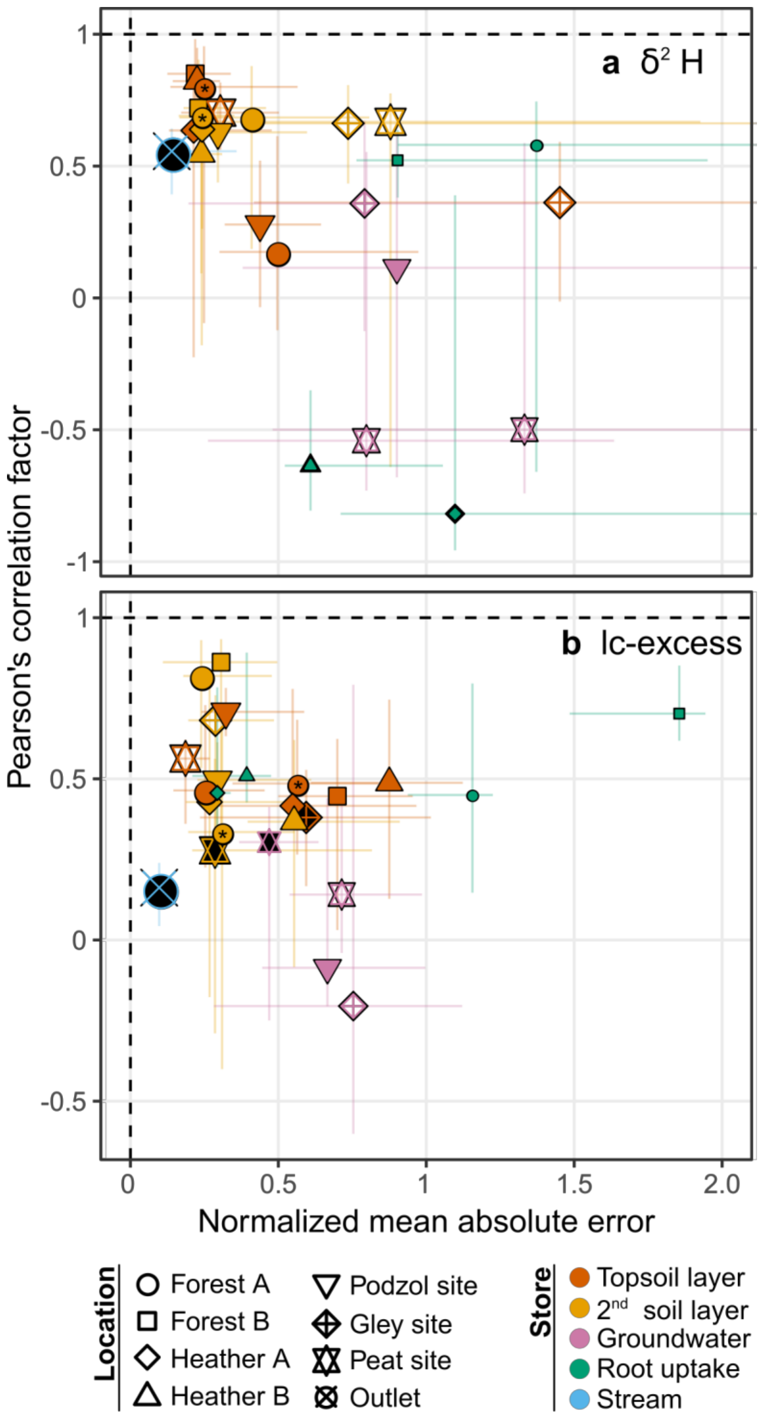

*modelled and observed time series, for **(a)** δ^2H and **(b)** lc-excess, showing the median and 90%-spread over the ensemble. The size of each symbol is proportional to the logarithm of the number of observation points available. Performances in soil compartments at Forest site A are further separated between periods 2013 and 2015-2016 (the latter indicated with an asterisk), corresponding to two separate field data collection campaigns. Two groundwater wells are presents at the peat site.*

As pointed out in Biondi et al. (2012) and elsewhere, normalized MAE provides a more balanced evaluation, permits a direct comparison between different types of observables of varying distributions and dynamics, and is sensitive to model biases. The Pearson's correlation on the other hand captures very well if the model and observables have similar variances, but does not capture biases and is not robust to outliers, especially for time series with few points and/or low variability (groundwater and xylem). In response to this comment these edits have been brought to the main text in Sect 3.4 (P13L26):

"As outlined in Sect. 1, our model evaluation is meant to test the ability of EcH2O to generically simulate isotope dynamics across compartments. We used mean absolute error (MAE) to quantify model-data fit for all isotopic outputs, some of which present low temporal variability, have skewed distributions, or have a relatively lower sampling record and resulting in typical hydrograph-oriented efficiency metrics (e.g., Nash-Sutcliffe or Kling-Gupta, Nash and Sutcliffe, 1970; Kling et al., 2012) being less applicable. The median value are shown on corresponding time series (Figs. 3–7). It is then normalized by each dataset range and used in conjunction with Pearson's correlation factor in Fig. 8 as a summary of model performance. The correlation coefficient axis in this dual model performance space represents the quality of the model in representing the variation of the data, while the normalized MAE axis provides information on the accuracy (bias) of the model."

And in section 4.1 (P17L13):

A summary of model performance is shown in Fig. 8 for all sites/compartments, using the dual space of normalized MAE (using each dataset range, x-axis) and Pearson's linear correlation factor (y-axis). The vast majority of median normalized MAE were below 1, and more than half of evaluated datasets showed values below 0.5. Values above 0.7 were mostly found for groundwater and xylem compartments, a clustering especially marked for δ^2H. In addition, most median model-data correlations were significantly positive between 0.4 and 0.85, noting a tighter clustering around high values for δ^2H than lc-excess. Insignificant or negative correlations were mostly found where only a few data points were available (xylem) or where seasonal variability was low (e.g. groundwater). Interestingly, median model-data agreement in topsoil at Forest site A significantly differed between 2013 (mobile water sampling via lysimeters) and the 2015-2016 period (bulk water sampling via direct equilibration). This was notable in the dramatic increase of model-data correlation (0.17 to 0.8) and decrease of normalized MAE (0.5 to 0.25) for topsoil δ^2H in the latter case, which is consistent with our interpretation that the simulated soil water composition represents that of bulk water."

P14 Sect 4.1. The time series section is detailed and provide considerable amount of information. However, it is also difficult for the reader to quickly get a grasp of the main strength and weaknesses of the model. Please consider including e.g., scatterplots.

Fig. 8 of the revised manuscript provides the recommended scatterplots (see reply to previous referee comment). We have also edited the manuscript to facilitate the interpretation of the figure and guide the reader through the description of the evaluation metrics (at the very end of Sect. 3.4).

P21 Fig 9, P23 Fig 10: Possibly consider moving some of the maps to the SI, and condense the information by grouping (by e.g., riparian/upstream/downstream etc types of regions).

Please refer to our reply to General Comment 5.

P26L9- "By keeping the. . ." Parts of this could also be modelling rationale that could been useful in the introduction section or model set-up.

Following this suggestion, we have emphasized this aspect in the abstract (see related comment above), and at the end of the introduction just after the list of research questions (also reformulated, see related comment above):

"These questions are here addressed by testing the new tracer-enhanced model (EcH_2O-iso, Sect. 2) in a small, low-energy montane catchment (Sect. 3). This site has previously been modelled applying EcH_2O for calibration, using multiple datasets of long-term ecohydrological fluxes and storage variables (Kuppel et al., 2018). We take advantage of this earlier work as a reference ensemble of calibrated model parameterizations, and no additional isotopic calibration is conducted. In addition to using long-term, high resolution isotopic datasets for rainfall and runoff (^2H and ^{18}O), we assess the spatio-temporal variations of model-data agreement in soil water, groundwater, and plant xylem at different locations (Sect 4.1). Following this generic evaluation, the model is used to infer seasonally-varying patterns of water fluxes and isotopes signatures (Sect. 4.2), and water age (Sect. 4.3). Model strengths and weaknesses, insights in processes and potential ways forward are discussed in Sect. 5, before drawing conclusions in Sect. 6."

P3019: "ecohydrological feedbacks". A bit general, and not clear what the authors mean. Ecosystem response in terms of CO2 fertilisation and root depth development?

The term "reciprocal ecohydrological feedbacks" here only encapsulates the reciprocal feedbacks between plant water use and terrestrial water pathways, in the face of environmental change. Given the simplified biogeochemistry used in EcH_2O, the effect of CO2 fertilization, of changes in nutrient availability, or of rooting depth development cannot be explored at present. We have modified this sentence in the revised manuscript as follows:

"[…] Complementing more conceptual approaches, the physical basis of the EcH_2O-iso model further provides the potential to extrapolate these insights beyond recorded conditions and scales, and to notably project the reciprocal feedbacks between plant water use, hydrological pathways and potential environmental changes."

References

Berry, Z. C., Evaristo, J., Moore, G., Poca, M., Steppe, K., Verrot, L., Asbjornsen, H., Borma, L. S., Bretfeld, M., Hervé-Fernández, P., Seyfried, M., Schwendenmann, L., Sinacore, K., De Wispelaere, L., and McDonnell, J.: The two water worlds hypothesis: Addressing multiple working hypotheses and proposing a way forward, Ecohydrology, p. e1843, https://doi.org/10.1002/eco.1843, 2017.

Biondi, D., Freni, G., Iacobellis, V., Mascaro, G. and Montanari, A.: Validation of hydrological models: Conceptual basis, methodological approaches and a proposal for a code of practice, Phys. Chem. Earth, Parts A/B/C, 42–44, 70–76, doi:10.1016/j.pce.2011.07.037, 2012.

Birkel, C. and Soulsby, C.: Advancing tracer-aided rainfall–runoff modelling: a review of progress, problems and unrealised potential, Hydrol. Process., 29(25), 5227–5240, 2015.

Coenders-Gerrits, A. M. J., van der Ent, R. J., Bogaard, T. A., Wang-Erlandsson, L., Hrachowitz, M. and Savenije, H. H. G.: Uncertainties in transpiration estimates, Nature, 506(7478), E1–E2, doi:10.1038/nature12925, 2014.

Evaristo, J., Jasechko, S. and McDonnell, J. J.: Global separation of plant transpiration from groundwater and streamflow, Nature, 525(7567), 91–94, doi:10.1038/nature14983, 2015.

Good, S. P., Noone, D. and Bowen, G.: Hydrologic connectivity constrains partitioning of global terrestrial water fluxes, Science, 349(6244), 175–177, doi:10.1126/science.aaa5931, 2015.

Jasechko, S., Sharp, Z. D., Gibson, J. J., Birks, S. J., Yi, Y. and Fawcett, P. J.: Terrestrial water fluxes dominated by transpiration, Nature, 496(7445), 347–50, doi:10.1038/nature11983, 2013.

Kling, H., Fuchs, M., Paulin, M.: Runoff conditions in the upper Danube basin under an ensemble of climate change scenarios. J. Hydrol. 424, 264–277, 2012.

Krause, P., Boyle, D.P., Bäse, F.: Comparison of different efficiency criteria for hydrological model assessment. Adv. Geosci. 5, 89–97, 2005.

Kuppel, S., Tetzlaff, D., Maneta, M. P., and Soulsby, C.: What can we learn from multi-data calibration of a process-based ecohydrological model?, Environmental Modelling & Software, 101, 301–316, https://doi.org/10.1016/j.envsoft.2018.01.001, 2018.

Legates, D.R., McCabe, G.J.: Evaluating the use of "goodness-of-fit" measures in hydrologic and hydroclimatic model validation. Water Resour. Res. 35, 233–241, 1999.

Lozano-Parra, J., Maneta, M. P., and Schnabel, S.: Climate and topographic controls on simulated pasture production in a semiarid Mediterranean watershed with scattered tree cover, Hydrology and Earth System Sciences, 18, 1439, 2014.

McGuire, K. J. and McDonnell, J. J.: A review and evaluation of catchment transit time modeling, J. Hydrol., 330(3), 543–563, 2006.

Maneta, M. P. and Silverman, N. L.: A spatially distributed model to simulate water, energy, and vegetation dynamics using information from regional climate models, Earth Interactions, 17, 1–44, 2013.

Schlesinger, W. H. and Jasechko, S.: Transpiration in the global water cycle, Agric. For. Meteorol., 189–190, 115–117, doi:10.1016/j.agrformet.2014.01.011, 2014.

Simeone, C.: Coupled ecohydrology and plant hydraulics model predicts Ponderosa seedling mortality and lower treeline in the US Northern Rocky Mountains, Master Thesis, University of Montana. [online] Available from: https://scholarworks.umt.edu/etd/11128, 2018.

Sprenger, M., Tetzlaff, D., Buttle, J., Laudon, H., Leistert, H., Mitchell, C. P., Snelgrove, J., Weiler, M. and Soulsby, C.: Measuring and Modeling Stable Isotopes of Mobile and Bulk Soil Water, Vadose Zone J., 17(1), 2018.

Troy, T. J., Pavao-Zuckerman, M. and Evans, T. P.: Debates—Perspectives on socio-hydrology: Socio-hydrologic modeling: Tradeoffs, hypothesis testing, and validation, Water Resour. Res., 51(6), 4806–4814, 2015.

Wei, Z., Yoshimura, K., Wang, L., Miralles, D. G., Jasechko, S. and Lee, X.: Revisiting the contribution of transpiration to global terrestrial evapotranspiration, Geophys. Res. Lett., 44(6), 2792–2801, doi:10.1002/2016GL072235, 2017.

Zhang, M., Liu, N., Harper, R., Li, Q., Liu, K., Wei, X., Ning, D., Hou, Y. and Liu, S.: A global review on hydrological responses to forest change across multiple spatial scales: Importance of scale, climate, forest type and hydrological regime, J. Hydrol., 546, 44–59, 2017.

Response to Referee 2

The authors would like to thank the Referee #2 for her/his valuable comments and suggestions to strengthen the analysis presented in this manuscript. They have been taken into account in the revised manuscript, as follows (original referee's comments in bold):

Kuppel et al. presents a physically-based ecohydrological model EcH2O-iso that can track water isotopic tracers (2H and 18O) and age. The EcH2O-iso is an extension of the EcH2O model (Maneta and Silverman, 2013). The EcH2O-iso model was evaluated at the Bruntland Burn catchment in the Scottish Highlands, and the simulation results show reasonable agreements with the isotopic measurements. The paper is well written and structured, and it could be a potentially useful contribution to the literature. However, the authors used very general terms in many parts of their model evaluation, which makes it difficult to assess the reliability of their results. For example, no statistics were shown on any of the time series plots, so there is no way that the readers can examine the model performance. Therefore, a major revision is suggested to improve the presentation of the current manuscript.

We thank the reviewer for this suggestion. The mean absolute error (MAE) values have been added to all relevant time series in the revised manuscript (showing the ensemble median only, so as not to overload the figures), complementing the evaluation metrics provided in summary Fig. 8. The latter has according been modified, by using normalized MAE (using each datasets range) against the Pearson's correlation factor.

Additionally, we added a justification for using these metrics at the end of Sect. 3.4 (P13L26):

"As outlined in Sect. 1, our model evaluation is meant to test the ability of EcH2O to generically simulate isotope dynamics across compartments. We used mean absolute error (MAE) to quantify model-data fit for all isotopic outputs, some of which present low temporal variability, have skewed distributions, or have a relatively lower sampling record and resulting in typical hydrograph-oriented efficiency metrics (e.g., Nash-Sutcliffe or Kling-Gupta, Nash and Sutcliffe, 1970; Kling et al., 2012) being less applicable. The median value are shown on corresponding time series (Figs. 3–7). It is then normalized by each dataset range and used in conjunction with Pearson's correlation factor in Fig. 8 as a summary of model performance. The correlation coefficient axis in this dual model performance space represents the quality of the model in representing the variation of the data, while the normalized MAE axis provides information on the accuracy (bias) of the model."

Finally, some descriptions of results have been made more precise, especially in the abstract and conclusions. Specific changes to the manuscript are detailed in 'specific comments'.

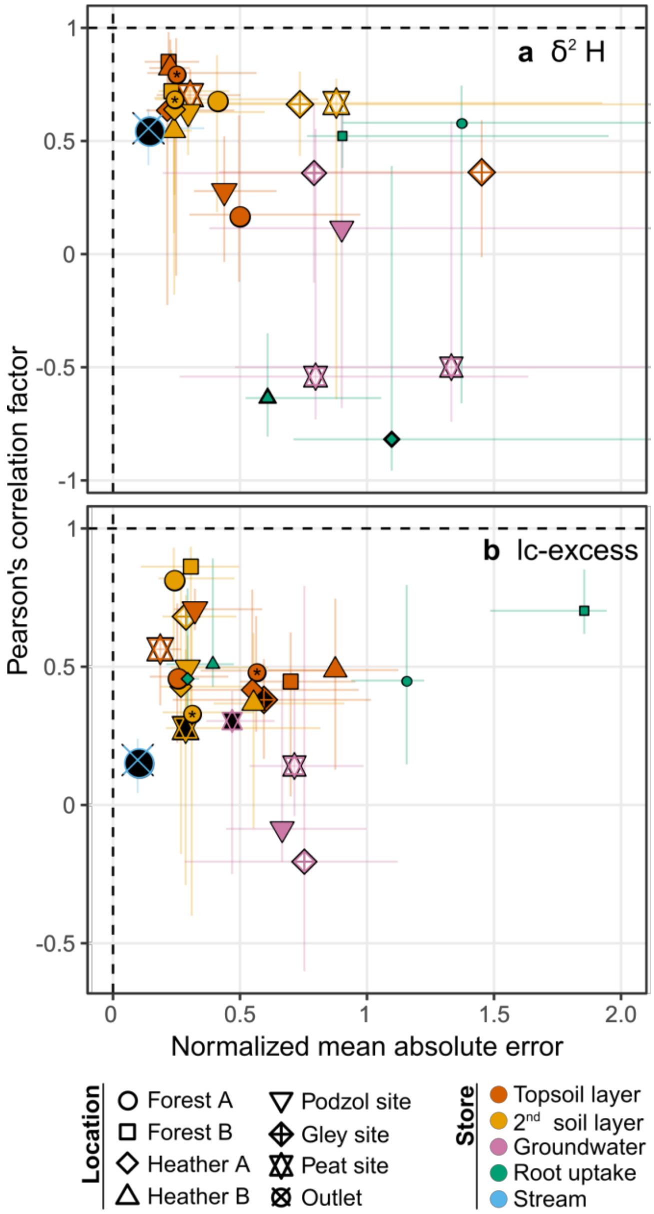

Figure 8. *Summary of model performance in the dual space of mean absolute error (normalized by the observed range of values) and Pearson's correlation factor between modelled and observed time series, for* ***(a)*** *δ^2H and* ***(b)*** *lc-excess, showing the median and 90%-spread over the ensemble. The size of each symbol is proportional to the logarithm of the number of observation points available. Performances in soil compartments at Forest site A are further separated between periods 2013 and 2015-2016 (the latter indicated with an asterisk), corresponding to two separate field data collection campaigns. Two groundwater wells are presents at the peat site.*

<u>Specific comments</u>

Pg2, L9-12: The statement provided here seems not directly related to the paragraph above and below it. It is not clear what was the authors' attempt to deliver here. Also, what is "simplistic" meant by the authors with regard to the hydrology in land surface models?

The phrasing was awkward and has been edited for clarity. Our intent was to indicate that land surface models are the only type of process-based models operating at scales larger than the hillslope where isotope tracking has been implemented (to our knowledge). However, simplifications in the representation of hydrological pathways, such as lateral connectivity, make them of limited applicability to understand water mixing and storage dynamics. In the revised manuscript, this paragraph has been reformulated as follows:

"[...] While the simulation of energy budgets and biogeochemical cycles is increasingly detailed in these land surface models -sometimes including vegetation dynamics-, the

hydrology has, however, remained somewhat simplistic (or even absent) regarding lateral transfers as overland flow, shallow and deeper subsurface flows, and channel routing (Fan, 2015). This makes it difficult to take advantage of isotopes tracking to characterise the role of cascading downstream water redistribution in the spatial patterns of catchment functioning. […]"

Pg3, L28-31: It is not clear how these questions being addressed in the paper. It would be very helpful if the authors could add more details about the experimental design to illustrate how these questions were linked to the results.

We have modified the end of the introduction in the revised manuscript, so that the connection between research questions (now modified following Referee #1's suggestion) and our experimental/analytical design is clear (from P3L20 onwards):

"This model was chosen because it provides a physically-based, yet computationally-efficient representation of energy-water-ecosystem couplings where intra-catchment connectivity (both vertical and lateral) can be explicitly resolved. In addition, EcH$_2$O separately solves the energy balance at the top of the canopy and at the soil surface, allowing a process-based separation of E_s, E_t, and E_c. The novel isotopic and age tracking module is designed in a fashion directly consistent with the original model structure, assuming full mixing in each model compartment, and crucially without catchment-specific parameterization. The conceptualisation of evaporation fractionation uses the well-known Craig-Gordon approach (Craig and Gordon, 1965).

We ask the following questions:

- *To what extent can a hydrometrically-calibrated, physically-based hydrologic model correctly reproduce internal catchment dynamics of isotopes?*
- *What are the limitations of these isotopic simulations? Do they relate to the underlying model physics and/or to the tracking approach adopted?*
- *How useful and transferrable is this model framework for simulating spatio-temporal patterns of isotopes and water ages?*

These questions are here addressed by testing this new tracer-enhanced model (EcH$_2$O-iso, Sect. 2) in a small, low-energy montane catchment (Sect. 3). This site has previously been modelled applying the original EcH$_2$O model for calibration, using multiple datasets of long-term ecohydrological fluxes and storage variables (Kuppel et al., 2018). We take advantage of this earlier work as a reference ensemble of calibrated model parameterizations, and no additional isotopic calibration is conducted. In addition to using long-term, high resolution isotopic datasets for rainfall and runoff (^{2}H and ^{18}O), we assess the spatio-temporal variations of model-data agreement in soil water, groundwater, and plant xylem at different locations (Sect 4.1). Following this generic evaluation, the model is used to infer seasonally-varying patterns of water fluxes and isotopes signatures (Sect. 4.2), and water age (Sect. 4.3). Model strengths and weaknesses, insights in processes and potential ways forward are discussed in Sect. 5, before drawing conclusions in Sect. 6."

Pg4, L4: It might be better to change "climate" to "microclimate" since the spatial and temporal scales used in the model is relatively small than the scales used in climate science.

Since the model is designed to be used at a range of spatial scales, including regional studies (Simeone, 2018), in the revised manuscript we have used the term "local climate".

Pg4, L11: What is the temperature threshold for the partitioning between liquid and snow components? How does the model quantify snowpack depth for a given amount of precipitating snow?

For this threshold we use a default value of 2°C from Maneta and Silvermann (2013). Snowpack depth is not quantified in the model; only the snow water equivalent is being output by the model, and has been used for evaluation in Maneta and Silvermann (2013). In the revised manuscript, the corresponding section of the paragraph now reads:
"[...]. The capacity-excess P (i.e., throughfall) is partitioned between liquid and snow components using a snow-rain temperature threshold (fixed to 2 °C) together with the minimum and maximum air temperature at each time step. [...]"

Pg4, L12: Canopy conductance is a key factor determining the amount of canopy transpiration. How is canopy conductance represented in the model? Is it simulated at each model time step?

Stomatal conductance is represented by a Jarvis-type multiplicative model to account for the four major environmental stressors driving stomatal conductance, and then upscaled to canopy conductance using the leaf area index (LAI) (Maneta & Silverman, 2013):

$$g_{canopy} = g_{stoma}^{max} \cdot LAI \cdot f_{light} \cdot f_{temp} \cdot f_{VPD} \cdot f_{moist}.$$

Stomatal conductance is calculated for each vegetation type in each cell of the model. Here, g_{stoma}^{max} is the maximum stomatal conductance (a calibrated parameter), while f_{light}, f_{temp}, f_{VPD}, and f_{ψ} are efficiency factors (range 0-1), respectively, which account for the effect of incoming shortwave radiation ($R_{SW\downarrow}$), air temperature (T_a), vapor pressure deficit at the leaf-air interface ($e_a^* - e_a$), and soil matric potential (ψ). All these variables are calculated at each time step for each vegetation type present in the grid cells, noting that f_{ψ} is iteratively updated within the Newton-Rapson loop used to solve the 3-equations system for the canopy-level energy balance (see Appendix A1 in Kuppel et al., 2018 for further details):

$$f_{light} = \frac{R_{SW\downarrow}}{R_{SW\downarrow} + \phi_{SW\downarrow}}$$

$$f_{temp} = \left[\left(\frac{T_a - T_{min}}{T_{opt} - T_{min}}\right)\left(\frac{T_{max} - T_a}{T_{max} - T_{opt}}\right)\right]^{\left(\frac{T_{max} - T_{opt}}{T_{opt} - T_{min}}\right)}$$

$$f_{VPD} = exp\left[-\phi_{e_a} \cdot (e_a^* - e_a)\right]$$

$$f_{\psi} = \frac{1}{1 + \left(\frac{\psi}{\psi_d}\right)^c}$$

where $\phi_{SW\downarrow}$, T_{min}, T_{opt}, T_{max}, ϕ_{e_a}, ψ_d, and c are empirical coefficients whose values are taken from the literature ($\phi_{SW\downarrow}$, T_{min}, T_{max}, ϕ_{e_a}) or calibrated (T_{opt}, ψ_d, and c). While adding this full description is beyond the scope of the paper, in the revised manuscript we modified the sentence highlighted for the Referee, as follows:

"The canopy energy balance then separately yields plant transpiration (E_t) and evaporation of intercepted water (E_c). The calculation of E_t uses, for each vegetation type, the canopy conductance at each time step based on a Jarvis-type multiplicative model accounting for environmental limitations of incoming solar radiation, T_a, vapor pressure deficit at the leaf surface, and soil water potential (see Maneta and Silverman (2013) and Appendices in Kuppel et al. (2018) for a more detailed description). Infiltration of surface water [...]"

Pg6, L3: Δt is redundant here as it has been defined right above eqn (2).

This redundant definition has been removed.

Pg8, L13: Could the authors provide any reference for the amount of PET estimated at the study site?

We noticed that the value reported here is an estimate of actual evapotranspiration derived from applying the Penman-Monteith equation adjusted for heather shrub aerodynamic roughness (Birkel et al., 2011). This correction, reference, and precision has been added to the revised manuscript.

Pg11, L27-29: Were there any missing data during the measurement period? If so, what was the gap-filling treatment for the meteorological observations? Also, what was the temporal resolution of the meteorological observations?

The three weather stations at the catchment provided micrometeorological measurements at an original resolution of 15 minutes. Some measurements were sparsely missing in each of the stations records, with gaps ranging from one 15-min time step to a few days (notably during severe rainstorms at the beginning of 2016). There was however no instance of data simultaneously missing from all three stations, so that the daily inputs used for our simulations did not require a specific temporal gap-filling approach in the preprocessing stage. The revised manuscript includes information about the original temporal resolution of the raw meteorological data.

Pg 12, L 13: How did the authors determine the transient dynamics has been removed after a 3-year spin up period?

It was achieved by visual inspection of the time series of hydrometric and isotopic variables at the set of locations used in this study: through incrementing the spinup length starting from 1 to 6 years; no significant changes or trends were observed beyond 3 years of spinup. We added this precision in the revised manuscript (P12L11):

"For all simulations a 3-year spin up period was added using the first three years of isotopic and climatic model inputs, as preliminary sensitivity tests combined with a visual inspection of simulated hydrometric and isotopic time series at the locations used in this study (Sect. 3.2) indicated it was sufficient to remove transient dynamics."

Pg 12, L21: Why did the authors set the depth of the first soil layer to 0.001 m? How sensitive does the model respond to the changes in the depth of the first soil layer?

The depth of the first layer was set to 0.001 m at locations where a significant proportion (>0.5) of the grid cell area is bare soil, which always corresponds to locations with exposed bare rock. This choice was made to limit the local soil evaporation simulated by the model (which only occurs in the first soil layer and thus is strongly controlled by its depth), and avoid producing an unrealistic degree of isotopic fractionation. Sensitivity tests shows that the overall effect was small in simulating the water balance given the relatively small area covered by exposed rock, and that the isotopic composition in downstream soils and in the stream channel was barely affected by this choice of a very thin topsoil. In the revised manuscript, the corresponding sentence has been modified as follows:

"To avoid an overestimation of local soil evaporation and resulting isotopic fractionation in grid cells of exposed rock/scree, for simplicity we fixed the depth of the first soil layer to 0.001 m wherever the fraction of bare soil was larger than 0.5 – after performing a sensitivity analysis showing little effect on catchment water balance and downstream isotopic budgets."

Pg 13, L11: It should be Eq. 20 instead of Eq. 19.

It has been corrected in the revised manuscript.

Pg 19, L 26-27: How is the seasonal change of vegetation represented in the model? Was the increase of ecosystem transpiration resulted from the increase of vegetation leaf area or the increase of canopy conductance? Did the authors check the water loss from canopy evaporation? How much of difference did the model simulate between canopy evaporation and soil evaporation?

For this study, we adopted the same configuration as Kuppel et al. (2018) where vegetation dynamics is turned off, i.e. leaf area index (LAI) remains constant. As a result, the variation in ecosystem transpiration results from that of canopy conductance (see our reply about its calculation a few comments above), and that of vapor gradient at the leaf surface (see also Eq. A4 in Kuppel et al. (2018)). We have added this precision in Sect. 3.3 (P12L20) of the revised manuscript:
"As in Kuppel et al. (2018), the dynamic vegetation allocation module is switched off, so that leaf area index remains equal to initial values of 2.9, 1.6, 3.5, and 2 $m^2.m^{-2}$ for Scots pines, heather shrubs, peat moss and grasslands, respectively (Albrektson, 1984; Calder et al., 1984; Bond-Lamberty and Gower, 2007; Moors et al., 1998)."

The simulation ensemble provides a catchment-wide values of 354±50 mm/yr for canopy evaporation (here understood as interception losses plus transpiration), which is much higher than soil evaporation (59±22 mm/yr). Note that this large dominance of canopy evaporation (~85-90% of the evaporative losses) over soil evaporation was also highlighted by observation-based, plot-scale studies at the same catchment in a Scots pine stand (Wang et al., 2017a) and at a heather plot (Wang et al., 2017b).

Pg29, L23: Please change "T he" to The.

It has been corrected in the revised manuscript.

Pg30, L13-14: This is a very general statement. It would be very helpful if the authors could revise it with more specific terms so the readers can catch up easily.

This is a good suggestion, and we provide more specific summary in the revised manuscript: *"Evaluated against a multi-site, extensive isotopic dataset encompassing a wide range of ecohydrological compartments (soil moisture, groundwater, plant xylem, and stream water) across hydropedological units, the model has generically shown good performance in reproducing the seasonal and higher-frequency variations of absolute and relative isotopic content (δ^2H and lc-excess, respectively)."*

Pg30, L14-15: Again, it is difficult for the readers to understand why this wound indicate the model is correct in both energy celerity and flow velocity viewpoints. It might be useful to explain what exactly are the energy celerity and flow velocity viewpoints meant by the authors.

The definition of celerity and velocity viewpoints, given in the abstract and introduction, are here repeated for clarity in the revised manuscript:

"This isotope-based evaluation suggests a correct capture of the velocity fields (i.e., how fast water parcels move) across the catchment, and complements a previous calibration and evaluation mostly using hydrometric observations (water fluxes and stores) which indicated a good simulation of catchment functioning from a celerity viewpoint (i.e., how fast energy propagates via the hydraulic gradient) (Kuppel et al., 2018). Satisfying this dual velocity-celerity perspective is key to characterizing water pathways […]"

References

Albrektson, A.: Sapwood basal area and needle mass of Scots pine (Pinus sylvestris L.) trees in central Sweden, Forestry, 57(1), 35–43, 1984.

Birkel, C., Tetzlaff, D., Dunn, S. M., and Soulsby, C.: Using time domain and geographic source tracers to conceptualize streamflow generation processes in lumped rainfall-runoff models, Water Resour. Res., 47, W02 515, https://doi.org/10.1029/2010WR009547, 2011.

Bond-Lamberty, B. and Gower, S. T.: Estimation of stand-level leaf area for boreal bryophytes, Oecologia, 151(4), 584–592, doi:10.1007/s00442-006-0619-5, 2007.

Calder, I. R., Hall, R. L., Harding, R. J. and Wright, I. R.: The use of a wet-surface weighing lysimeter system in rainfall interception studies of heather (Calluna vulgaris), J. Clim. Appl. Meteorol., 23(3), 461–473, 1984.

Craig, H. and Gordon, L. I.: Deuterium and oxygen 18 variations in the ocean and the marine atmosphere, Stable Isotopes in Oceanic Studies and Paleotemperatures, 1965.

Kuppel, S., Tetzlaff, D., Maneta, M. P., and Soulsby, C.: What can we learn from multi-data calibration of a process-based ecohydrological model?, Environmental Modelling & Software, 101, 301–316, https://doi.org/10.1016/j.envsoft.2018.01.001, 2018.

Lozano-Parra, J., Maneta, M. P., and Schnabel, S.: Climate and topographic controls on simulated pasture production in a semiarid Mediterranean watershed with scattered tree cover, Hydrology and Earth System Sciences, 18, 1439, 2014.

Moors, E., Stricker, J. and van der Abeele, G.: Evapotranspiration of cut over bog covered by Molinia Caerulea, Wagenigen., 1998.

Maneta, M. P. and Silverman, N. L.: A spatially distributed model to simulate water, energy, and vegetation dynamics using information from regional climate models, Earth Interactions, 17, 1–44, 2013.

Simeone, C.: Coupled ecohydrology and plant hydraulics model predicts Ponderosa seedling mortality and lower treeline in the US Northern Rocky Mountains, Master Thesis,

University of Montana. [online] Available from: https://scholarworks.umt.edu/etd/11128, 2018.
Wang, H., Tetzlaff, D., Dick, J.J., Soulsby, C.:. Assessing the environmental controls on Scots pine transpiration and the implications for water partitioning in a boreal headwater catchment. Agric. For. Meteorol. 240, 58e66, 2017a.
Wang, H., Tetzlaff, D., Soulsby, C.:. Testing the maximum entropy production approach for estimating evapotranspiration from closed canopy shrubland in a low-energy humid environment. Hydrol. Process., 31, 4613-4621, 2017b.

Response to Referee 3

The authors would like to thank the Referee #3 for her/his valuable comments to deepen the discussion of the conceptualisation adopted and the results. It has been taken into account in the revised manuscript and we reply point-by-point in the following (original referee's comments in bold).

This review report is for the manuscript, entitled: "EcH2O-iso 1.0: Water isotopes and age tracking in a process-based distributed ecohydrological model" by Kuppel et al.. This study embedded the water isotopic tracers and age into an ecohydrological model, EcH2O and then applied this model onto a small catchment. This model, therefore, could simulate the spatio-temporal variation of water flux and water isotopic composition in soil moisture, plant xylem, and groundwater. Overall speaking, I enjoyed reading this study which, indeed, is a great and innovative work. The spatio-temporal patterns of water isotopes can be demonstrated now and the hypothesis we have been concerned can be tested. The simulation is promising, which indicates that the present concepts and knowledge are tentatively correct. However, there are still some concerns that should be addressed for completing the statements.

First of all, this study simulated the hydrological processes without parameterization and calibration. Although the lack of calibration is a good way to test hypothesis comprehensively, it would lower the practical applicability for transferring this model to other catchments. This Aberdeen catchment with intensive observations is quite unique around the world. Therefore, it would be great to discuss the potential parameterization, particularly for the soil moisture, transpiration, and groundwater. The parameterization could not only increase the applicability for other catchments, but also help to introduce the landscape characteristics into the parameters, which is an important concern of critical zones where researchers attempt to incorporate the geophysical characterization into substance transport.

We appreciate this comment. We must emphasize first that the ensemble of parameters sets used for the presented simulations derives from a multi-objective calibration conducted using hydrometrics and energy balance datasets as constraints (see Sect. 3.3), following the methodology of Kuppel et al. (2018). Most likely further calibration using isotopes datasets would introduce additional independent information capable of further refining the identification of model parameters. However, we chose not to conduct such calibration in order to put the new isotope tracking model to a fundamental test: we simply assess how the original EcH_2O structure (informed by hydrometry-based parameterization and successfully evaluated) performs when applying the current "tracer tracking" conceptualization.
This first step is in our view necessary to develop a solid and hypothesis-driven contribution to the emerging velocity-celerity (i.e., looking at both hydrological response and tracer transport) modelling community, even before engaging in the provision of a ready-to-use numerical tool. Although the positive results we present are very encouraging, our "minimalistic" approach also facilitates translating the model-data mismatches into specific development needs (as discussed in Sect. 5), something which would have been challenging otherwise, given the relative complexity of the original EcH2O model itself.

We agree with the Referee that our catchment is unique in terms data availability. Hydrologists using this model in other catchments will mostly have hydrometry-related datasets available for calibration, with perhaps a few (if any) isotopic datasets. Assessing the information transferability from one viewpoint (energy celerity, provided by hydrometric datasets) to the other (water velocity as represented by isotopic composition and water ages), and their compatibility, is a reason why we did not include our isotopic datasets in the calibration.
We are nonetheless aware of the pressing need for tracer-enabled models such as EcH_2O-iso to retrieve landscape-relevant model parameterizations to leverage information-rich combinations of hydrometric and isotopic datasets. We are currently working on such a calibration approach using isotopes, along with further hypothesis-testing regarding soil mixing. We have added this aspect to the end of the revised abstract:
"[...] Balancing the need for basic hypothesis testing with that of improved simulations of catchment dynamics for a range of applications (e.g., plant water use under changing environmental conditions, water quality issues, and calibration-derived estimates of landscape characteristics), further works could also benefit from including isotope-based calibration."

Secondly, the water isotopic measurement in soil moisture is very difficult and tricky. As mentioned by Orlowski et al. (2016), it is intricate to determine the soil water isotopic composition. Presently, this model integrated all soil layers into one storage, which is acceptable, but can the authors explain more on what kind of soil water they simulated and what is their opinion about this issue in modeling work?
Finally, the observed lc-excess values of groundwater are higher than simulated ones indicating the exaggerated mixing across the soil profile. However, evaporation from shallow groundwater could raise the lc-excess variability as well. Can the authors explain more to this concern and provide some thinking for further modeling development?

We grouped the two above comments by the Referee since they are interlinked.

Being able to compare simulated soil water isotopic composition with measurement representing a similar spatial footprint is key for correct model evaluation. Currently, the soil hydrology of EcH2O differentiates between three vertical layers in each grid cell, (whose thicknesses are calibrated parameters). Our results present the soil water isotopic composition (Figs. 3-4) of the first two layers and correspond to bulk soil water. Although we mention it in the results and discussion section (P14L17, P18L10, and P26L23), this is missing from the method section. In the revised manuscript, we have added this precision in this isotopic model description (P6L9):
"Note that because of its representation of a single, fully-mixed pool in each soil layer, EcH_2O-iso essentially provides a bulk water values for isotopic content and water ages. This needs to be kept in mind when comparing with soil isotopic datasets (see Sect. 3.2 and Sect. 4) and for the discussion (Sect. 5)."

A significant contribution of the reported model-data lc-excess discrepancy can probably be attributed to the coarse vertical discretization of the soil profile (3 layers), which enhances mixing compared to approaches that use a finer discretization of the soil profile (e.g. Sprenger et al., 2018). Overestimated mixing may be a reason for the buffered simulated isotopic signal and high lc-excess in the soil profile and in the groundwater. This explanation is unsatisfying

because it is rooted in the arbitrary numerical partitioning of the soil, and not on a hypothesis about hydrologic function. An alternative and more satisfying reason may be inadequacies of the full-mixing assumption and the need for a second type of water pool in each soil layer mixing at a different rate, which is a hypotheses guiding current model development. This dual mixing hypothesis relates to preferential flow pathways and is controlled by the degree of tension under which the water is held in the soil and the macro- to micro-scale variability of pore size (Beven and Germann, 2013). Despite being a long-standing issue in hydrological conceptualisation (Beven and Germann, 1982), associated efforts for catchment modelling are relatively rare and only recently gain momentum (e.g., Stump, 2007; Vogel et al., 2010; Sprenger et al., 2018; Smith et al., 2018). Without getting into the complexity (and potentially prohibitive computational cost) of applying a detailed description of a dual-porosity-based routing in the subsurface (e.g., Hutson and Wagenet, 1995) to the structure of the EcH_2O-iso model, we are currently exploring a parsimonious implementation for future studies with EcH_2O-iso. We have amended the corresponding part of Sect. 5.2 in the revised manuscript (P28L21):
"[…] dynamics and tracer mixing (Beven and Germann, 2013). This would first involve implementing conceptualisation of micro-topographic controls on overland flow (Frei et al., 2010). Secondly, the significance of sub-surface dual pore space (matrix-macropore) representations of tracer flow paths and mixing has long been put forward (Beven and Germann, 1982) but modelling efforts relevant to catchment hydrology remain somewhat scarce (Stumpp et al., 2007; Stumpp and Maloszewski, 2010; Vogel et al., 2010; Sprenger et al., 2018; Smith et al., 2018). Bridging these detailed plot-to-hillslope-scale descriptions […]"

Finally, evaporation of shallow groundwater is not explicitly taken into account in the current EcH_2O-iso formulation of evaporative losses and isotopic fractionation. While these processes are not likely a major contributor to water fluxes and isotopic fractionation in our catchment (as hinted by the positive lc-excess values), future developments should take into account these process, which can become significant in locations with higher evaporative demand (e.g., Soylu et al., 2011).

Thirdly, the simulated and observed deuterium composition and lc-excess in forest sites exist large discrepancies. It was straightforwardly attributed to the dependency among species. It indicated that vegetation pumping has great differences among species (e.g. heather and forest). It will be great if the authors can give some suggestions for further parameterization.

The last paragraph of Sect. 5.2 (P28L19), discusses the observed model-data mismatch in Scot pine xylem and highlights limitations in our approach because: 1) we assumed soil-dependent root-profile, instead of a vegetation-dependent parameterization, and 2) unrepresented processes that could cause isotopic fractionation at different stage of xylem water cycling, e,g. during root uptake, via inner-stem exchange (e.g., xylem-phloem cycling) and via evaporation through the bark (see references in Sect. 5.2). These mechanisms are complex, non-exclusive, and the lack of a scientific consensus has made them a very active topic of ecophysiological research (Poca, *personal communication*). It is therefore difficult to suggest specific parameterization, but a first step to obtain probably requires to increase the temporal resolution of measurements and use it to derive a relationship that can be incorporated in models and that capture short-term variability (e.g., Martín-Gómez et al., 2016).

References

Beven, K. and Germann, P.: Macropores and water flow in soils, Water Resour. Res., 18(5), 1311–1325, 1982.

Beven, K. and Germann, P.: Macropores and water flow in soils revisited, Water Resour. Res., 49(6), 3071–3092, doi:10.1002/wrcr.20156, 2013.

Hutson, J. L. and Wagenet, R. J.: A multiregion model describing water flow and solute transport in heterogeneous soils, Soil Sci. Soc. Am. J., 59(3), 743–751, 1995.

Martín-Gómez, P., Serrano, L. and Ferrio, J. P.: Short-term dynamics of evaporative enrichment of xylem water in woody stems: implications for ecohydrology, Tree Physiol., 37(4), 511–522, 2016.

Smith, A. A., Tetzlaff, D. and Soulsby, C.: Using StorAge Selection functions to quantify ecohydrological controls on the time-variant age of evapotranspiration, soil water, and recharge, Hydrol Earth Syst Sci Discuss, 2018, 1–25, doi:10.5194/hess-2018-57, 2018.

Soylu, M. E., Istanbulluoglu, E., Lenters, J. D., and Wang, T.: Quantifying the impact of groundwater depth on evapotranspiration in a semi-arid grassland region, Hydrol. Earth Syst. Sci., 15, 787-806, https://doi.org/10.5194/hess-15-787-2011, 2011.

Sprenger, M., Tetzlaff, D., Buttle, J., Laudon, H., Leistert, H., Mitchell, C. P., Snelgrove, J., Weiler, M. and Soulsby, C.: Measuring and Modeling Stable Isotopes of Mobile and Bulk Soil Water, Vadose Zone J., 17(1), 2018.

Stumpp, C. and Maloszewski, P.: Quantification of preferential flow and flow heterogeneities in an unsaturated soil planted with different crops using the environmental isotope $\delta^{18}O$, Journal of Hydrology, 394, 407–415, 2010.

Stumpp, C., Maloszewski, P., Stichler, W., and Maciejewski, S.: Quantification of the heterogeneity of the unsaturated zone based on environ mental deuterium observed in lysimeter experiments, Hydrological Sciences Journal, 52, 748–762, 2007.

Vogel, T., Sanda, M., Dusek, J., Dohnal, M., and Votrubova, J.: Using Oxygen-18 to Study the Role of Preferential Flow in the Formation of Hillslope Runoff, Vadose Zone Journal, 9, 252–259, https://doi.org/10.2136/vzj2009.0066, 2010.

EcH_2O-iso 1.0: Water isotopes and age tracking in a process-based, distributed ecohydrological model

Sylvain Kuppel[1], Doerthe Tetzlaff[1,2,3], Marco P. Maneta[4], and Chris Soulsby[1,2]

[1]Northern Rivers Institute, University of Aberdeen, Aberdeen, AB24 3UF, United Kingdom.
[2]Leibniz Institute of Freshwater Ecology and Inland Fisheries, Berlin, 12587, Germany.
[3]Department of Geography, Humboldt University Berlin, Berlin, 10099, Germany.
[4]Geosciences Department, University of Montana, Missoula, MT 59812-1296, USA

Correspondence: D. Tetzlaff (d.tetzlaff@igb-berlin.de)

Abstract. We introduce EcH_2O-iso, a new development of the physically-based, fully-distributed ecohydrological model EcH_2O where the tracking of water isotopic tracers (^{2}H and ^{18}O) and age has been incorporated. EcH_2O-iso is evaluated at a montane, low-energy experimental catchment in ~~eastern~~ northern Scotland using 16 independent isotope time series from various landscape positions and compartments; encompassing soil water, groundwater, stream water, and plant xylem. ~~We find a good model-observation match in most cases, despite having only calibrated the model using hydrometric data and energy fluxes. These results provide further~~ The simulation results show consistent isotopic ranges and temporal variability (seasonal and higher-frequency) across the soil profile at most sites (especially on hillslopes), broad model-data agreement in heather xylem, and consistent deuterium dynamics in stream water and in groundwater. Since EcH_2O-iso was calibrated only using hydrometric and energy flux datasets, tracking water composition provides a truly independent validation of the physical basis of the model for successfully capturing catchment hydrological functioning, both in terms of the celerity in energy propagation shaping the hydrological response (e.g. runoff generation under prevailing hydraulic gradients) and flow velocities of water molecules (e.g., in consistent tracer concentrations at given locations and times). ~~We also~~ Additionally, we show that the spatially-distributed formulation of EcH_2O-iso ~~provides a powerful tool for quantitatively linking~~ has the potential to quantitatively link water stores and fluxes with spatio-temporal patterns of isotopes ratios and water ages. ~~Finally, our study highlights some~~ However, our case study also highlights model-data discrepancies in some compartments, such as an over-dampened variability in groundwater and stream water lc-excess, and over-fractionated riparian topsoils. The adopted minimalistic framework, without site-specific parameterization of isotopes and age tracking, allows us to learn from these mismatches in further model development and benchmarking needs, ~~refined using isotope-based calibration, for hypothesis testing and~~ while taking into account the idiosyncracies of our study catchment. Notably, we suggest that more advanced conceptualisation of soil water mixing and of plant water use would be needed to reproduce some of the observed patterns. Balancing the need for basic hypothesis testing with that of improved simulations of catchment dynamics ~~that is transferable beyond the catchment landscape studied here.~~ for a range of applications (e.g., plant water use under changing environmental conditions, water quality issues, and calibration-derived estimates of landscape characteristics), further work could also benefit from including isotope-based calibration.

1 Introduction

Before being evaporated to the atmosphere or routed to the oceans, continental precipitation transits in soils, plants, aquifers, and rivers. All these pathways in the "critical zone" (National Research Council, 2012) shape the coupling between hydrology and biogeochemistry, and impose controls on many ecological and geomorphological processes. In turn, these interactions determine the partitioning of water trajectories between storage, bypass, mixing, recharge and evapotranspiration (Brooks et al., 2015). In this respect, conservative tracers such as stable water isotopes (^{1}H, ^{2}H, ^{16}O, and ^{18}O) represent a useful "water fingerprinting" tool to research these mechanisms due to the process-dependent asymmetrical dynamics of heavier and lighter isotopes. Combined with a quantification of water flux rates and storage dynamics – either measured or modelled –, ~~characterizing~~ characterising isotopic composition provides powerful insights into water pathways at scales ranging from the pedon (Sprenger et al., 2018) to the catchment landscape (McGuire and McDonnell, 2006; Birkel and Soulsby, 2015)~~, and even to~~ . At larger scales, such approaches can yield global estimates of terrestrial water flux partitioning (Good et al., 2015)~~. Furthermore, tracers~~ , where recent scrutiny has been brought upon separating plant transpiration from other source of evaporative losses (e.g., Jasechko et al., 2013; Coenders-Gerrits et al., 2014; Schlesinger and Jasechko, 2014; Wei et al., 2017). At catchment and watershed scales, an understanding of landscape functioning in turn helps designing robust models to predicts the impact of climate extremes and environmental changes in society-relevant issues such as water resources management, flood forecasting, and impact assessment of land cover – land use change (e.g., Troy et al., 2015; Zhang et al., 2017).

Tracers have been of particular importance in understanding catchment functioning, as they highlight pore velocities of water molecules (i.e., how fast does a given parcel of water move) in a way that distinguishes this from the celerity (i.e., how fast energy propagates via the hydraulic gradient) of the rainfall-runoff response (McDonnell and Beven, 2014).

Historically, isotopic transport models were initially developed at the plot scale (∼1-100 m^2) to represent 1-D isotope transfers in the soil profile and at the surface-atmosphere interface (Mathieu and Bariac, 1996; Melayah et al., 1996; Braud et al., 2005, 2009; Haverd and Cuntz, 2010; Soderberg et al., 2012; Sprenger et al., 2018). Process-based simulation of isotopic trajectories has also been considered in larger-scale studies using land surface models (Haverd et al., 2011; Henderson-Sellers, 2006) where couplings with atmospheric isotopic circulation can be captured (Haese et al., 2013; Risi et al., 2016; Wong et al., 2017). While the simulation of energy budgets and biogeochemical cycles is increasingly detailed in these land surface models –sometimes including vegetation dynamics–, the hydrology has, however, remained somewhat simplistic ~~. These shortcomings in explicitly taking into account~~ (or even absent) regarding the simulation of lateral transfers as overland flow, shallow and deeper subsurface flows, and channel routing (Fan, 2015)~~make~~ . This makes it difficult to take advantage of isotope tracking to characterise the role of cascading downstream water redistribution in the spatial patterns of catchment functioning.

In parallel, isotopes have been used to explore water velocities, travel times and ages in catchments using analytical and conceptual models (e.g., Neal et al., 1988; Barnes and Bonell, 1996; Weiler et al., 2003; Sayama and McDonnell, 2009; Birkel et al., 2015; McGuire and McDonnell, 2015). These numerical tools allow testing hypotheses regarding how catchment storage relates to hydrological fluxes via mixing (or the relative absence thereof), and extending insights to spatio-temporal scales and variables inaccessible to current observation methods. An example of the latter is the estimation of water age, for which such models hold great promise (Dunn et al., 2007; McGuire and McDonnell, 2006; Sayama and McDonnell, 2009), with a more recent focus on the statistical properties of water transit time with time-varying and/or spatially-distributed conceptualizations (Botter et al., 2010; Birkel et al., 2012; Heidbüchel et al., 2012; Harman, 2015; Rinaldo et al., 2015; Benettin et al., 2017; Hesse et al., 2017). Additionally, the distinct information content of tracer observations, compared to more traditional hydrometric data, dictates that the integration of the two offers a strong hypothesis-testing framework for catchment model development (Uhlenbrook and Sieber, 2005; Fenicia et al., 2008; McDonnell and Beven, 2014). This opportunity is reinforced by decreasing costs of stable isotope analysis, now allowing for collection of daily (or more frequent) time series over several years (Kirchner and Neal, 2013) to inform simulations.

Yet, applications of a velocity-celerity framework in model-data fusion for catchment-scale hydrology remains relatively rare (Birkel and Soulsby, 2015). Such studies are urgently needed at this scale where the emphasis is mainly on the characterization of water pathways from precipitation to streamflow generation and/or evaporative losses. Recent efforts have nonetheless provided insights, either into whole-catchment dynamics with conceptual rainfall-runoff models (Birkel et al., 2011; Stadnyk et al., 2013; Hrachowitz et al., 2013; van Huijgevoort et al., 2016; Smith et al., 2016; Ala-aho et al., 2017; Knighton et al., 2017); or at finer detail (Soulsby et al., 2015) and using process-based 2-D hillslope models (Windhorst et al., 2014). We argue that extending tracer-aided approaches to physically-based models could resolve both intra- and whole-catchment dynamics of stable water isotopes and bridge perspectives at multiple and process-specific scales, as ~~largely~~ recently shown in hydrometric-based studies (e.g., Endrizzi et al., 2014; Pierini et al., 2014; Niu and Phanikumar, 2015; Manoli et al., 2017). This process-oriented characterisation could also include non-conservative isotope behaviour such as evaporative fractionation, whereby ~~water with~~ lighter isotopes (^{1}H and ^{16}O) preferentially ~~evaporates~~ evaporate (Gat, 1996), and whose impact on downstream water signatures has been highlighted even in energy-limited landscapes (Sprenger et al., 2017a). Birkel et al. (2014) and Knighton et al. (2017) are amongst the rare attempts to include fractionation in catchment-scale studies, albeit with conceptual rainfall-runoff models. Investigation of internal catchment heterogeneity, marked in some geographical settings (Tetzlaff et al., 2013), is facilitated by spatially-distributed resolutions of the catchment domain. In previous tracer-aided catchment modelling however, this aspect is either indirectly considered – e.g., a semi-distributed separation of non-saturated/saturated domains (Birkel et al., 2015) – or simply absent. Where spatial distribution has been taken into account in the model structure (van Huijgevoort et al., 2016; Ala-aho et al., 2017), fractionation processes were not included.

Finally, plants dynamically modulate ~~evaporative losses (ET~~terrestrial evaporation (E) – green water, *sensu* Falkenmark and Rockström (2006) – in the landscape water balance. This crucially drives the partitioning between soil evaporation (E_s), evaporation of canopy-intercepted water (E_c), and plant transpiration (~~T~~E_t). The two former pathways can result in evaporative fractionation, and root uptake for transpiration is usually considered non-fractionating (e.g., Wershaw et al., 1966; Dawson and Ehleringer, 1991; Harwood et al., 1999), although whether this is the case has recently been subject of debate (Lin and da SL Sternberg, 1993; Zhao et al., 2016; Vargas et al., 2017). While these different isotopic dynamics are of key importance in disentangling ecohydrological couplings in tracer-aided modelling, previous approaches generally lack a process-based conceptualisation of vegetation. Knighton et al. (2017) separately distinguished ~~T from other ET~~ E_t from other E components in catchment-wide isotopic model-data fusion. However, their spatially-lumped approach was parsimonious, using empirical partitioning of potential evapotranspiration which has high uncertainty in natural ecosystems (Kool et al., 2014).

Here, we implement isotope and age tracking in the physically-based, fully-distributed model EcH_2O (Maneta and Silverman, 2013). Notably, this model This model was chosen because it provides a physically-based, yet computationally-efficient representation of energy-water-ecosystem couplings where intra-catchment connectivity (both vertical and lateral) is explicitly resolved. In addition, EcH_2O separately solves the energy balance at the top of the canopy and at the soil surface, allowing a process-based separation of soil evaporation, transpiration, and canopy evaporationE_s, E_t, and E_c. The novel isotopic and age tracking module is designed in a fashion manner directly consistent with the original model structure, assuming full mixing in each model compartment, and with very limited empirical crucially without catchment-specific parameterization. The critical conceptualisation of evaporation fractionation uses the well-known Craig-Gordon approach (Craig and Gordon, 1965). The

We ask the following questions:

- To what extent can a hydrometrically-calibrated, physically-based hydrologic model correctly reproduce internal catchment dynamics of isotopes?
- What are the limitations of these isotopic simulations? Do they relate to the underlying model physics and/or to the tracking approach adopted?
- How useful and transferrable is this model framework for simulating spatio-temporal patterns of isotopes and water ages?

These questions are here addressed by testing the new tracer-enhanced model (EcH_2O-iso) is tested , Sect. 2) in a small, low-energy montane catchment where, in addition to (Sect. 3). This site has previously been modelled applying EcH_2O for calibration, using multiple datasets of long-term ecohydrological fluxes and storage variables (Kuppel et al., 2018). We take advantage of this earlier work as a reference ensemble of calibrated model parameterizations, and no additional isotopic calibration is conducted. In addition to using long-term, high resolution isotopic datasets for rainfall and runoff (^2H and ^{18}O), we assess the spatio-temporal variation variations of model-data agreement in soil water, groundwater, and plant xylem . Crucially, no isotopic calibration is conducted. The site has previously been modelled aplying EcH_2O for calibration, using multiple datasets of ecohydrological fluxes and storage variables (Kuppel et al., 2018). We ask the following questions: *1)* To what extent can a hydrometrically-calibrated, physically-based hydrologic model correctly reproduce internal catchment dynamics of isotopes? *2)* What are the limitations of these isotopic simulations? Do they relate to the physics and /or to mixing assumptions? *3)* What are the implications and opportunities for simulating spatio-temporal patterns of isotopes and water ages? at different locations (Sect 4.1). Following this generic evaluation, the model is used to infer seasonally-varying patterns of water fluxes and isotopes signatures (Sect. 4.2), and water age (Sect. 4.3). Model strengths and weaknesses, insights in processes and potential ways forward are discussed in Sect. 5, before drawing conclusions in Sect. 6.

2 Model description

2.1 Presentation of the The EcH$_2$O model

The ecohydrological model EcH$_2$O combines a land surface module for calculating vertical energy balances (canopy and understory), with a kinematic-wave-based scheme for lateral and vertical water transfers, while vegetation productivity, allocation and growth is derived from plant transpiration (Maneta and Silverman, 2013). Energy fluxes, water fluxes and storage, and vegetation state are explicitly coupled to capture the feedbacks between ecosystem productivity, hydrology and local climate, at time steps larger or equal to that of the meteorological inputs (precipitation P, incoming longwave and shortwave solar radiation, air temperature T_a (maximum, average, and minimum), relative humidity, and wind speed). In addition, the flexible definition of the spatial domain in EcH$_2$O allows for applications at a range of scales: from the plot (Maneta and Silverman, 2013), to small catchments (1-10 km^2 – Lozano-Parra et al., 2014; Kuppel et al., 2018), to larger watersheds (10^2-10^3 km^2 – Maneta and Silverman, 2013 Despite some potential limitations due to the absence of diffusion-driven water redistribution or an explicit biogeochemical cycle providing ecosystem respiration, the model yielded satisfactory results and insights across the diversity of climatic settings (semiarid to humid) and scientific foci (e.g., water balance, energy balance, or plant hydraulics) covered by the aforementioned studies. A comprehensive description of the model EcH$_2$O can be found in (Maneta and Silverman, 2013), and subsequent developments in ? Lozano-Parra et al. (2014) and Kuppel et al. (2018).

We provide here a brief step-wise overview, focused on the different hydrological compartments and transfers simulated in EcH$_2$O at the grid cell level (Fig. 1). For each vegetation cover present in a grid cell, a linear bucket approach is used for canopy interception. The capacity-excess P (i.e., throughfall) is below-canopy throughfall) and P over bare soil are partitioned between liquid and snow components using for each time step a snow-rain temperature threshold (fixed to 2°C) together with the minimum and maximum air temperature , together with a snow-rain temperature thresholdat each time step. The canopy energy balance then separately yields plant transpiration from canopy conductance, (E_t) and evaporation of intercepted water . Infiltration of liquid throughfall in the topsoil (E_c). The calculation of E_t uses, for each vegetation type, the canopy conductance at each time step based on a Jarvis-type multiplicative model accounting for environmental limitations from incoming solar radiation, T_a, vapor pressure deficit at the leaf surface, and soil water potential (see Maneta and Silverman (2013) and Appendices in Kuppel et al. (2018) for a more detailed description). Infiltration of surface water in the top soil layer is computed using a Green and Ampt approximation of Richard's equation. Subsequent soil water content above field capacity (gravitational water) percolates to the underlying soil layers, with fixed bedrock seepage – out of the system – as a lower boundary condition (Fig. 1). Soil evaporation (limited to the topsoiltop soil layer) and snowmelt (resulting in surface ponding, Fig. 1) under each vegetation type are calculated by solving the energy balance at the surface(soil or snowpack). Following a local drainage direction derived from the input elevation map, lateral water routing is simulated at three levels: in the deepest soil layer, groundwater seeps in the channel (if present) while the remainder is transferred laterally using a 1D kinematic wave, and can result in saturation return flow in downstream cells. All remaining ponded water becomes overland flow; reinfiltrating further downstream or running off until it reaches an outlet or a cell within the stream network; stream water routing is also computed within a 1D kinematic wave approximation.

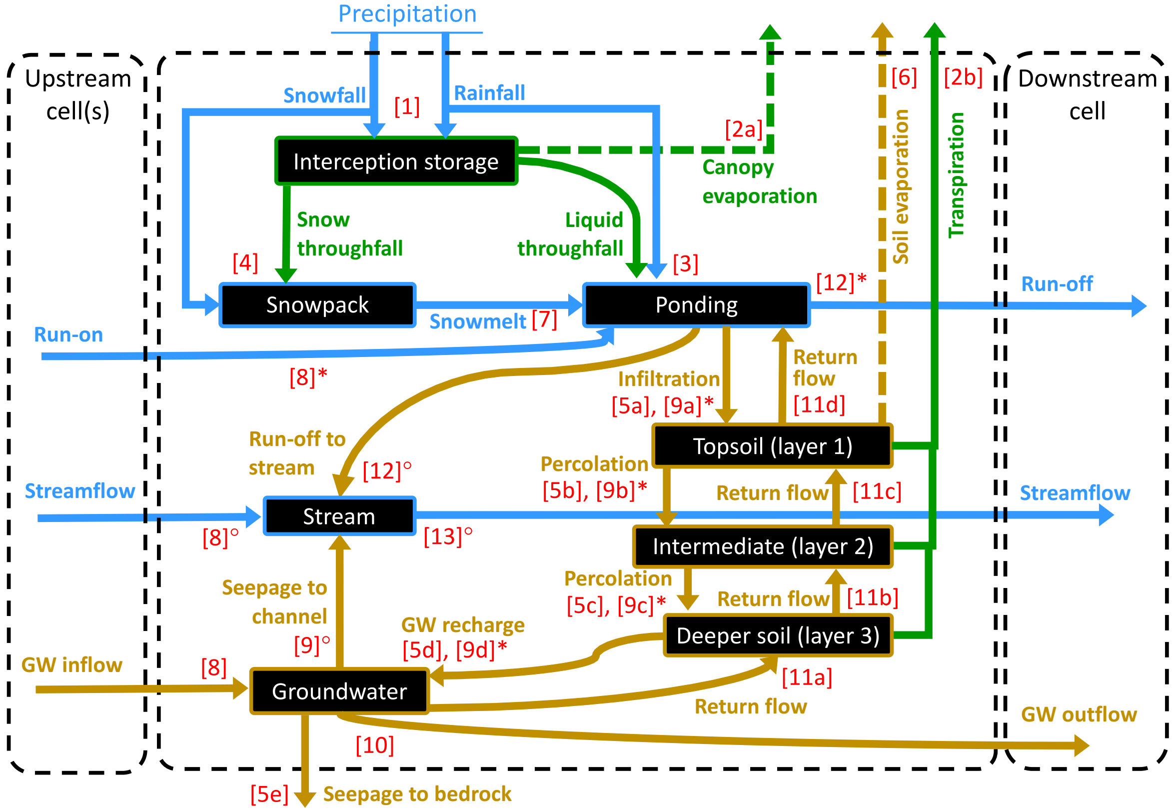

Figure 1. Water compartments (black rectangles) and fluxes (coloured arrows) as represented in EcH_2O, with the dashed arrows indicating processes where isotopic fractionation is simulated. The numbers between brackets reflect the sequence of calculation within a time step. Note that water routing (steps [8] to [13]) differs between cells where a stream is present (○) or not (∗).

~~Water compartments (black rectangles) and fluxes (coloured arrows) as represented in EcH_2O, with the numbers between brackets reflecting the sequence of calculation within a time step. Note that water routing (steps 8to 13) differs between cells where a stream is present (○) or not (∗).~~

2.2 Implementation of isotopic and age mixing

The conceptualization of water mixing equally applies for all the tracked quantities implemented in the model (isotopes and age), so that a generic notation C is in this section used to designate both isotopic tracer composition (^{2}H and ^{18}O) and water age. The only ~~specificities~~ specific conceptualisation of isotope dynamics in EcH_2O-iso relates to fractionation (see Sect. 2.3), while precipitation inputs have a fixed age of zero and the water age in all compartments is ~~incremented~~ increased at the end of each simulation time step by the length of the latter. The delta notation (δ) for isotopic composition quantifies, for a given water sample, the difference in the mass ratio of heavy to light isotopes (R) as compared to the Vienna Standard Mean Ocean Water (VSMOW): $\delta = \left(\frac{R_{sample}}{R_{VSMOW}} - 1\right) \times 10^3$ $\delta = \left(\frac{R_{\text{sample}}}{R_{\text{VSMOW}}} - 1\right) \times 10^3$. First, the instantaneous mass balance for water signature is:

$$\frac{d\left(V_{res}C_{res}\right)}{dt} \frac{d\left(V_{\text{res}}C_{\text{res}}\right)}{dt} = \sum_{k=1}^{N_{in}\, N_{\text{in}}} q_{in,k\,\text{in},k} C_{in,k\,\text{in},k} - q_{out\,\text{out}} C_{res\,\text{res}} \tag{1}$$

where V_{res} and C_{res} V_{res} and C_{res} are, respectively, the volume and signature (δ^2H , $\delta^{18}O$, or age) of the water in the reservoir, t is time, q_{out} q_{out} is the flux of water exiting the reservoir, and $q_{in,k}$ and $C_{in,k}$ $q_{\text{in},k}$ and $C_{\text{in},k}$ are, respectively, the flux and signature of water entering the reservoir from each the N_{in} N_{in} adjacent upstream locations. An implicit first-order finite-difference scheme is used to compute mixing during a given time interval Δt :

$$V_{res\,\text{res}}{}^{t+\Delta t} C_{res\,\text{res}}{}^{t+\Delta t} - V_{res\,\text{res}}{}^{t} C_{res\,\text{res}}{}^{t} = \left(\sum_{k=1}^{N_{in}\, N_{\text{in}}} q_{in,k\,\text{in},k} C_{in,k\,\text{in},k}{}^{t+\Delta t} - q_{out\,\text{out}} C_{res\,\text{res}}{}^{t+\Delta t}\right) \cdot \Delta t, \tag{2}$$

where $V_{res}^{t+\Delta t}$ and $C_{res}^{t+\Delta t}$ $V_{\text{res}}^{t+\Delta t}$ and $C_{\text{res}}^{t+\Delta t}$ are, respectively, the volume and water signature in the reservoir after mixing, V_{res}^t and C_{res}^t V_{res}^t and C_{res}^t are the volume and water signature in the reservoir before mixing, $C_{in,k}^{t+\Delta t}$ and $C_{\text{in},k}^{t+\Delta t}$ is the signature of the k-th input source after mixing in the latter(following the implicit approach), and Δt is the time step. Replacing $V_{res}^{t+\Delta t}$ by $V_{res}^t + \left(\sum_{k=1}^{N_{in}} q_{in,k} - q_{out}\right) \cdot \Delta t$. Replacing $V_{\text{res}}^{t+\Delta t}$ by $V_{\text{res}}^t + \left(\sum_{k=1}^{N_{\text{in}}} q_{\text{in},k} - q_{\text{out}}\right) \cdot \Delta t$ in Eq. (2) finally yields:

$$C_{res\,\text{res}}{}^{t+\Delta t} = \frac{V_{res}^t C_{res}^t + \left(\sum_{k=1}^{N_{in}} q_{in,k} C_{in,k}^{t+\Delta t}\right)\Delta t}{V_{res}^t + \left(\sum_{k=1}^{N_{in}} q_{in,k}\right)\Delta t} \frac{V_{\text{res}}^t C_{\text{res}}^t + \left(\sum_{k=1}^{N_{\text{in}}} q_{\text{in},k} C_{\text{in},k}^{t+\Delta t}\right)\Delta t}{V_{\text{res}}^t + \left(\sum_{k=1}^{N_{\text{in}}} q_{\text{in},k}\right)\Delta t}. \tag{3}$$

In practice, Eq. (3) is applied in EcH$_2$O-iso at every sub-time step where water transfers are computed, in the sequence shown in Fig. 1. Note that $C_{res}^{t+\Delta t}$ $C_{\text{res}}^{t+\Delta t}$ in Eq. (3) only depends on the magnitude of the summed incoming flux $\sum_{k=1}^{N_{in}} q_{in,k}$ $\sum_{k=1}^{N_{\text{in}}} q_{\text{in},k}$. Flow to the downstream cell is fully mixed – right-hand terms of Eq. (2). Full mixing was used as a simplifying approximation because this model is to be first evaluated in a wet environment (Tetzlaff et al., 2014; Sprenger et al., 2017a) with relatively long time steps (i.e. daily, see Sect. 3.3). Note that because of its representation of a single, fully-mixed pool in each soil layer, EcH$_2$O-iso essentially provides bulk water values for isotopic content and water age. This needs to be kept in mind when comparing the simulations with soil isotopic datasets (see Sect. 3.2 and Sect. 4) and for the discussion (Sect. 5).

One exception to immediate mixing is the snowpack, where the snowmelt flux (q_{out}^{melt}) ($q_{\text{out}}^{\text{melt}}$) is assumed to tap first into the snow throughfall of the same day (q_{in}^{snow} time step ($q_{\text{in}}^{\text{snow}}$) if present, before mobilizing mobilising older snow, fully mixed in the snowpack. Consequently, the signatures of the snowpack ($C_{pack}^{t+\Delta t}$ $C_{\text{pack}}^{t+\Delta t}$) and snowmelt water ($C_{melt}^{t+\Delta t}$ $C_{\text{melt}}^{t+\Delta t}$) which goes into the surface reservoir in EcH$_2$O-iso at step 7 (Fig. 1) are calculated as follows:

$$C_{pack\,\text{pack}}{}^{t+\Delta t} = \frac{V_{pack}^t C_{pack}^t + max\left(0, q_{in}^{snow} - q_{out}^{melt}\right) C_{rain}^{t+\Delta t}\Delta t}{V_{pack}^t + max\left(0, q_{in}^{snow} - q_{out}^{melt}\right)\Delta t} \frac{V_{\text{pack}}^t C_{\text{pack}}^t + \max\left(0, q_{\text{in}}^{\text{snow}} - q_{\text{out}}^{\text{melt}}\right) C_{\text{rain}}^{t+\Delta t}\Delta t}{V_{\text{pack}}^t + \max\left(0, q_{\text{in}}^{\text{snow}} - q_{\text{out}}^{\text{melt}}\right)\Delta t} \tag{4}$$

$$C_{melt\,\text{melt}}{}^{t+\Delta t} = \frac{max\left(0, q_{out}^{melt} - q_{in}^{snow}\right) C_{pack}^{t+\Delta t} + q_{in}^{snow} C_{rain}^{t+\Delta t}}{max\left(q_{in}^{snow}, q_{out}^{melt}\right)} \frac{\max\left(0, q_{\text{out}}^{\text{melt}} - q_{\text{in}}^{\text{snow}}\right) C_{\text{pack}}^{t+\Delta t} + q_{\text{in}}^{\text{snow}} C_{\text{rain}}^{t+\Delta t}}{\max\left(q_{\text{in}}^{\text{snow}}, q_{\text{out}}^{\text{melt}}\right)} \tag{5}$$

~~No spill-over of canopy-intercepted water is simulated in this bucket-type approach of~~ Only the same-time-step precipitation can contribute to throughfall in the EcH$_2$O model, whenever the resulting canopy storage exceeds the maximum canopy storage capacity (Maneta and Silverman, 2013), the latter being constant in our simulations. As a result, ~~intercepted water~~ all intercepted water eventually evaporates from the canopy and does not interact with the surface/subsurface. Therefore, throughfall water (liquid and snow) is assumed to have the isotopic composition of same-time-step precipitation and age zero. This simplification is reasonable for our study site where vegetation interception has only a trivial effect on the isotopic partitioning of rainwater (Soulsby et al., 2017), yet further developments could be implemented for model application in different eco-climatic settings.

Finally, transpiration is considered as a non-fractionating process. This is based on previous work (Wershaw et al., 1966; Dawson and Ehleringer, 1991; Harwood et al., 1999), and the fact that non-steady state effects cancel out at the daily time-step (Farquhar et al., 2007). However, this simple conceptualisation is increasingly questioned (Lin and da SL Sternberg, 1993; Zhao et al., 2016; Vargas et al., 2017), and the implications for our study will be discussed later. Here, during the canopy energy balance (step [2] in Fig. 1), the signature of transpired water ~~C_T~~ $C_{\mathrm{E_t}}$ is taken as the weighted sum of the signature in the three soil layers:

$$C_{\sout{T}\mathrm{E_t}} = f_{\sout{L1}\mathrm{L1}} C_{\sout{soilL1}\mathrm{soilL1}} + f_{\sout{L2}\mathrm{L2}} C_{\sout{soilL2}\mathrm{soilL2}} + f_{\sout{L3}\mathrm{L3}} C_{\sout{soilL3}\mathrm{soilL3}}, \quad (6)$$

where ~~f_{L1}, f_{L2}, and f_{L3}~~ f_{L1}, f_{L2}, and f_{L3} are the respective fractions of roots in each layer, as described in Eq. (A8) in Kuppel et al. (2018).

2.3 Isotopic fractionation from soil evaporation

The change in isotopic composition of the first soil layer during soil evaporation (step [6] in Fig. 1) is simulated using the Craig-Gordon model Craig and Gordon (1965); Gat (1995), without any empirical parameterization specific to our study. In this section, generically refers to the standardized isotopic ratio in for either ^{2}H or ^{18}O. For each time step t:

$$\delta_{\sout{soilL1}\mathrm{soilL1}}{}^{t+\Delta t} = \delta^* - \left(\delta^* - \delta_{\sout{soilL1}\mathrm{soilL1}}{}^{t}\right) f^m, \quad (7)$$

where f is the remaining fraction of water after evaporation (~~$f = V^{t+\Delta t}_{soilL1} / V^t_{soil}$~~ $f = V^{t+\Delta t}_{\mathrm{soilL1}} / V^t_{\mathrm{soilL1}}$), while δ^* is the limiting isotopic composition given the local atmospheric conditions in ‰(Gat and Levy, 1978) and m is the dimensionless enrichment slope (Welhan and Fritz, 1977; Allison and Leaney, 1982). Their formulation is generalized following Good et al. (2014):

$$\delta^* = \sout{\frac{h_a\delta_a + h_s\cdot\varepsilon^+ + \varepsilon_k}{h_a - (h_s\cdot\varepsilon^+ + \varepsilon_k)\cdot 10^{-3}}} \frac{h_\mathrm{a}\delta_\mathrm{a} + h_\mathrm{s}\cdot\varepsilon^+ + \varepsilon_\mathrm{k}}{h_\mathrm{a} - (h_\mathrm{s}\cdot\varepsilon^+ + \varepsilon_\mathrm{k})\cdot 10^{-3}} \quad (8)$$

$$m = \sout{\frac{h_a - (h_s\cdot\varepsilon^+ + \varepsilon_k)\cdot 10^{-3}}{h_s - h_a + \varepsilon_k\cdot 10^{-3}}} \frac{h_\mathrm{a} - (h_\mathrm{s}\cdot\varepsilon^+ + \varepsilon_\mathrm{k})\cdot 10^{-3}}{h_\mathrm{s} - h_\mathrm{a} + \varepsilon_\mathrm{k}\cdot 10^{-3}} \quad (9)$$

The different terms in Eqs. (8) and (9) are sequentially defined as follows:

- δ_a δ_{a} is the stable isotope composition of the ambient air moisture in ‰, derived from that of the precipitation by assuming isotopic equilibrium Gat (1995); Gibson and Reid (2014):

$$\delta_{a\mathrm{a}} = \frac{\delta_{rain} - \varepsilon^+}{\alpha^+} \frac{\delta_{\mathrm{rain}} - \varepsilon^+}{\alpha^+} \tag{10}$$

- ε^+ is a factor (in ‰) derived from the equilibrium fractionation α^+ of water between the liquid and vapour phases (Skrzypek et al., 2015):

$$\varepsilon^+ = \left(1 - 1/\alpha^+\right) \cdot 10^3 \approx \left(\alpha^+ - 1\right) \cdot 10^3, \tag{11}$$

with α^+ taken as temperature-dependent following Horita and Wesolowski (1994), here using the air temperature T_a : T_{a} :

$$10^3 \cdot \ln \alpha^+_{^2H} = \frac{1158.8}{10^9} \cdot T_{a\mathrm{a}}{}^3 - \frac{1620.1}{10^6} \cdot T_{a\mathrm{a}}{}^2 - \frac{794.84}{10^3} \cdot T_{a\mathrm{a}} - 161.04 + \frac{2.9992}{T_a^3} \frac{2.9992}{T_{\mathrm{a}}^3} \cdot 10^9 \tag{12}$$

$$10^3 \cdot \ln \alpha^+_{^{18}O} = -7.685 + \frac{6.7123}{T_a} \frac{6.7123}{T_{\mathrm{a}}} \cdot 10^3 - \frac{1.6664}{T_a^2} \frac{1.6664}{T_{\mathrm{a}}^2} \cdot 10^6 + \frac{0.35041}{T_a^3} \frac{0.35041}{T_{\mathrm{a}}^3} \cdot 10^9 \tag{13}$$

- ε_k ε_{k} accounts for the diffusion-controlled fractionation in air (Craig and Gordon, 1965):

$$\varepsilon_{k\mathrm{k}} = \left(h_{s\mathrm{s}} - h_{a\mathrm{a}}\right) \cdot n \cdot \left(1 - \frac{D_i}{D}\right), \tag{14}$$

where D_i/D is the diffusivity ratio of the gaseous water molecules bearing an isotope *i* to that of lighter isotopic water. We use literature values given by Vogt (1976), as suggested in Horita et al. (2008): 0.9877 for $D_{^1H^2HO}/D_{H_2O}$ and 0.9859 for $D_{H_2^{18}O}/D_{H_2^{16}O}$.

- n translates the dominant mode of transport of water molecule at the surface. We adopted a time-varying formulation taking into account soil water content θ (Braud et al., 2005; Mathieu and Bariac, 1996):

$$n = 1 - 0.5 \cdot \frac{(\theta - \theta_r)}{\phi - \theta_r} \frac{(\theta - \theta_{\mathrm{r}})}{\phi - \theta_{\mathrm{r}}} \tag{15}$$

where ϕ and θ_r θ_{r} are, respectively, the soil porosity and residual water content. n increases from 0.5 in a saturated soil to 1 for a dry soil where diffusion is the dominant mode of transport.

- h_a h_{a} is the relative humidity of the atmosphere (measured at the weather stations, see Sect. 3.2) after being normalized to the saturated vapor pressure e^* at the soil surface (Gat, 1995):

$$h_{a\mathrm{a}} = h_{a,measured\,\mathrm{a,measured}} \cdot \frac{e^*(T_a)}{e^*(T_s)} \frac{e^*(T_{\mathrm{a}})}{e^*(T_{\mathrm{s}})}, \tag{16}$$

where the surface temperature T_s T_{s} is given at each time step from solving the surface energy balance equation (Maneta and Silverman, 2013).

- Finally, h_s h_s is the relative humidity of the air of the soil pores, following the formulation of soil evaporation flux E E_s in EcH_2O (Eqs. 9-10 in Maneta and Silverman, 2013):

$$h_{ss} = \beta + (1-\beta)\cdot h_{aa}, \tag{17}$$

where β is adjusted as a growing function of the volumetric water content θ , equal to 1 whenever θ is superior or equal to field capacity θ_{fc} (Lee and Pielke, 1992):

$$\beta = min\,\mathrm{min}\left(1, \frac{1}{4}\left[1 - cos\frac{\theta}{\theta_{fc}}\frac{\theta}{\theta_{\mathrm{fc}}}\pi\right]^2\right). \tag{18}$$

3 Data and methods

3.1 Study site

Simulations were conducted for the Bruntland Burn (BB) catchment in the Scottish Highlands (57°8'N 3°20'W) (Fig. 2a-b). It is a small (3.2 km^2) headwater catchment of the Dee, a major Scottish river providing freshwater resources for 250,000 people in the Aberdeen urban area, having EU conservation designations, and hosting ecosystem services (e.g., Atlantic salmon fishery). Annual precipitation averages around 1000 mm, with a mild seasonal cycle (Fig 2c). The water balance is energy-limited, given the northern latitude, with 400 mm of annual potential evapotranspiration (PET) evapotranspiration with pronounced seasonality in daily losses: from 0.5 mm in winter to 4 mm in summer (Birkel et al., 2011). Mean annual temperature is 7°C and no monthly-averaged temperatures fall below 0°C, the climate qualifies as temperate to boreal oceanic; less than 5% of precipitation usually occurs as snowfall.

The topography of the BB reflects glacier retreat, with elevation ranging from 220 m.a.s.l in the wide valley bottom to 560 m.a.s.l on above the steeper slopes (Fig. 2a). Glacial drift deposits cover 60-70% of the catchment bedrock (granite, schist and other meta-sediments) and forms the dominant soil parent material (Soulsby et al., 2007). Mostly saturated, these deposits are important reservoirs of groundwater, sustaining base flows in the stream and maintaining persistent wet conditions across the valley bottom (Soulsby et al., 2016). Thin regosols (rankers) dominate the pedology of the catchment above 400 m.a.s.l., where drift deposits are marginal (Fig. 2a). Freely-draining shallow podzols (<0.7 m deep) dominate steeper hillslopes, overlying moraines and marginal ice deposits. Finally, deep (>1 m) soils with high organic matter content (histosols: peat and gley) characterize the riparian area (Fig. 2a). The histosols are saturated most of the time, so that rainfall events generate runoff mostly via rapid saturation overland flow, with a surface connectivity in the podzols limited to the wettest periods (Tetzlaff et al., 2014). Spatial patterns of land cover reflect these hydropedological units (Fig. 2b). Heather shrublands (*Calluna vulgaris* and *Erica* spp.) are the dominant cover over podzols and rankers. Such a land use results from red deer (*Cervus elaphus*) and sheep overgrazing, at the expense of naturally-occurring Scots pine trees (*Pinus sylvestris L.*), which are now mostly found in the steep sections of the northern hillslopes and in the plantation areas neighbouring the stream outlet. Finally, grasses (*Molinia caerulea*) cover the riparian gley soils, while the peat is dominated by bog mosses (*Sphagnum spp.*).

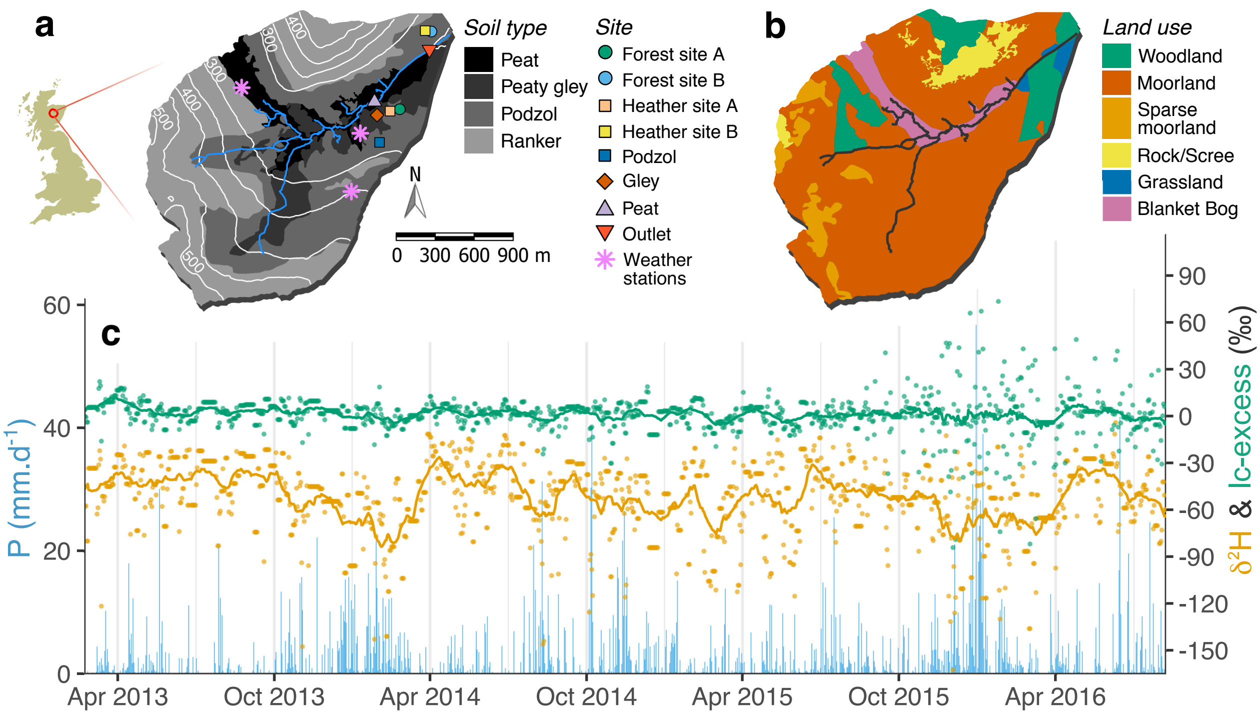

Figure 2. Bruntland Burn catchment characteristics, showing **(a)** topography, soil cover as derived from the Hydrology of Soil Types (HOST) classification types, stream network, and measurements sites locations, and **(b)** land use type. **(c)** Time series of measured precipitation amount (blue bars, daily) and isotopic signatures, δ^2H (orange) and lc-excess (green), showing daily values (dots) and the 30-day running mean (solid lines).

3.2 Datasets

We used the wealth of diverse and often multi-year time series available at different locations in the BB catchment (Fig. 2a). These measurements capture numerous ecohydrological processes and observables, used either for model inputs, or calibration/evaluation of simulations (Table 1). A brief description follows.

3.2.1 Isotopic measurements

At the catchment outlet, rainfall and stream water have been sampled daily for isotope analysis from June 2011 to the present, providing an isotope time series of unusual high frequency and longevity. Samples have been collected using an ISCO 3700 automatic sampler (Teledyne Isco, Lincoln, USA). The auto-sampler bottles were emptied at fortnightly frequency or higher, while paraffin was added to each bottle to prevent evaporation.

Stable isotope measurements in the soil fall into two categories, differing in the sampling method and time period. Between 2011 and 2013, soil water was extracted at 0.1, 0.3, and 0.5 m ~~depth~~ depths at four locations: Peat, Gley, and Podzol sites (weekly), and Forest site A (fortnightly) (Fig. 2a). Since MacroRhizon suction lysimeters were used (Rhizosphere Research

Table 1. Local datasets used in this study, grouped by location and purpose: model evaluation (■), model calibration (▲), and model inputs (♦). For soil isotopes, [a] and [b] respectively indicate suction-lysimetric sampling (2013) and direct equilibration from soil sampling (2015-2016). Other notations: Srf – surface water, GW – groundwater, P – precipitation, SWC – soil water content, ~~Tp~~ E_t – transpiration, NR – net radiation, ∗ – relative air humidity, precipitation, air temperature, and wind speed, • – synoptic collection campaign at 92 to 94 locations (see text).

	Water isotopes						Water fluxes & stores			Meteorology	
Locations	Soil	Srf	GW	Xylem	Stream	P	SWC	Pine ~~Tp~~ E_t	Discharge	NR	Other*
Forest site A	■ [a,b]			■				▲			
Forest site B	■ [b]			■			▲	▲			
Heather site A	■ [b]			■							
Heather site B	■ [b]			■							
Podzol	■ [a]		■				▲				
Gley	■ [a]		■				▲				
Peat	■ [a]		■				▲				
Riparian area•		■			■						
Outlet					■	♦			▲		
Weather stations										▲	♦

Products, Wageningen, Netherlands) (Tetzlaff et al., 2014), isotopic ~~characterization~~ characterisation represents the mobile water held under lower tensions (Sprenger et al., 2015). From September 2015 to August 2016, near-monthly soil water sampling was carried out at four ~~sites~~ locations (Forest sites A and B, and Heather sites A and B) using soil samples collected with a spade from four layers (~~0-0~~0–0.05, 0.05~~-0.1, 0.10~~–0.1, 0.1–0.15, and ~~015-0~~0.15–0.2 ~~.~~m) with five replicates for each. Isotopic analysis followed on water extracted by the direct equilibration method (Wassenaar et al., 2008), thus fully accounting for bulk pore water, as described by Sprenger et al. (2017a). Conceptually, the lysimeters can be viewed as sampling the "fast domain" of soil water held under low tension, whilst direct equilibration characterises the "bulk" soil water which also includes the "slow domain" of water held under higher tensions.

Groundwater samples were collected monthly between August 2015 and September 2016, at four wells (>1.6 m) covering a representative transect from the hillslope to valley bottom (Scheliga et al., 2017) encompassing the main hydropedological units; Peat (2 wells), Gley and Podzol sites (Fig. 2a). Vegetation xylem water was collected between ~~Autumn~~ autumn 2015 and ~~Spring-Summer~~ spring-summer 2016, using cryogenic extraction from Scots Pine xylem cores at 1.5 m height (Forest sites A and B) and from heather twigs (Heather sites A and B) (Fig. 2a). Sampling was made at near-monthly resolution (n = 7) with five replicas for each extraction (Geris et al., 2017). We also used isotopic measurements from a synoptic sampling campaign conducted in the drainage network of pools and channels across the valley bottom of the Bruntland Burn on 20th February (92 locations) and 24th May (94 locations) of the year 2013, covering contrasting catchment wetness states. On those days, water was also sampled along the perennial stream network at 10 locations (Lessels et al., 2016).

Air tight ~~vial~~ vials were used to store all water samples, which were kept refrigerated until they were analysed. The soil samples were equilibrated and extracted water analysed within a week of collection (Sprenger et al., 2017a). In both cases, stable isotopic composition was determined using Los Gatos laser isotope spectrometers (DLT-100 and OA-ICSO models; Los Gatos Research, Inc., San Jose, USA), with reported measurement uncertainties of 0.4 and <0.55 ‰(δ^2H), and 0.1 and <0.25 ‰(δ^{18}O), respectively.

3.2.2 Hydrometric and meteorological data

Daily soil moisture data was derived from 15-minute retrievals at four locations: three along the peat-gley-podzol transect presented in Sect. 3.2.1 (Tetzlaff et al., 2014), and in a Scots pine stand (Forest site B, Fig. 2a). Time domain reflectometry (TDR) soil moisture probes (Campbell Scientific, Inc. USA) were located at different depths (0.1, 0.3, and 0.5 m – only 0.1 and 0.3 m in the peat), and replicated $\sim$ 2 m apart. During two growing seasons, Scots pine transpiration was measured at Forest site A (July – September 2015) and at Forest site B (April – September 2016) (Fig. 2a), by installing Granier-type thermal dissipation sap flow sensors (Dynamax Inc., Houston, USA) on 10 and 14 trees, respectively. Depending on its stem diameter (10 to 32 cm), each tree had 2 to 4 sensors. At the end of each study period, incremental wood core sampling in surrounding trees provided sapwood-area-to-tree-diameter relationships, used to derive stand-scale transpiration estimates (Wang et al., 2017a), which were then daily averaged. At the catchment outlet (Fig. 2a), 15-minute stage height records (Odyssey capacitance probe, Christchurch, New Zealand) were used to generate daily discharge observations, with a rating curve previously calibrated for a stable stream section.

Finally, meteorological observations used as model inputs (P, ~~air temperature~~ T_a, relative humidity, and wind speed) and for calibration (net radiation) were primarily ~~measured~~ daily-averaged from 15-minutes measurements at the three meteorological stations ~~which were~~ installed at different landscape positions (valley bottom, bog, and hilltop, Fig. 2a) and operated from July 2014. Prior to that period, a square elevation inverse distance-weighted algorithm was applied to interpolate local precipitation values from five Scottish Environment Protection Agency (SEPA) rain gauges located within 10 km of the Bruntland Burn catchment ~~Birkel et al. (2011)~~(Birkel et al., 2011). Daily mean T_a, relative humidity and wind speed values were then available from the Centre for Environmental Data Analysis (CEDA) at the Balmoral station (5km NW) (Met Office, 2017). The ERA-Interim climate reanalysis dataset (Dee et al., 2011) was used to retrieve daily minimum and maximum T_a (prior to July 2014), and incoming ~~shortwave~~ solar and longwave radiation (whole study period). Finally, we applied altitudinal effects on P and T_a were accounted for: we applied a 5.5% increase of P every 100 m.a.s.l. (Ala-aho et al., 2017), and a 0.6°C decrease per 100 m.a.s.l, from the moist adiabatic temperature lapse rate (Goody and Yung, 1995).

3.3 Model set-up and calibration

The methodology closely follows the approach detailed in Kuppel et al. (2018). Here, we only provide a brief summary and highlight the modifications adopted for this study.

All simulations were performed on daily time steps, at a 100× 100 m^2 resolution. This choice of coarser grid cells – from 30× 30 m^2 in Kuppel et al. (2018) – was made to decrease computation time while preserving reasonable spatial variability across the catchment. The simulation period extends from February 2013 to August 2016, for which a continuous record of daily δ^2H and δ^{18}O in precipitation input was available (see Sect. 3.2.1). For all simulations a 3-year spin up period was added using the first three years of isotopic and climatic model inputs, as preliminary tests suggested this spin up was enough sensitivity tests combined with visual inspection of simulated hydrometric and isotopic time series at the location used in this study (see Sect. 3.2) indicated it was sufficient to remove transient dynamics.

Based on the soil classes defined by the Hydrology of Soil Types (HOST), four hydropedological units were defined (Fig. 2a) (Tetzlaff et al., 2007) to map soil hydrological properties in the modelled domain. Physical soil characteristics relating to the energy balance were considered as uniform across the catchment, similar to Kuppel et al. (2018) (see Table S1 therein). Land cover was divided into five classes, four of them vegetated: Scots pine, heather shrubs, peat moss, and grasslands. From extensive land use mapping (Fig. 2b), the cover fraction of each vegetation type was estimated by combining 1× 1 m^2-resolution LiDAR canopy cover measurements (Lessels et al., 2016), aerial imagery and typical vegetation patterns in the different soil units (Tetzlaff et al., 2007; Kuppel et al., 2018). In addition, we took into account occurrence of exposed rock by fixing As in Kuppel et al. (2018), the dynamic vegetation allocation module is switched off, so that leaf area index remains equal to initial values of 2.9, 1.6, 3.5, and 2 m^2.m^{-2} for Scots pines, heather shrubs, peat moss and grasslands, respectively (Albrektson, 1984; Calder et al., 1984; Bond-Lamberty and Gower, 2007; Moors et al., 1998). To avoid an overestimation of local soil evaporation and resulting isotopic fractionation in grid cells of exposed rock/scree, for simplicity we fixed the depth of the first soil layer to 0.001 m to limit soil evaporation wherever the fraction of bare soil was larger than 0.5 – after performing a sensitivity analysis showing little effect on catchment water balance and downstream isotopic budgets.

Finally, the calibrated model parameters (Table S1), and associated sampling ranges, are those presented in Kuppel et al. (2018). The parameter space was sampled using a uniform Monte-Carlo approach. The corresponding 150,000 simulations were constrained by simultaneously using jointly constrained combining measurements of stream discharge, soil moisture (4 sites), pine transpiration E_t (2 sites) and net radiation (3 sites) over the whole simulations period. (Table 1) whenever the observation periods overlapped with the current simulations (Feb 2013 – Aug 2016, Fig. S1). For soil moisture observations, a b-spline curve was fitted to the measured profile (to account for non-monotonic variations) on each sampling date, followed by a vertical integration. It enabled a consistent comparison against simulations in each of the upper two hydrological layers of EcH_2O (cf. Fig. 1), while profile-averaged values were used for calibration in Kuppel et al. (2018). Constraints were combined in a multi-criteria objective function based on the cumulative distribution functions (CDF) of dataset-specific goodness-of-fit (GOF) (Ala-aho et al., 2017): mean absolute error for stream discharge and root mean square error for all others observations. This method allows retention of model parameter sets that give most behavioural simulations *simultaneously* across different variables (Kuppel et al., 2018). We retained the 30 “best” of these parameterizations as a testbed for ensemble simulations of stable water isotopes and water age dynamics presented in this study.

3.4 Analysis

Daily, seasonal and inter-annual climate variability results result in changing isotopic composition of precipitation inputs. Equilibrium isotopic fractionation processes result in a strong correlation between rainfall δ^2H and $\delta\,^{18}$O across the globe, defining a global meteoric water line (GMWL, Dansgaard, 1964). At the BB catchment, there is a seasonal trend of more enriched values in summer and depleted in winter (e.g. Fig. 2c). A local meteoric water line (LMWL) was defined, using daily values from February 2013 to August 2016 and weighting by precipitation inputs ($r^2 = 0.96$, $p < 0.001$):

$$\delta^2 H = 7.8 \cdot \delta^{18} O + 4.9. \tag{19}$$

The line-conditioned excess (hereafter, lc-excess) was defined as the residual from the LMWL (Landwehr and Coplen, 2006):

$$lc-excess\text{lc-excess} = \delta^2 H - a_{LMWL\,\mathrm{LMWL}} \cdot \delta^{18} O - b_{LMWL\,\mathrm{LMWL}}, \tag{20}$$

with a_{LMWL} = 7.8, b_{LMWL} = 4.9 ‰(Eq. 1920). As oxygen has a higher atomic weight, non-equilibrium fractionation during the liquid-to-vapour phase change will preferentially evaporate (in terms of statistical expectation) $^1H^2H^{16}O$ molecules rather than the heavy isotopologue $^1H_2{}^{18}O$ (Craig et al., 1963). The isotopic signature of a water sample affected by evaporation thus shows negative lc-excess values, as δ ^{18}O in non-evaporated water enriches faster than δ^2H, and plots under the LMWL in the dual-isotope space (Landwehr et al., 2014). For these reasons, we preferred combining δ^2H and lc-excess in our analysis (over separately looking at both δ^2H and δ ^{18}O), to simultaneously highlight absolute isotopic dynamics and evaporative fractionation. Note that lc-excess was also preferred over the oft-used deuterium-excess, which translates the deviation of δ^2H from the GMWL (Dansgaard, 1964). While the two quantities are mathematically similar, lc-excess displays much smaller seasonal dynamics from the near-0 ‰value of precipitation inputs, thus it advantageously allows separation of fractionation impacts from overall isotopes dynamics (Sprenger et al., 2017a).

Similar to soil moisture observations, measured and simulated isotopic values in the soil are conceptually different: datasets are collected at specific depths (see Sect. 3.2.1), whilst model outputs provide average values for the different hydrological layers (Fig. 1). While original quantities were preserved for temporal analysis of the results, we additionally provided a formal quantification of model-data agreement. To do so, we reconstructed layer-integrated isotopic datasets at each soil sampling site, following the same interpolation-integration methodology used for soil moisture for computing model-data goodness-of-fit during calibration (Sect. 3.3). ~~Model evaluation then used model-to-data ratio of standard deviations, and~~

As outlined in Sect. 1, our model evaluation is meant to test the ability of EcH$_2$O-iso to generically simulate isotope dynamics across compartments. We used mean absolute error (MAE) to quantify model-data fit for all isotopic outputs, some of which present low temporal variability, have skewed distributions, or have a relatively lower sampling record, resulting in typical hydrograph-oriented efficiency metrics (e.g., Nash-Sutcliffe or Kling-Gupta, Nash and Sutcliffe, 1970; Kling et al., 2012) being less applicable. The median value are shown on corresponding time series (Figs. 3–7), and normalized by each dataset range and used in conjunction with Pearson's correlation factor ~~.~~ in Fig. 8 as a summary of model performance. The correlation coefficient axis in this dual model performance space represents the quality of model in representing the variation of the data, while the normalized MAE axis provides information on the accuracy (bias) of the model.

4 Results

4.1 Time series

Seasonal dynamics of soil water isotopes were well captured on the hillslopes, as exemplified at two sites in Fig. 3: one located in the shrub-dominated moorland (Podzol site), the other in a Scots pine plantation (Forest site B), noting that the graphs cover different hydrological years dictated by data availability. Model-data agreement was consistent for δ^2H, keeping in mind that while measurements were depth-specific, simulated values were averaged over the first and second hydrological layers (Fig. 1). As a result of model calibration (see Sect. 3.3), the thickness of the first (topsoil) and second layers span 0.10-0.19 m and 0.02-0.39 m in the simulated podzol soil unit, respectively (not shown). Still, at the podzol site the model captured well the vertical variability δ^2H across the summer of 2013, but overestimated topsoil enrichment during the following winter (Fig. 3a). Lc-excess was generally underestimated in the topsoil top soil layer there, with negative simulated values indicating evaporative influence generally not found in the data. At Forest site B, both δ^2H and lc-excess dynamics showed modelled ranges consistent with measurements. Note, however, that EcH$_2$O-iso simulated a vertical profile during the winter 2016 with richer δ^2H in the deeper layer, a condition that was only occasionally found in δ^2H measurements (Nov 2015 and Jan 2016). At both sites, the temporal dynamics of soil moisture were well captured by the model (bottom rows), although . We note however that the observed decrease of moisture content with depth – especially marked at forest site B – was generally not reproducedby the gravity-driven physics of , as the vertically-constant parameterization of soil hydrology in EcH$_2$O (Brooks-Corey conceptualisation; Maneta and Silverman, 2013) does not allow sufficient water retention in highly organic upper soil layers.

Isotopic consistency was also found further in the valley bottom, as shown at the peat site in the riparian area (Fig. 4). The bimodal summer δ^2H enrichment measured was well captured in the topsoil layer of the model (thickness: 0.02-0.25 m), as were the mildly-negative lc-excess values. In addition, the weak variability and range of measured δ^2H and lc-excess at greater depths were consistently reproduced. As for the podzol site, we noted in the peat higher peak enrichment values from the model than for the available data. As for other elements of the analysis, we remind here that soil isotopic data was sampled differently at the three sites: lysimeters extraction was used for the podzol and peat sites, therefore characterizing characterising mobile water in the fast domain, while the direct equilibration analysis conducted at Forest site B effectively applies to bulk water including water held under higher tension. The model essentially gives a bulk isotopic composition of stored water (Sect. 2), which might also explain why results were comparatively better at Forest site B.

We also explored the accuracy of simulated spatial patterns of isotopic signatures in the riparian zone, using two synoptic sampling surveys of surface water and stream water (Sect. 3.2.1) on separate days in late winter and late spring of 2013 (Fig. 4d-g). A good agreement was found for δ^2H in the main branch of the stream network on both dates, while there was a tendency to overestimate δ^2H values in the northwest part of the riparian area. Model-data fit of lc-excess mostly oscillated between good and a few per mille underestimation, depending on the location. For both δ^2H and lc-excess there was fine-scale spatial variability in the model-data fit, especially marked in late May and in the main channel. This reflects both the spatial

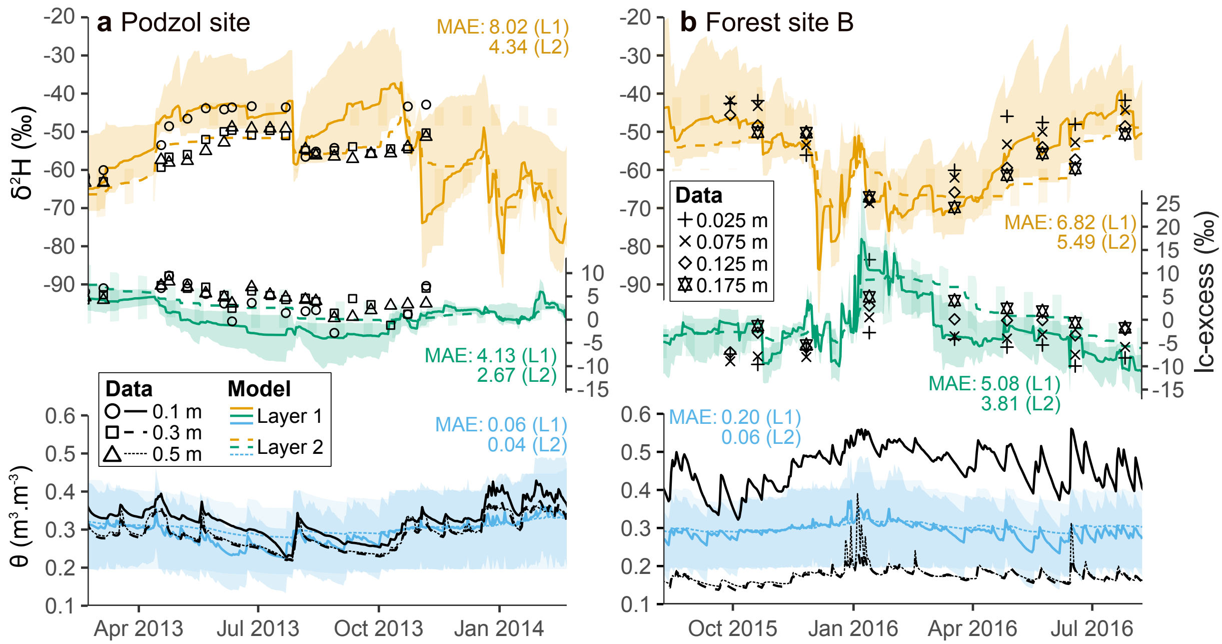

Figure 3. Time series isotopic composition (δ^2H – top, and lc-excess – middle) and soil volumetric water (bottom) at two sites located in the hillslopes; **(a)** one dominated by a heather shrub cover and **(b)** the other in a pine-dominated area. Black symbols and lines show measurements at a given depth while colours display the ensemble medians and 90%-intervals of simulations in the two uppermost soil layers, and the the median mean absolute error (MAE) between model and data are shown.

variability of measurements (Lessels et al., 2016; Sprenger et al., 2017b) and the different resolution of sampling ($\sim$ 10 metres intervals) and the much coarser grid of the simulations (100×100 m^2).

Figure 5 shows EcH$_2$O-iso's simulation of the isotopic imprint of plant water uptake in the transpiration flux. The isotopic composition of xylem water samples was directly compared to that of root water uptake simulated from the canopy energy balance (sub-step [2b] in Fig. 1). At the heather sites, the simulated ranges were consistent from model to data, with an excellent model-data fit for lc-excess despite the low 90% -spread of simulations outputs (Figs. 5a and 5b). The seasonal cycle of simulated δ^2H conversely seemed opposite to that of xylem samples, which showed gradual enrichment in winter followed by depletion at beginning of the growing season, but the lack of data from January to April limits general seasonal interpretation. At the forest sites, simulation results were very similar, noting that Forest site A corresponds to the same model grid cell as Heather site A (Figs. 5c and 5d). However, the measured isotopic composition in xylem was quite different for Scots Pine compared to the heather, in two ways. First, the seasonal trends of δ^2H were reversed, resulting in a good agreement with the modelled seasonality. Second, measured δ^2H and lc-excess showed consistently lower values as compared to the heather sites, by 5-24 ‰for δ^2H and 4-13 ‰for lc-excess (δ^{18}O was only slightly positively biased, not shown). ~~Aa~~ As a consequence, simulations showed a permanent positive offset for Scots pine water use despite consistent seasonality.

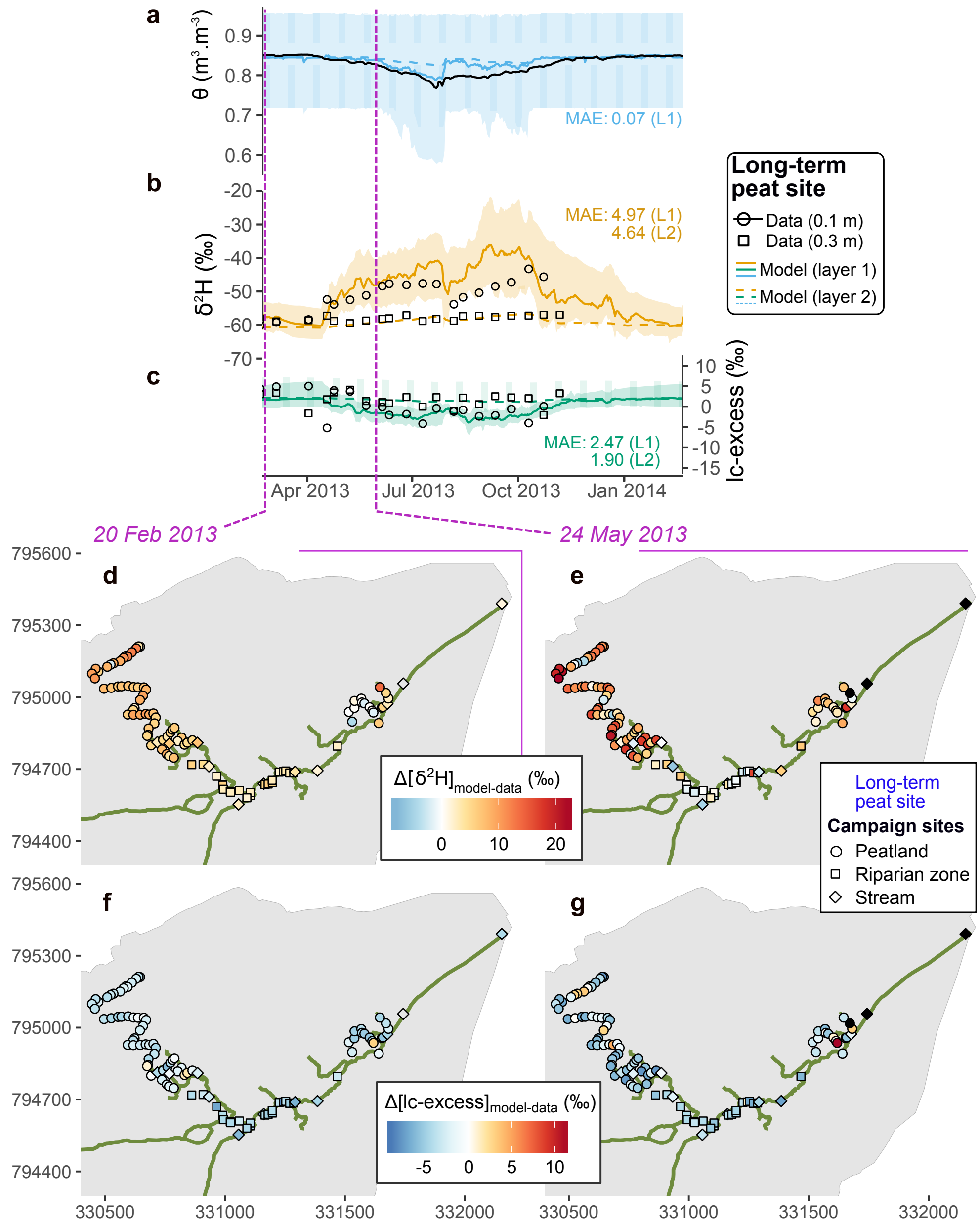

Figure 4. (a-c) Time series of soil volumetric water content (θ) and isotopic composition (δ^2H and lc-excess) at the peat site indicated by purple cross in the bottom maps. Measurements at a given depth are shown in black while colours display the ensemble medians and 90%-intervals of simulations in the two uppermost soil layers. **(d-g)** Model-minus-data difference at two given days when samples were collected in the valley bottom, for deuterium **(d-e)** and lc-excess **(f-g)**; black symbols indicate an absence of sample on one of the two dates, and the median model-data MAE values are shown.

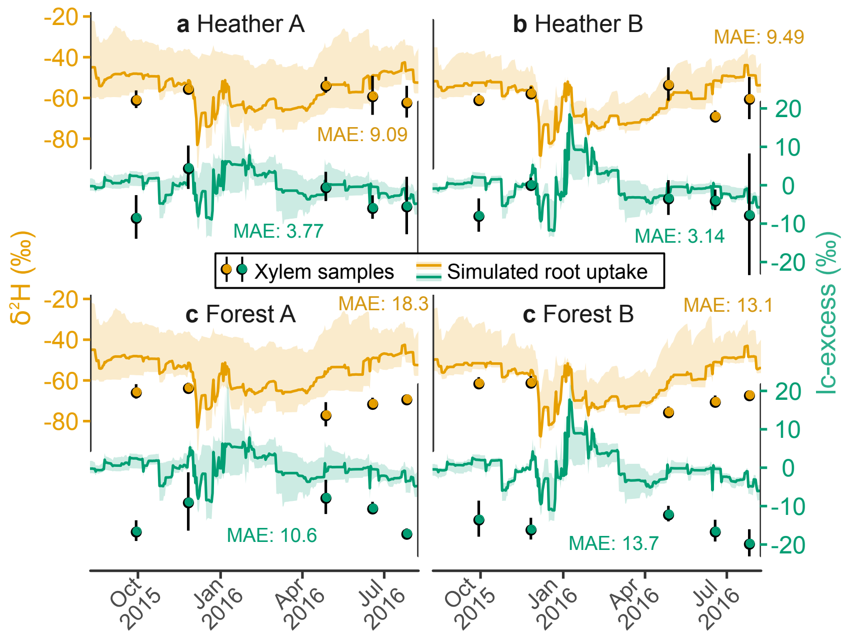

Figure 5. Time series of deuterium composition (orange) and lc-excess (green) in the xylem of two heather shrublands (Heather Site A and B) and two Scots pine stands (Forest Site A and B). Measurements are shown with symbols with one standard deviation across replicas, while solid lines display ensemble medians and 90%-intervals of simulations, and the corresponding median model-data MAE values are shown.

Isotopic variability was comparatively much lower for the groundwater both in time and across monitored wells, and a general agreement was found in the simulations (Fig. 6). The deuterium signal was robustly reproduced, with all measured values falling in the 90% -spread of simulation ensemble. However, the model tended to slightly underestimate lc-excess, with simulated values near zero while measurements were mostly centered on 3 ‰. In addition, the short-term lc-excess variability was somewhat underestimated in the riparian area.

Figure 7 shows the model-data comparison at the catchment outlet. The ~~flow (Fig. 7a) and~~ overall signal of stream water δ^2H (Fig ~~7b) was~~ 7a) and discharge values (Fig. 7c) were well reproduced by the model, with consistent “transition” periods of progressive enrichment when atmospheric demand increased and the catchment got drier. Most behavioural models in the ensemble did not completely capture the full extent of winter δ^2H depletion, and the seasonal minimum of δ^2H generally fell below the 90%-spread of the ensemble. However, seasonal variations of modelled lc-excess in the stream were in phase with the datasets throughout the study period: minimum in summer, maximum in winter, although simulated variability was more damped than for δ^2H, with a slight negative bias ~~.~~ (Fig. 7b).

A summary of model performance is shown in Fig. 8 for all sites/compartments, using the dual space of ~~model-data linear correlation (~~normalized MAE (using each dataset range, x-axis) and ~~model-to-data ratio of variability (observation-normalized standard deviations,~~ Pearson’s linear correlation factor (y-axis). ~~Most~~ The vast majority of median normalized MAE were below

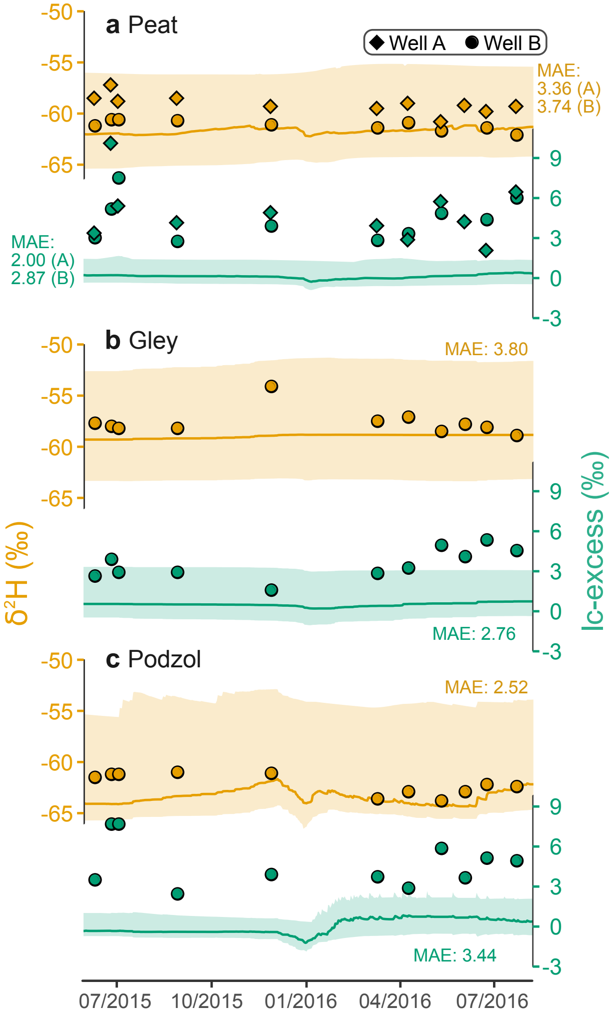

Figure 6. Time series of deuterium composition (orange) and lc-excess (green) in groundwater at different locations in the catchment. Measurement are shown with symbols – with two wells on the same simulated peat grid cell, on opposite sides of the stream –, while solid lines and ribbons show the median and 90%-confidence interval of ensemble simulations, and the median model-data MAE values are shown.

1, and more than half of evaluated datasets showed values below 0.5. Values above 0.7 were mostly found for groundwater and xylem compartments, a clustering especially marked for δ^2H. In addition, most median model-data correlations were significantly positive between ~~0.5~~ 0.4 and 0.85, ~~while insignificant~~ noting a tighter clustering around high values for δ^2H than lc-excess. Insignificant or negative correlations were mostly found where only a few data points were available (xylem) or where seasonal variability was low (e.g. groundwater). ~~In addition, δ^2H variability ratio between model and data was often close to 1, while values for lc-excess were more variable. Some model overestimations of isotopic variability were evident, most often in the topsoil layer (Forest B and Heather sites) but also in the second layers for lc-excess at the Gley site.~~ Interestingly, median

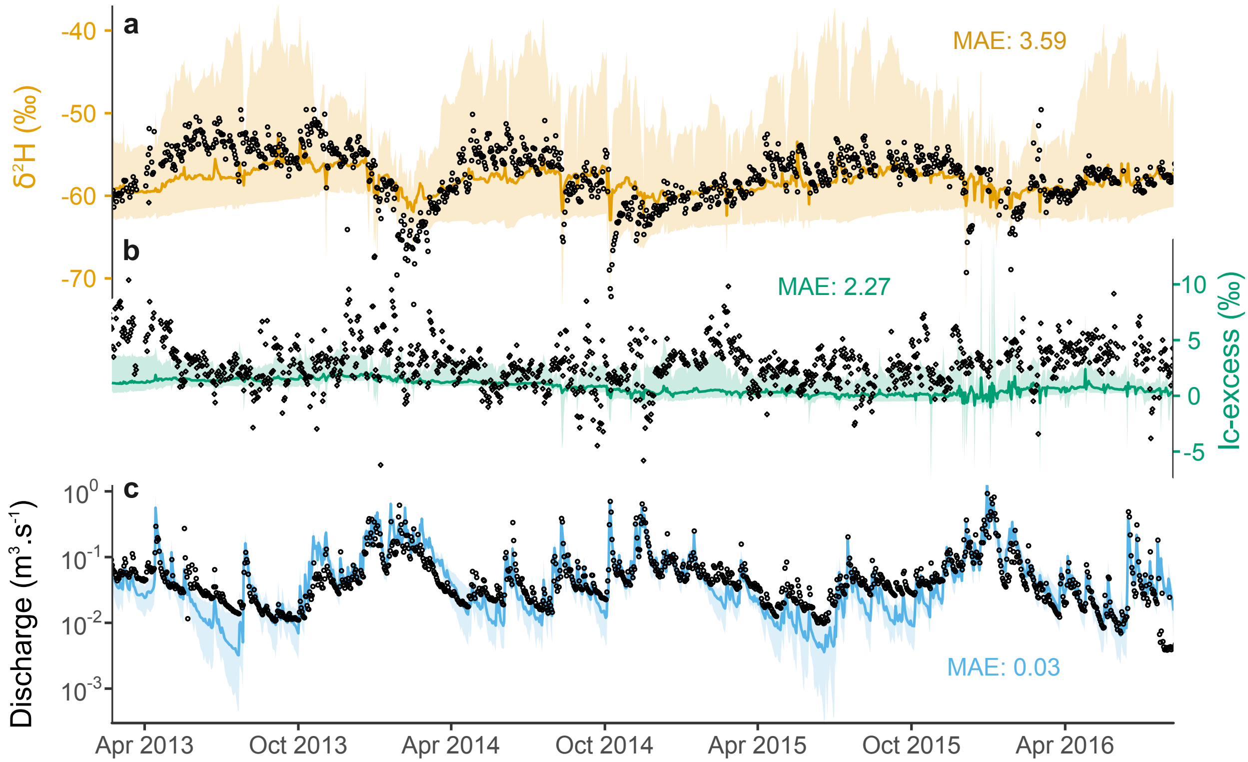

Figure 7. Time series of stream ~~**(a)** discharge and~~ isotopic composition – ~~**(b)**~~ **(a)** δ^2H and ~~**(c)**~~ **(b)** lc-excess – and **(c)** discharge at the catchment outlet. Measurements are shown with black open symbols while colours display the medians and 90%-confidence intervals of ensemble simulations, and the model-data MAE values are displayed.

model-data agreement in topsoil at Forest site A significantly differed between 2013 (mobile water sampling via lysimeters) and the 2015-2016 period (bulk water sampling via direct equilibration). This was notable in the dramatic increase of model-data correlation ~~and near-one variability ratio~~ (0.17 to 0.8) and decrease of normalized MAE (0.5 to 0.25) for topsoil δ^2H in the latter case, which is consistent with ~~the hypothesis~~ our interpretation that the simulated soil water composition represents that of bulk water.

4.2 Simulated hydrometric and isotopic spatial patterns

Figure 9 provides a spatially-distributed, seasonal view of the ensemble-median of outgoing water fluxes across the catchment over the simulation period. Lateral connectivity was markedly higher during the wetter first half of the hydrological year (October - March, Fig. 9a-b). During this colder, most energy-limited period, surface runoff –cumulative along the flow path, as runoff can cross several grid cells within one time step– was significant in many cells where the slopes transition to the valley bottom (up to 53 mm·d^{-1}, i.e., 0.006 m^3·s^{-1}), as well as on some surrounding hillslopes in the southern/south-western part of

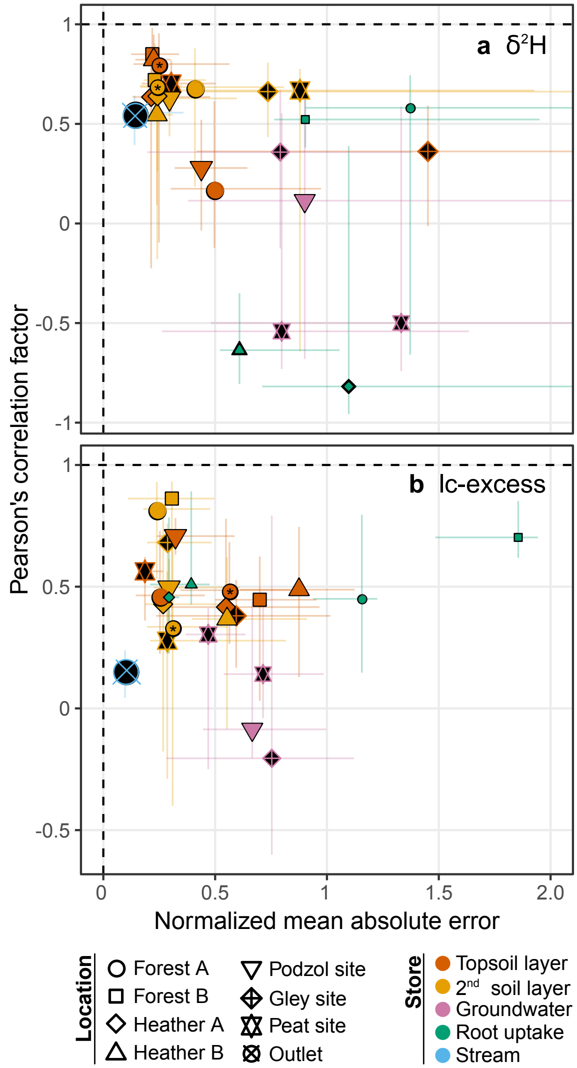

Figure 8. Summary of model performance in the dual space of ~~model-data~~ mean absolute error (normalized by the observed range of values) and Pearson's correlation factor ~~and ratio~~ between modelled and observed time series, ~~shown~~ for **(a)** δ^2H and **(b)** lc-excess, showing the median and 90%-spread over the ensemble. The size of each symbol is proportional to the logarithm of the number of ~~daily field data~~ observation points available. Performances in soil compartments at Forest site A are further separated between periods 2013 and 2015-2016 (the latter indicated with an asterisk), corresponding to two separate field data collection campaigns. Two groundwater wells are presents at the peat site.

the catchment (Fig. 9a). Throughout the spring-summer, very few of these overland flow corridors were usually hydrologically active; only in response to larger storm events. In parallel, lateral subsurface connectivity in autumn-winter time was quite widespread across the catchment, particularly concerning the two southernmost stream tributaries where subsurface flux largely exceeded surface runoff (up to 90 mm·d^{-1}, Fig. 9b). Some of these subsurface connections were still active during the growing season, albeit weaker (< 40 mm·d^{-1}). Given the predominance of subsurface flow near the channel, return flow dominated the vertical water budget (exfiltration minus infiltration > 0) throughout the year at junctions with the main stream and further downstream, especially in the winter (Fig. 9c). The rest of the catchment was dominated by infiltration, with average net rates of a few mm·d^{-1}. Evaporative losses of soil water were much smaller and had a different seasonality than infiltration and throughflow (Fig. 9d-e). In autumn-winter, soil evaporation (E_s) was similar in magnitude to ecosystem transpiration ~~(T_c,~~ E_t (integrated over all vegetation cover for each grid cell), although at local scales both fluxes remained below a few tenths of mm·d^{-1} (catchment average: 0.11 mm·d^{-1} for both E_s and ~~T~~E_{et}). Conversely, ecosystem transpiration clearly dominated during the rest of hydrological year, with a catchment-averaged rate almost four times higher than that of soil evaporation (0.61 versus 0.16 mm·d^{-1}, respectively). In both cases, the highest values were found in the riparian area, although the spatial contrast was more marked for soil evaporation.

This spatio-temporal variability in water fluxes was somewhat reflected in that of isotopic patterns (~~Figs. 10-11~~δ^2H in Fig. 10a, and lc-excess in Fig. S2). δ^2H in the topsoil went from markedly depleted winter values (average: -61 ‰) to maximum enrichment in spring-summer with larger spatial variability (average: -44 ‰) (Fig. 10a). These temporal variations were well within that of δ^2H in precipitation inputs (Fig. 2c). Yet, the increasing spatial variability of topsoil δ^2H in spring-summer, and the much more pronounced relative seasonality of topsoil lc-excess (Fig. ~~11a~~S2a) (compared to that in precipitation, Fig. 2c), indicated a significant influence of evaporation fractionation on isotopic patterns. During the spring-summer period the highest δ^2H values, and most negative lc-excess values, were found in the organic soils of the valley bottom and on the higher hillslopes. These locations are where soil evaporation was highest (Fig. 9d) or where the soils are thinnest (rankers regosols, Fig. 2a). The effect of isotopic fractionation crucially depends on relative storage change (Eq. 7), thus it had large values either because absolute evaporation was high (valley bottom) or because the available storage was limited (thin soils). Conversely, spring-summer lc-excess values were near zero (or even slightly positive), and δ^2H enrichment less pronounced, in most of the topsoil grid cells where the stream is also present, corresponding to the locations where upslope-routed groundwater exfiltrated (Fig. 9c). Finally, positive winter values for lc-excess across the catchment's topsoil hints at a widespread dominance of winter precipitation and mixing processes (via surface connectivity and infiltration, Fig. 9), over fractionating ones.

The isotopic signature (δ^2H and lc-excess) in water used by plants for transpiration largely displayed a damped reflection of the topsoil patterns (Figs. ~~10-11 b~~10a and S2a). This reflects distributed root uptake across the soil profile, reaching deeper soil compartments where seasonal isotope dynamics were less marked. One consequence is that the model simulated more isotopically-depleted plant water use in the thin regosols of the upper hillslopes compared to the very shallow topsoil layer (northern and western parts of the catchment).

~~Seasonal average of lc-excess in the Bruntland Burn over the period 2013 – 2016, showing the ensemble median of simulations in **(a)** the topsoil layer, **(b)** root water uptake (summed of vegetation covers) and **(c)** groundwater.~~

Finally, groundwater δ^2H patterns were comparatively more uniform across the catchment ($\sigma_{spatial}$ = 1.9 ‰) and across seasons (Fig. 10c). Most depleted values were found in the podzolic hillslopes and across the valley bottom, a feature more marked in winter and spring. Lc-excess mostly displayed positive values throughout the year, except for some weakly negative autumn values on the higher hillslopes (Fig. ~~11c~~S2c). Markedly positive values were generally found in the organic soil of the

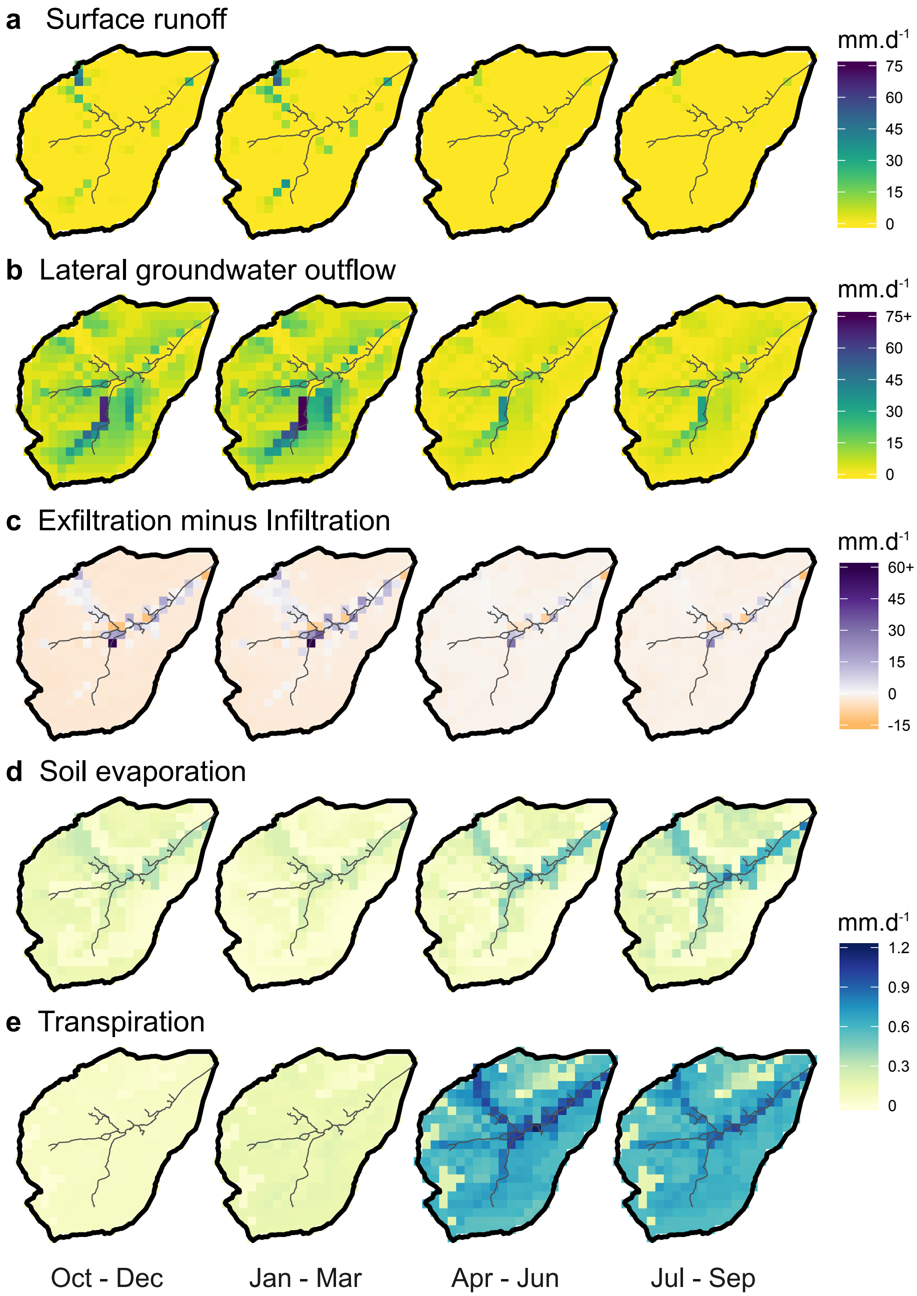

Figure 9. Seasonally-averaged daily outgoing water fluxes in the Bruntland Burn over the period 2013 – 2016, showing the ensemble median of simulated **(a-b)** cell-to-cell lateral flow, **(c)** net vertical liquid flow and **(d-e)** evaporative losses via soil evaporation and transpiration, respectively.

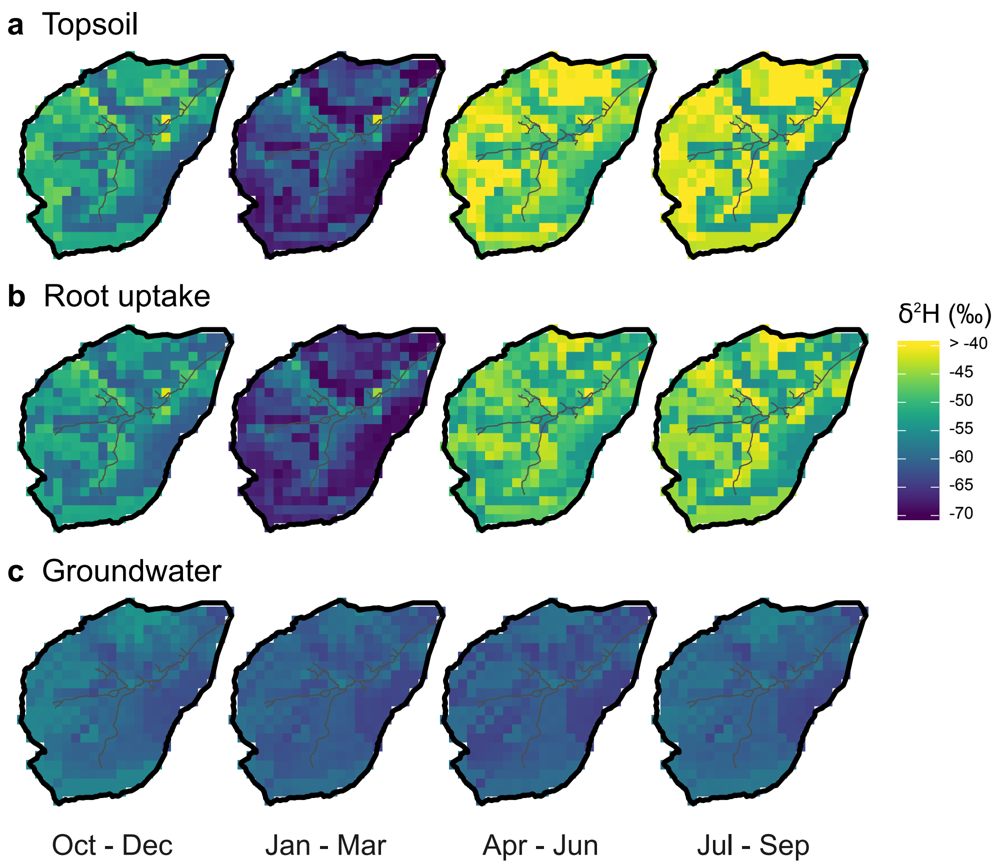

Figure 10. Seasonal average of δ^2H in the Bruntland Burn over the period 2013 – 2016, showing the ensemble median of simulations in **(a)** the topsoil layer, **(b)** root water uptake (summed of vegetation covers) and **(c)** groundwater.

valley bottom where fluxes converge. Note that positive values were more spatially homogeneous during winter and spring time, highlighting subsurface recharge lagging behind the more superficial compartments by a few months.

4.3 Water ages

Simulated water ages showed significant variability across locations in the catchment, as well as a marked seasonality at most sites selected for the analysis (Fig. ~~12~~11). For convenience, the sites chosen for analysis in Fig. ~~12a-d~~ 11a-d were the same as those where isotopic model-data evaluation was conducted. In general, modelled water age increased with distance downhill, consistent with freely-draining hillslopes sustaining groundwater fluxes into the riparian area. In the soils, water age ranged from a few weeks on the hillslopes to several years in the valley bottom peat where the top soil is affected by exfiltration of older groundwater from upslope areas. Groundwater age was more homogeneous across the watershed but still showed significant differences, averaging one year ~~of age~~ in the podzol-covered locations, compared to 2-to-3 years in the riparian area. Seasonal variations were most significant on the hillslopes, from week-old waters in winter to water ages of 2-to-6 months during the growing season in the vadose zone. Weaker intrinsic seasonal variability was generally found in groundwater, which is consistent with the very flat simulated isotope dynamics (Fig. 6). The age of water uptaken by plants followed the topsoil age patterns in most cases, reflecting the relatively young water ages from shallow rooting depths. One exception is Forest site A, where the contribution of older water from the second soil layer during the growing season had a clear effect on the age of the water used by vegetation. This latter site interestingly displayed older water ages compared to other hillslopes locations, suggesting slower drainage conditions, likely linked to less marked local topography and receipt of older water from upslope. In addition, the gley site displayed ~~a~~ rather dynamic behaviour in the upper soil layers, similar to podzols, while the turnover of groundwater there was the lowest among all locations, suggesting it is confined and disconnected from the soil profile. Finally, at the peat site, younger water ages were found in groundwater compared to upper soil layers. This surprising result was likely linked to permanently saturated soils with limited infiltration (disconnection from the surface and overland flow) and recharge (disconnection from confined groundwater) where lateral soil water movement was not simulated, but lateral transfers and mixing occurred in the underlying groundwater.

Spatial variability was also found in stream water age, as shown in previously referred-to sites and arbitrarily defined locations along the channel network (Fig. ~~12e~~11e). In two of the main tributaries of the BB (HW2 and HW3), simulated water ages were significantly younger ($\sim$ 0.5-1.5 years) than along the rest of the channel network (1.4$\sim$ 2.8 years). The older water ages found in HW1 might be linked to the presence of high water storage in drift deposits and an extensive raised peat bog in this portion of the valley bottom (Sprenger et al., 2017b), while the streams in HW2 and HW3 emerge further upslope at the drift-free ranker-podzol transition (Fig. 2a). There is a localized increase in water age when moving downstream towards the peat site, consistent with increased groundwater exfiltration (Fig. 9c) where stream water is a few weeks older than at the catchment outlet. In this lower part of the catchment lower temporal variability was also evident (1.8$\sim$ 2.4 years). Again, this might be derived from groundwater influxes and the extensive presence of saturated peat soils in this part of the catchment, compared to other sections of the stream.

5 Discussion

5.1 Performance of the tracer-enhanced model

The model-data comparison demonstrated that EcH$_2$O-iso captured a significant part of the isotopic behaviour across multiple ecohydrological compartments and landscape positions monitored in the study catchment. Because no calibration was performed on the isotopic components, these results reveal that the water mixing and storage and the water pathways simulated by the hydrologic core of EcH$_2$O-iso correctly reflect the dominant hydrologic dynamics of the basin (Kuppel et al., 2018). Hydrological states and fluxes in the model evolve driven by the *celerity* of propagation of local energy gradients (e.g. gravity-driven hydraulic gradient) throughout the landscape, with no direct knowledge about which “water parcels” (e.g., old or young, upslope or downslope) have been mobilized during a given hydrological response (Kirchner, 2003). Conversely, correctly capturing isotope dynamics is conditioned to accurately simulating patterns of water particle ~~velocities~~*velocities*, i.e. to routing the correct water parcels all the way from precipitation to their fate in the stream or as evaporative outputs (McDonnell and

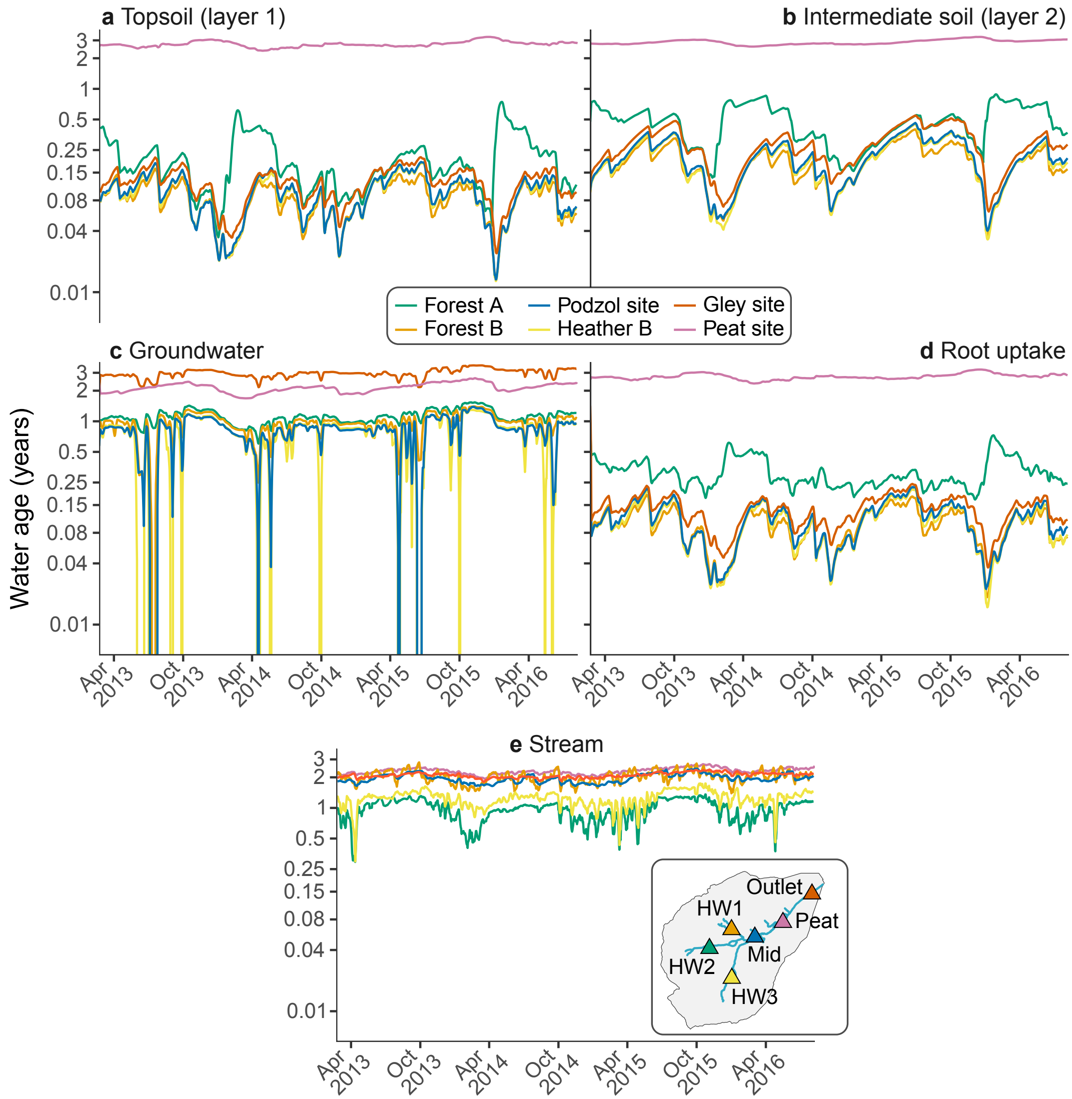

Figure 11. Ensemble median of simulated water age at the different sites used for model evaluation (except for Heather site A) in each corresponding compartment **(a-d)**, and in the stream at several locations along the channel network (shown on the inset map, **e**) . To improve visibility, all curves have been smoothed using a 7-day moving average window.

Beven, 2014). Therefore, the general performances achieved ~~by our~~ in the present celerity-velocity framework give reasonable confidence in the mechanistic description of energy-water-plant couplings adopted by the EcH_2O-iso model.

Despite some of the discrepancies presented and discussed below, the overall isotopic model-observation fit is ~~remarkable~~ very encouraging because the evaluated ensemble of model configurations was not derived from any tracer-aided calibration, but solely used the information content brought by hydrometric and energy balance datasets in an independent calibration exercise similar to Kuppel et al. (2018). Further, the implementation of water isotope and age tracking, consistent with the original structure of EcH_2O and including evaporation fractionation of isotopes, was straightforward and followed well-established methodologies (Eqs. 4-18) without any parameterization specific to the study site. By keeping both the isotopic module and calibration as minimalistic as possible, our approach avoids adding new, unnecessary degrees of freedom and reduces the risk of overfitting. Specific model performance might thus be lower than what could be achieved using a dual hydrometric-isotope calibration approach (Birkel et al., 2014; van Huijgevoort et al., 2016; Knighton et al., 2017), but because the isotopic signal remains truly independent of the hydrologic calibration our approach allows unique critical analysis and insight into the physical hypotheses underlying simulated flow generation and water mixing.

5.2 Insights into critical processes for model future development

The timing of seasonal isotopic dynamics as well as higher-frequency responses were well simulated in the vast majority of cases (summary in Fig. 8), together with value ranges also broadly consistent with observations. Yet, the amplitudes of modelled temporal isotopic responses displayed variable degrees of agreement with that of measured signals. In general, dynamics of deuterium were better reproduced than that of lc-excess, with a trend to underestimate lc-excess in several compartments.

One of these model-data mismatches is the overly enriched signal in the topsoil of the riparian sites during the growing season (Figs. 4, 8). The concomitant underestimated lc-excess hints at an excessive evaporation fractionation signal. As pointed out in section 4.1, these discrepancies can partially derive from the different ~~support~~ information represented by model and observations. For instance, the model simulates the composition of the bulk topsoil water, whereas the observations may reflect only the composition of the free draining portion of the soil water. At the long-term riparian locations (Peat and Gley sites, Fig. 2a), collection by suction lysimeters (Tetzlaff et al., 2014) was used, sampling water under low tension and less affected by fractionation (Brooks et al., 2010; Sprenger et al., 2017b). In addition, the samples from a synoptic field campaign across the extended riparian area in flowing surface waters and ponds on two dates (Lessels et al., 2016) were directly compared to simulated topsoil water (Fig. 4d-g). This was because the current formulation of EcH_2O-iso routes all surface water to the next downstream cell and thus does not account for free-standing water such as the ponds and zero-order streams typically forming outside summer in the BB, particularly in the north west of the catchment (Lessels et al., 2016). Yet, the sampled surface water in the riparian area has been shown to have spatially-varying sources, presenting distinctively enriched or depleted δ^2H signals depending if the source is soil water or groundwater, respectively (Lessels et al., 2016). Systematically comparing soil water to sampled surface water might thus explain the overestimation of δ^2H, especially in the north-west part of the catchment where limited groundwater seepage is modelled (Fig. 9c). Secondly, the riparian topsoil in EcH_2O-iso might function as an "evaporation hotspot" to a greater extent than has been found in corresponding sampled surface water locations (Sprenger et al., 2017b). Indeed, topsoil water is not laterally connected in the model, so that evaporation fractionation remains local (horizontally) but immediately mixes across the whole layer – as compared to a vertically-stratified isotopic profile in poorly mixed ponded areas. In addition, while fractionation is modest ~~as~~ compared to other climatic settings~~at our site~~, measurements have shown that ponds and zero-order channels that are not fully evaporated connect to the channel network in spring-summer and drive the seasonal isotopic enrichment observed in the stream (Sprenger et al., 2017b). Further support for this hypothesis was found by disabling evaporative fractionation in our simulations: seasonal variability of isotopes in the stream almost completely disappeared, while short-term, event-driven dynamics remained (not shown). Beyond the idiosyncrasies of our study catchment, and the gap between fine-scale wetland heterogeneity and our model resolution (100×100 m^2), a large body of literature has reported the importance of riparian wetlands as time-varying "chemostats" controlling stream water quality (e.g., Billett and Cresser, 1992; Smart et al., 2001; Spence and Woo, 2003) or "isostats" mixing isotope signals (Tetzlaff et al., 2014). Since modelled soil water is not laterally routed to the channel during the onset of the growing season, this might explain some underestimation of summer δ^2H in the stream outlet, as well as the reported lack of seasonal variability for instream lc-excess (Fig. 7). Further developments of the model to include ponding effects and/or a more dynamic channel network (rather than fixed, as currently conceptualised), would help capture these seasonally-varying flow paths in the variably-saturated valley bottom of low-energy landscapes.

The isotope and age tracking adopts a complete and instantaneous mixing scheme at each sub-time step where water transfers are computed between the spatially-distributed compartments of the simulated domain. This working hypothesis was chosen for simplicity, given the wet and cool climate conditions and the relatively long (daily) simulation time steps. The spatio-temporal variability of simulated fluxes and stores somewhat results in a time-variant partial mixing at the catchment scale at the stream outlet (van Huijgevoort et al., 2016). However, we note, for example, that our simulations of groundwater lc-excess showed an underestimated variability and a consistent negative bias towards near-zero values (Fig. 6). It indicates that the simulated recharge signal is very damped throughout the year and slightly biased towards the signature of over-enriched, evaporation-affected recharge. This contrasts with the evidenced dominance of winter recharge given the markedly positive lc-excess values observed at the monitored wells (Scheliga et al., 2017) as well as in other catchments with comparable eco-climatic settings (O'Driscoll et al., 2005; Yeh et al., 2011; Bertrand et al., 2014). It might point to an exaggerated mixing across the soil profile in our simulations, overly flattening the precipitation signature and overestimating fractionation signal in the water percolating to the water table. Given that groundwater directly sustains 19 (±16) % of annual stream flow in our ensemble simulations (not shown), one can link this lack of variability in groundwater lc-excess to that simulated in stream water (Fig. 7). While such a link between the degree of unsaturated zone mixing and stream isotopes was not evidenced by Knighton et al. (2017), there was a much lower contribution of baseflow to discharge in the intermittent catchment they modelled. More generally, further developments would benefit from incorporating insights from the growing body of literature on the importance of preferential flow in driving catchment dynamics and tracer mixing (Beven and Germann, 2013). This would first involve implementing conceptualisation of micro-topographic controls on overland flow (Frei et al., 2010)~~and~~ . Secondly, the significance of sub-surface dual pore space (matrix-macropore) representations of tracer flow paths and mixing ~~(Stumpp et al., 2007; Stumpp and Maloszewski, 2010; Vogel et al., 2010; Sprenger et al., 2018)~~has long been put forward (Beven and Germann, 1982) but modelling efforts relevant to catchment hydrology remain somewhat scarce (Stumpp et al., 2007; Stumpp a Bridging these detailed ~~plot-scale~~ plot-to-hillslope-scale descriptions with a physically-based ecohydrological model such as EcH$_2$O-iso will likely require a simplified, parsimoniously parameterized implementation and calibration with tracer data.

Our modelling experiment also helps to evaluate the ~~conceptualization~~ conceptualisation of isotopic fractionation in the soil water of wet, energy-limited catchments. The evaporative fractionation is described by the well-established Craig-Gordon model (Craig and Gordon, 1965), supplemented here with a soil-adapted formulation following Mathieu and Bariac (1996) and

Good et al. (2014). As reviewed by Horita et al. (2008), the Craig-Gordon model is very sensitive to the isotopic composition of atmospheric moisture (δ_a), the relative humidity of the atmosphere at the surface (h_a) and the kinetic fractionation factor (ϵ_k). We assumed isotopic equilibrium between rainfall and atmospheric moisture (Eq. 10), as is commonly done when no direct measurement of δ_a is available (Horita et al., 2008). While this empirical, and here spatially-uniform, approach is valid on monthly time scales in temperate climates (Schoch-Fischer et al., 1983; Jacob and Sonntag, 1991), discrepancies can arise on shorter time scales and/or when local evaporation significantly feeds atmospheric moisture (Krabbenhoft et al., 1990). Second, h_a estimates can be a large source of error in wet environments where h_a>0.75 (Kumar and Nachiappan, 1999), which is often the case in our catchment (Wang et al., 2017b). Furthermore, we found a marked sensitivity of isotope dynamics to the strategy used to calculate ϵ_k (Eq. 14), consistent with Haese et al. (2013), who found a large impact on simulated soil δ^{18}O in northern latitudes. We chose to use a formulation based on isotopic diffusivity ratios; the latter were taken from Vogt (1976) because their experimental protocol covered a comparatively large range of humidity conditions. Yet it seems that very few (if any) experimental studies estimating these ratios spanned the very humid conditions found at the BB, and further empirical data could help reduce the associated uncertainties (Horita et al., 2008).

Finally, we showed that our root uptake simulations for heather shrubs closely broadly matched the measured isotopic signature in plant xylem. Conversely, a systematic, positive model offset was found for both δ^2H and lc-excess in Scots pines despite the fact that the model correctly captured the temporal dynamics (Fig. 5). Our simulations assumed identical, exponential root profiles for all vegetation types within soil types, e.g. the podzol, where these experimental heather and forest sites are found (Kuppel et al., 2018), thus species-dependent use of soil water from depth-specific isotopic signature cannot be captured. Heather shrubs have, however, a shallow root system (typically < 5 cm, Geris et al., 2017) and thus its source water might be more affected by evaporation than Scots pine (which can be deeper-rooted). However, the observed lc-excess values in the soil of Scots pine (-13 to 5.5 ‰; Fig. 3b, Forest site A not shown) were significantly higher than those measured in the pine xylem (-19.6 to -7.6 ‰, Fig. 5c-d). It mostly seems to stem from significant recorded deuterium depletion while oxygen-18 ratios were consistent or slightly depleted as compared to soil samples, and we found larger simulations biases (relative to the mean value) in xylem for deuterium than for oxygen-18 ratios (not shown). Such isotopic departures between soil and xylem water have been reported in a number of experimental studies, although primarily conducted in seasonally-drier environments (Lin and da SL Sternberg, 1993; Zhao et al., 2016; Vargas et al., 2017). Several mechanisms have been proposed, including a discrimination of heavier isotopes during water uptake controlled by root aquaporins (Mamonov et al., 2007) or mycorrhizal associations (Berry et al., 2017), phloem-xylem water cycling on several time scales (Hölttä et al., 2006; De Schepper and Steppe, 2010; Pfautsch et al., 2015; Stanfield et al., 2017), and stem water evaporation through the bark (Dawson and Ehleringer, 1993). While exploring the relevance of these mechanisms to the ecosystems here simulated goes far beyond the scope if this study, it is clear that the complexity of isotopic dynamics in plant xylem cannot be fully captured simply based on a root-profile-weighted mixing of soil pools.

5.3 Opportunities for ~~characterizing~~ characterising water pathways

The development of EcH_2O-iso is a methodological "middle ~~ground~~path" for modelling conservative tracer transport, between detailed plot-scale models across the soil-vegetation-atmosphere continuum (e.g., Mathieu and Bariac, 1996; Melayah et al., 1996; Braud et al., 2005; Haverd and Cuntz, 2010), catchment rainfall-runoff models (Birkel and Soulsby, 2015; McGuire and McDonnell, 2015; van Huijgevoort et al., 2016; Knighton et al., 2017), and land surface models for earth system studies (Haese et al., 2013; Risi et al., 2016; Wong et al., 2017). This reflects the reasons why the original EcH_2O model was developed, namely to provide a physically-based, yet computationally-efficient representation of energy-water-ecosystem couplings where intra-catchment connectivity (both vertical and lateral) could be explicitly resolved (Maneta and Silverman, 2013). The combination of these features is critical, since explicit lateral connectivity (surface, subsurface, and channel) is typically the missing piece in land surface models (Fan, 2015) and in plot-scale approaches, and the coupling with vegetation processes is typically missing in rainfall-runoff models (van Huijgevoort et al., 2016). The newly developed model provides, for the first time, a transferable, process-based linkage of spatial-temporal patterns of water fluxes (Fig. 9) with those of isotopic tracers (~~Fig. 10-11~~Figs. 10 and S2) across a headwater catchment.

Here, a major focus has been put on the isotopic analysis to evaluate the consistency of EcH_2O-iso using the wealth of data available at the study site, and the limitations stemming from the unavoidable technical trade-off we adopted. Yet, principles used for isotope tracking were applied to track water age across the ecohydrological compartments (Fig. ~~12~~11). This provides a more complete picture of catchment functioning than stream water age, although the latter metric provides an important first-order benchmark for comparison with other modelling approaches. ~~T he~~ The mean stream water age of ∼2.1 yrs is consistent with isotope-calibrated rainfall-runoff approaches reporting ∼ 1.55 yrs (van Huijgevoort et al., 2016; Ala-aho et al., 2017) and ∼1.8 yrs (Soulsby et al., 2015). The low temporal variability found here yields higher discrepancies when considering flow-weighted median ages: ∼2 yrs against 1.2 yrs found by Soulsby et al. (2015) and ∼1 yr reported using transport model driven by StorAge Selection functions (Benettin et al., 2017). We notably find a slower water turnover in the valley bottom soils (∼2.8 yrs) as compared to compared to the spatially-distributed approach of van Huijgevoort et al. (2016) (∼2 yrs), and EcH_2O-iso conversely simulates much younger water ages in the groundwater both on the hillslope and in the valley bottom (∼ 0.9 and ∼2.2 yrs, vs. ∼2.9 and ∼3.4 yrs, respectively) and on the hillslope soils (∼0.2 yr vs. ∼0.8 yr) than van Huijgevoort et al. (2016). Keeping in mind that these discrepancies might arise from differences in modelling and calibration approaches, these mismatches may also confirm a tendency of EcH_2O-iso to overemphasize the role of the riparian area as a hydrologic buffer and mixing zone, as well as the contribution of groundwater, in damping the stream isotope response which could be addressed by strategies suggested in preceding sections.

6 Conclusions

The EcH_2O-iso model presented in this study is, to our knowledge, the first to simulate catchment dynamics of water isotopes (^2H and ^{18}O) and age by combining a physically-based description of hydrological stores and fluxes, a spatially-distributed simulation domain, a predictive vegetation component, and non-conservative isotopic processes (evaporative fractionation).

~~The model has been rigorously tested with an~~ Evaluated against a multi-site, extensive isotopic dataset ~~, in~~ encompassing a wide range of ecohydrological compartments ~~of the study region, and has shown very good performance~~ (soil moisture, groundwater, plant xylem, and stream water) across hydropedological units, the model has generally shown good performance in reproducing the seasonal and higher-frequency variations of absolute and relative isotopic content (δ^2H and lc-excess, respectively). Despite some limitations, this isotope-based evaluation suggests a reasonable capture of the *velocity* fields (i.e., how fast water parcels move) across the catchment, and complements a previous calibration and evaluation mostly using hydrometric observations (water fluxes and storage dynamics) which indicated a good simulation of catchment functioning from a *celerity* viewpoint (i.e., how fast energy propagates via the hydraulic gradient) (Kuppel et al., 2018). ~~This indicates that the model is correctly capturing the main elements of the catchment functioning as seen from both energy celerity and flow velocity viewpoints.~~ Satisfying this dual velocity-celerity perspective is key to ~~characterizing~~ characterising water pathways and quantifying the associated travel times in different ecohydrological compartments of headwater landscapes. Complementing more conceptual approaches, the physical basis of the EcH_2O-iso model further provides the potential to extrapolate these insights beyond recorded conditions and scales, and to notably project ~~ecohydrological feedbacks of~~ the reciprocal feedbacks between plant water use, hydrological pathways and potential environmental changes.

The relatively simple ~~conceptualization~~ conceptualisation of compartment-scale velocities, e.g. assuming complete mixing and without site-specific parameterization, and the absence of isotopic calibration, already make the current results particularly encouraging. It also provides a useful framework for ~~hierarchizing~~ hierarchising model development and benchmarking needs~~, specific or not to the physics of a high-latitude, low-energy, wet and steep headwater catchment such as the one simulated here. In particular,~~ . For example, some of the model-data discrepancies in our results stress the necessary incorporation of partial mixing hypotheses, likely to be critical in drier and/or flatter landscapes where diffusive water movement ~~prevail~~prevails. Second, our model-data analysis of isotope dynamics strongly reflects fractionation effects, be it via soil evaporation or species-specific plant water use. ~~Together with the presented model , these considerations~~ Finally, the versatility of climatic settings in which the original EcH_2O model has already been evaluated facilitates applying the presented methodology beyond the specifies of a high-latitude, low-energy, wet and steep headwater catchment such as the one simulated here. Further, the flexible spatial domain used by the model will help providing a process-based modelling framework for plot-to-catchment-scale hypothesis testing. This is timely for current challenges in critical zone science, such as exploring the occurrence and mechanisms behind the postulated ecohydrological separation of water fluxes (Berry et al., 2017).

Code and data availability. The source code of the EcH_2O-iso model is open source (https://bitbucket.org/sylka/ech2o_iso). The datasets used in this study are available from the PURE data repository of the University of Aberdeen (http://dx.doi.org/10.20392/0a7f3ba2-e6f3-40fd-b504-2eb44b76e515).

Competing interests. The authors declare that they have no conflict of interest.

Acknowledgements. This work was funded by the European Research Council (project GA 335910 VeWa). M. P. Maneta acknowledges support from the U.S National Science Foundation (project GSS 1461576) and U.S National Science Foundation EPSCoR Cooperative Agreement # EPS-1101342. The authors would like to acknowledge the support of the Maxwell compute cluster funded by the University of Aberdeen. Finally, the authors are grateful to the many people who have been involved in establishing and continuing data collection at the Bruntland Burn, particularly Christian Birkel, Maria Blumstock, Jon Dick, Josie Geris, Konrad Piegat, Bernhard Scheliga, Matthias Sprenger, Claire Tunaley, and Hailong Wang, and to Aaron Smith for fruitful discussions regarding the model development.

References

Ala-aho, P., Tetzlaff, D., McNamara, J. P., Laudon, H., and Soulsby, C.: Using isotopes to constrain water flux and age estimates in snow-influenced catchments using the STARR (Spatially distributed Tracer-Aided Rainfall–Runoff) model, Hydrology and Earth System Sciences, 21, 5089, 2017.

Albrektson, A.: Sapwood basal area and needle mass of Scots pine (Pinus sylvestris L.) trees in central Sweden, Forestry, 57, 35–43, http://forestry.oxfordjournals.org/content/57/1/35.short, 1984.

Allison, G. B. and Leaney, F. W.: Estimation of isotopic exchange parameters, using constant-feed pans, Journal of Hydrology, 55, 151–161, https://doi.org/10.1016/0022-1694(82)90126-3, 1982.

Barnes, C. J. and Bonell, M.: Application of unit hydrograph techniques to solute transport in catchments, Hydrological Processes, 10, 793–802, 1996.

Benettin, P., Soulsby, C., Birkel, C., Tetzlaff, D., Botter, G., and Rinaldo, A.: Using SAS functions and high-resolution isotope data to unravel travel time distributions in headwater catchments, Water Resources Research, 53, 1864–1878, 2017.

Berry, Z. C., Evaristo, J., Moore, G., Poca, M., Steppe, K., Verrot, L., Asbjornsen, H., Borma, L. S., Bretfeld, M., Hervé-Fernández, P., Seyfried, M., Schwendenmann, L., Sinacore, K., De Wispelaere, L., and McDonnell, J.: The two water worlds hypothesis: Addressing multiple working hypotheses and proposing a way forward, Ecohydrology, p. e1843, https://doi.org/10.1002/eco.1843, 2017.

Bertrand, G., Masini, J., Goldscheider, N., Meeks, J., Lavastre, V., Celle-Jeanton, H., Gobat, J.-M., and Hunkeler, D.: Determination of spatiotemporal variability of tree water uptake using stable isotopes (δ^18O, δ^2H) in an alluvial system supplied by a high-altitude watershed, Pfyn forest, Switzerland, Ecohydrology, 7, 319–333, 2014.

Beven, K. and Germann, P.: Macropores and water flow in soils, Water resources research, 18, 1311–1325, 1982.

Beven, K. and Germann, P.: Macropores and water flow in soils revisited, Water Resour. Res., 49, 3071–3092, https://doi.org/10.1002/wrcr.20156, 2013.

Billett, M. F. and Cresser, M. S.: Predicting stream-water quality using catchment and soil chemical characteristics, Environmental Pollution, 77, 263–268, 1992.

Birkel, C. and Soulsby, C.: Advancing tracer-aided rainfall–runoff modelling: a review of progress, problems and unrealised potential, Hydrol. Process., 29, 5227–5240, https://doi.org/10.1002/hyp.10594, 2015.

Birkel, C., Tetzlaff, D., Dunn, S. M., and Soulsby, C.: Using time domain and geographic source tracers to conceptualize streamflow generation processes in lumped rainfall-runoff models, Water Resour. Res., 47, W02 515, https://doi.org/10.1029/2010WR009547, 2011.

Birkel, C., Soulsby, C., Tetzlaff, D., Dunn, S., and Spezia, L.: High-frequency storm event isotope sampling reveals time-variant transit time distributions and influence of diurnal cycles, Hydrological Processes, 26, 308–316, 2012.

Birkel, C., Soulsby, C., and Tetzlaff, D.: Developing a consistent process-based conceptualization of catchment functioning using measurements of internal state variables, Water Resour. Res., 50, 3481–3501, https://doi.org/10.1002/2013WR014925, 2014.

Birkel, C., Soulsby, C., and Tetzlaff, D.: Conceptual modelling to assess how the interplay of hydrological connectivity, catchment storage and tracer dynamics controls nonstationary water age estimates, Hydrological Processes, 29, 2956–2969, 2015.

Bond-Lamberty, B. and Gower, S. T.: Estimation of stand-level leaf area for boreal bryophytes, Oecologia, 151, 584–592, https://doi.org/10.1007/s00442-006-0619-5, http://link.springer.com/10.1007/s00442-006-0619-5, 2007.

Botter, G., Bertuzzo, E., and Rinaldo, A.: Transport in the hydrologic response: Travel time distributions, soil moisture dynamics, and the old water paradox, Water Resources Research, 46, 2010.

Braud, I., Bariac, T., Gaudet, J. P., and Vauclin, M.: SiSPAT-Isotope, a coupled heat, water and stable isotope (HDO and H 2 18 O) transport model for bare soil. Part I. Model description and first verifications, Journal of Hydrology, 309, 277–300, 2005.

Braud, I., Bariac, T., Biron, P., and Vauclin, M.: Isotopic composition of bare soil evaporated water vapor. Part II: Modeling of RUBIC IV experimental results, Journal of hydrology, 369, 17–29, 2009.

Brooks, J. R., Barnard, H. R., Coulombe, R., and McDonnell, J. J.: Ecohydrologic separation of water between trees and streams in a Mediterranean climate, Nature Geoscience, 3, 100–104, 2010.

Brooks, P. D., Chorover, J., Fan, Y., Godsey, S. E., Maxwell, R. M., McNamara, J. P., and Tague, C.: Hydrological partitioning in the critical zone: Recent advances and opportunities for developing transferable understanding of water cycle dynamics, Water Resources Research, 51, 6973–6987, 2015.

Calder, I. R., Hall, R. L., Harding, R. J., and Wright, I. R.: The use of a wet-surface weighing lysimeter system in rainfall interception studies of heather (Calluna vulgaris), Journal of climate and applied meteorology, 23, 461–473, http://journals.ametsoc.org/doi/abs/10.1175/1520-0450(1984)023%3C0461%3ATUOAWS%3E2.0.CO%3B2, 1984.

Coenders-Gerrits, A. M. J., Van der Ent, R. J., Bogaard, T. A., Wang-Erlandsson, L., Hrachowitz, M., and Savenije, H. H. G.: Uncertainties in transpiration estimates, Nature, 506, E1, 2014.

Craig, H. and Gordon, L. I.: Deuterium and oxygen 18 variations in the ocean and the marine atmosphere, Stable Isotopes in Oceanic Studies and Paleotemperatures, 1965.

Craig, H., Gordon, L. I., and Horibe, Y.: Isotopic exchange effects in the evaporation of water: 1. Low-temperature experimental results, Journal of Geophysical Research, 68, 5079–5087, 1963.

Dansgaard, W.: Stable isotopes in precipitation, Tellus, 16, 436–468, 1964.

Dawson, T. E. and Ehleringer, J. R.: Streamside trees that do not use stream water, Nature, 350, 335–337, 1991.

Dawson, T. E. and Ehleringer, J. R.: Isotopic enrichment of water in the “woody” tissues of plants: implications for plant water source, water uptake, and other studies which use the stable isotopic composition of cellulose, Geochimica et Cosmochimica Acta, 57, 3487–3492, 1993.

De Schepper, V. and Steppe, K.: Development and verification of a water and sugar transport model using measured stem diameter variations, J Exp Bot, 61, 2083–2099, https://doi.org/10.1093/jxb/erq018, 2010.

Dee, D. P., Uppala, S. M., Simmons, A. J., Berrisford, P., Poli, P., Kobayashi, S., Andrae, U., Balmaseda, M. A., Balsamo, G., Bauer, P., Bechtold, P., Beljaars, A. C. M., van de Berg, L., Bidlot, J., Bormann, N., Delsol, C., Dragani, R., Fuentes, M., Geer, A. J., Haimberger, L., Healy, S. B., Hersbach, H., Hólm, E. V., Isaksen, L., Kållberg, P., Köhler, M., Matricardi, M., McNally, A. P., Monge-Sanz, B. M., Morcrette, J.-J., Park, B.-K., Peubey, C., de Rosnay, P., Tavolato, C., Thépaut, J.-N., and Vitart, F.: The ERA-Interim reanalysis: configuration and performance of the data assimilation system, Quarterly Journal of the Royal Meteorological Society, 137, 553–597, https://doi.org/10.1002/qj.828, 2011.

Dunn, S. M., McDonnell, J. J., and Vaché, K. B.: Factors influencing the residence time of catchment waters: A virtual experiment approach, Water Resour. Res., 43, W06 408, https://doi.org/10.1029/2006WR005393, 2007.

Endrizzi, S., Gruber, S., Dall'Amico, M., and Rigon, R.: GEOtop 2.0: simulating the combined energy and water balance at and below the land surface accounting for soil freezing, snow cover and terrain effects, Geosci. Model Dev., 7, 2831–2857, https://doi.org/10.5194/gmd-7-2831-2014, 2014.

Falkenmark, M. and Rockström, J.: The New Blue and Green Water Paradigm: Breaking New Ground for Water Resources Planning and Management, Journal of Water Resources Planning and Management, 132, 129–132, https://doi.org/10.1061/(ASCE)0733-9496(2006)132:3(129), 2006.

Fan, Y.: Groundwater in the Earth's critical zone: Relevance to large-scale patterns and processes, Water Resources Research, 51, https://doi.org/10.1002/ 2015WR017037., 2015.

Farquhar, G. D., Cernusak, L. A., and Barnes, B.: Heavy water fractionation during transpiration, Plant Physiology, 143, 11–18, 2007.

Fenicia, F., McDonnell, J. J., and Savenije, H. H.: Learning from model improvement: On the contribution of complementary data to process understanding, Water Resources Research, 44, 2008.

Frei, S., Lischeid, G., and Fleckenstein, J. H.: Effects of micro-topography on surface–subsurface exchange and runoff generation in a virtual riparian wetland — A modeling study, Advances in Water Resources, 33, 1388–1401, https://doi.org/10.1016/j.advwatres.2010.07.006, 2010.

Gat, J. R.: Stable isotopes of fresh and saline lakes, in: Physics and chemistry of lakes, pp. 139–165, Springer, 1995.

Gat, J. R.: Oxygen and hydrogen isotopes in the hydrologic cycle, Annual Review of Earth and Planetary Sciences, 24, 225–262, 1996.

Geris, J., Tetzlaff, D., McDonnell, J. J., and Soulsby, C.: Spatial and temporal patterns of soil water storage and vegetation water use in humid northern catchments, Science of The Total Environment, 595, 486–493, https://doi.org/10.1016/j.scitotenv.2017.03.275, 2017.

Gibson, J. J. and Reid, R.: Water balance along a chain of tundra lakes: A 20-year isotopic perspective, Journal of Hydrology, 519, Part B, 2148–2164, https://doi.org/10.1016/j.jhydrol.2014.10.011, 2014.

Good, S. P., Soderberg, K., Guan, K., King, E. G., Scanlon, T. M., and Caylor, K. K.: δ^2H isotopic flux partitioning of evapotranspiration over a grass field following a water pulse and subsequent dry down, Water Resources Research, 50, 1410–1432, 2014.

Good, S. P., Noone, D., and Bowen, G.: Hydrologic connectivity constrains partitioning of global terrestrial water fluxes, Science, 349, 175–177, https://doi.org/10.1126/science.aaa5931, 2015.

Goody, R. M. and Yung, Y. L.: Atmospheric radiation: theoretical basis, Oxford university press, 1995.

Haese, B., Werner, M., and Lohmann, G.: Stable water isotopes in the coupled atmosphere–land surface model ECHAM5-JSBACH, Geosci. Model Dev., 6, 1463–1480, https://doi.org/10.5194/gmd-6-1463-2013, 2013.

Harman, C. J.: Time-variable transit time distributions and transport: Theory and application to storage-dependent transport of chloride in a watershed, Water Resources Research, 51, 1–30, 2015.

Harwood, K. G., Gillon, J. S., Roberts, A., and Griffiths, H.: Determinants of isotopic coupling of CO_2 and water vapour within a *Quercus petraea* forest canopy, Oecologia, 119, 109–119, https://doi.org/10.1007/s004420050766, 1999.

Haverd, V. and Cuntz, M.: Soil–Litter–Iso: A one-dimensional model for coupled transport of heat, water and stable isotopes in soil with a litter layer and root extraction, Journal of Hydrology, 388, 438–455, 2010.

Haverd, V., Cuntz, M., Griffith, D., Keitel, C., Tadros, C., and Twining, J.: Measured deuterium in water vapour concentration does not improve the constraint on the partitioning of evapotranspiration in a tall forest canopy, as estimated using a soil vegetation atmosphere transfer model, Agricultural and forest meteorology, 151, 645–654, 2011.

Heidbüchel, I., Troch, P. A., Lyon, S. W., and Weiler, M.: The master transit time distribution of variable flow systems, Water Resources Research, 48, 2012.

Henderson-Sellers, A.: Improving land-surface parameterization schemes using stable water isotopes: Introducing the 'iPILPS' initiative, Global and Planetary Change, 51, 3–24, https://doi.org/10.1016/j.gloplacha.2005.12.009, 2006.

Hesse, F., Zink, M., Kumar, R., Samaniego, L., and Attinger, S.: Spatially distributed characterization of soil-moisture dynamics using travel-time distributions, Hydrology and Earth System Sciences, 21, 549, 2017.

Horita, J. and Wesolowski, D. J.: Liquid-vapor fractionation of oxygen and hydrogen isotopes of water from the freezing to the critical temperature, Geochimica et Cosmochimica Acta, 58, 3425–3437, https://doi.org/10.1016/0016-7037(94)90096-5, 1994.

Horita, J., Rozanski, K., and Cohen, S.: Isotope effects in the evaporation of water: a status report of the Craig–Gordon model, Isotopes in environmental and health studies, 44, 23–49, 2008.

Hrachowitz, M., Savenije, H., Bogaard, T. A., Soulsby, C., and Tetzlaff, D.: What can flux tracking teach us about water age distribution patterns and their temporal dynamics?, Hydrology and Earth System Sciences, 17 (2), 2013, 2013.

Hölttä, T., Vesala, T., Sevanto, S., Perämäki, M., and Nikinmaa, E.: Modeling xylem and phloem water flows in trees according to cohesion theory and Münch hypothesis, Trees, 20, 67–78, https://doi.org/10.1007/s00468-005-0014-6, 2006.

Jacob, H. and Sonntag, C.: An 8-year record of the seasonal variation of 2H and 18O in atmospheric water vapour and precipitation at Heidelberg, Germany, Tellus B, 43, 291–300, 1991.

Jasechko, S., Sharp, Z. D., Gibson, J. J., Birks, S. J., Yi, Y., and Fawcett, P. J.: Terrestrial water fluxes dominated by transpiration, Nature, 496, 347, 2013.

Kirchner, J. W.: A double paradox in catchment hydrology and geochemistry, Hydrological Processes, 17, 871–874, 2003.

Kirchner, J. W. and Neal, C.: Universal fractal scaling in stream chemistry and its implications for solute transport and water quality trend detection, Proceedings of the National Academy of Sciences, 110, 12 213–12 218, 2013.

Kling, H., Fuchs, M., and Paulin, M.: Runoff conditions in the upper Danube basin under an ensemble of climate change scenarios, Journal of Hydrology, 424, 264–277, http://www.sciencedirect.com/science/article/pii/S0022169412000431, 2012.

Knighton, J., Saia, S. M., Morris, C. K., Archiblad, J. A., and Walter, M. T.: Ecohydrologic considerations for modeling of stable water isotopes in a small intermittent watershed, Hydrol. Process., 31, 2438–2452, https://doi.org/10.1002/hyp.11194, 2017.

Kool, D., Agam, N., Lazarovitch, N., Heitman, J. L., Sauer, T. J., and Ben-Gal, A.: A review of approaches for evapotranspiration partitioning, Agricultural and Forest Meteorology, 184, 56–70, https://doi.org/10.1016/j.agrformet.2013.09.003, 2014.

Krabbenhoft, D. P., Bowser, C. J., Anderson, M. P., and Valley, J. W.: Estimating groundwater exchange with lakes: 1. The stable isotope mass balance method, Water Resources Research, 26, 2445–2453, 1990.

Kumar, B. and Nachiappan, R. P.: On the sensitivity of Craig and Gordon Model for the estimation of the isotopic composition of lake evaporates, Water Resour. Res., 35, 1689–1691, https://doi.org/10.1029/1999WR900011, 1999.

Kuppel, S., Tetzlaff, D., Maneta, M. P., and Soulsby, C.: What can we learn from multi-data calibration of a process-based ecohydrological model?, Environmental Modelling & Software, 101, 301–316, https://doi.org/10.1016/j.envsoft.2018.01.001, 2018.

Landwehr, J. M. and Coplen, T. B.: Line-conditioned excess: a new method for characterizing stable hydrogen and oxygen isotope ratios in hydrologic systems, in: International Conference on Isotopes in Environmental Studies, pp. 132–135, IAEA Vienna, 2006.

Landwehr, J. M., Coplen, T. B., and Stewart, D. W.: Spatial, seasonal, and source variability in the stable oxygen and hydrogen isotopic composition of tap waters throughout the USA, Hydrol. Process., 28, 5382–5422, https://doi.org/10.1002/hyp.10004, 2014.

Lee, T. J. and Pielke, R. A.: Estimating the soil surface specific humidity, Journal of Applied Meteorology, 31, 480–484, 1992.

Lessels, J. S., Tetzlaff, D., Birkel, C., Dick, J., and Soulsby, C.: Water sources and mixing in riparian wetlands revealed by tracers and geospatial analysis, Water Resour. Res., 52, 456–470, https://doi.org/10.1002/2015WR017519, 2016.

Lin, G. and da SL Sternberg, L.: Hydrogen isotopic fractionation by plant roots during water uptake in coastal wetland plants, in: Stable isotopes and plant carbon-water relations, pp. 497–510, Elsevier, 1993.

Lozano-Parra, J., Maneta, M. P., and Schnabel, S.: Climate and topographic controls on simulated pasture production in a semiarid Mediterranean watershed with scattered tree cover, Hydrology and Earth System Sciences, 18, 1439, 2014.

Mamonov, A. B., Coalson, R. D., Zeidel, M. L., and Mathai, J. C.: Water and Deuterium Oxide Permeability through Aquaporin 1: MD Predictions and Experimental Verification, The Journal of General Physiology, 130, 111–116, https://doi.org/10.1085/jgp.200709810, 2007.

Maneta, M. P. and Silverman, N. L.: A spatially distributed model to simulate water, energy, and vegetation dynamics using information from regional climate models, Earth Interactions, 17, 1–44, 2013.

Manoli, G., Huang, C.-W., Bonetti, S., Domec, J.-C., Marani, M., and Katul, G.: Competition for light and water in a coupled soil-plant system, Advances in Water Resources, 108, 216–230, https://doi.org/10.1016/j.advwatres.2017.08.004, 2017.

Mathieu, R. and Bariac, T.: An Isotopic Study (2H and 18O) of Water Movements in Clayey Soils Under a Semiarid Climate, Water Resour. Res., 32, 779–789, https://doi.org/10.1029/96WR00074, 1996.

McDonnell, J. J. and Beven, K.: Debates—The future of hydrological sciences: A (common) path forward? A call to action aimed at understanding velocities, celerities and residence time distributions of the headwater hydrograph, Water Resources Research, 50, 5342–5350, 2014.

McGuire, K. J. and McDonnell, J. J.: A review and evaluation of catchment transit time modeling, Journal of Hydrology, 330, 543–563, 2006.

McGuire, K. J. and McDonnell, J. J.: Tracer advances in catchment hydrology, Hydrological Processes, 29, 5135–5138, https://doi.org/10.1002/hyp.10740, 2015.

Melayah, A., Bruckler, L., and Bariac, T.: Modeling the Transport of Water Stable Isotopes in Unsaturated Soils Under Natural Conditions: 1. Theory, Water Resour. Res., 32, 2047–2054, https://doi.org/10.1029/96WR00674, 1996.

Met Office, .: Met Office Integrated Data Archive System (MIDAS) Land and Marine Surface Stations Data (1853-current), NCAS British Atmospheric Data Centre, http://catalogue.ceda.ac.uk/uuid/220a65615218d5c9cc9e4785a3234bd0, 2017.

Moors, E., Stricker, J., and van der Abeele, G.: Evapotranspiration of cut over bog covered by Molinia Caerulea, Tech. Rep. 73, Wagenigen, 1998.

Nash, J. and Sutcliffe, J.: River flow forecasting through conceptual models part I — A discussion of principles, Journal of Hydrology, 10, 282–290, https://doi.org/10.1016/0022-1694(70)90255-6, http://www.sciencedirect.com/science/article/pii/0022169470902556, 1970.

National Research Council, .: New Research Opportunities in the Earth Sciences, dOI: 10.17226/13236, 2012.

Neal, C., Christophersen, N., Neale, R., Smith, C. J., Whitehead, P. G., and Reynolds, B.: Chloride in precipitation and streamwater for the upland catchment of river severn, mid-wales; some consequences for hydrochemical models, Hydrol. Process., 2, 155–165, https://doi.org/10.1002/hyp.3360020206, 1988.

Niu, J. and Phanikumar, M. S.: Modeling watershed-scale solute transport using an integrated, process-based hydrologic model with applications to bacterial fate and transport, Journal of Hydrology, 529, Part 1, 35–48, https://doi.org/10.1016/j.jhydrol.2015.07.013, 2015.

O'Driscoll, M. A., DeWalle, D. R., McGuire, K. J., and Gburek, W. J.: Seasonal 18O variations and groundwater recharge for three landscape types in central Pennsylvania, USA, Journal of Hydrology, 303, 108–124, https://doi.org/10.1016/j.jhydrol.2004.08.020, 2005.

Pfautsch, S., Renard, J., Tjoelker, M. G., and Salih, A.: Phloem as capacitor: radial transfer of water into xylem of tree stems occurs via symplastic transport in ray parenchyma, Plant physiology, 167, 963–971, 2015.

Pierini, N. A., Vivoni, E. R., Robles-Morua, A., Scott, R. L., and Nearing, M. A.: Using observations and a distributed hydrologic model to explore runoff thresholds linked with mesquite encroachment in the Sonoran Desert, Water Resour. Res., 50, 8191–8215, https://doi.org/10.1002/2014WR015781, 2014.

Rinaldo, A., Benettin, P., Harman, C. J., Hrachowitz, M., McGuire, K. J., Van Der Velde, Y., Bertuzzo, E., and Botter, G.: Storage selection functions: A coherent framework for quantifying how catchments store and release water and solutes, Water Resources Research, 51, 4840–4847, 2015.

Risi, C., Ogée, J., Bony, S., Bariac, T., Raz-Yaseef, N., and others: The water isotopic version of the land-surface model ORCHIDEE: Implementation, evaluation, sensitivity to hydrological parameters, Hydrol Current Res, 7, 2, 2016.

Sayama, T. and McDonnell, J. J.: A new time-space accounting scheme to predict stream water residence time and hydrograph source components at the watershed scale, Water Resour. Res., 45, W07 401, https://doi.org/10.1029/2008WR007549, 2009.

Scheliga, B., Tetzlaff, D., Nuetzmann, G., and Soulsby, C.: Groundwater isoscapes in a montane headwater catchment show dominance of well-mixed storage, Hydrological Processes, 2017.

Schlesinger, W. H. and Jasechko, S.: Transpiration in the global water cycle, Agricultural and Forest Meteorology, 189, 115–117, 2014.

Schoch-Fischer, H., Rozanski, K., Jacob, H., Sonntag, C., Jouzel, I., Östlund, G., and Geyh, M. A.: Hydrometeorological factors controlling the time variation of D, 18 O and 3 H in atmospheric water vapour and precipitation in the northern westwind belt, IAEA,(ed.), Isotope Hydrology. Vienna, IAEA, pp. 3–30, 1983.

Simeone, C.: Coupled ecohydrology and plant hydraulics model predicts Ponderosa seedling mortality and lower treeline in the US Northern Rocky Mountains, Master's thesis, University of Montana, https://scholarworks.umt.edu/etd/11128, 2018.

Skrzypek, G., Myd\lowski, A., Dogramaci, S., Hedley, P., Gibson, J. J., and Grierson, P. F.: Estimation of evaporative loss based on the stable isotope composition of water using Hydrocalculator, Journal of Hydrology, 523, 781–789, 2015.

Smart, R. P., Soulsby, C., Cresser, M. S., Wade, A. J., Townend, J., Billett, M. F., and Langan, S.: Riparian zone influence on stream water chemistry at different spatial scales: a GIS-based modelling approach, an example for the Dee, NE Scotland, Science of The Total Environment, 280, 173–193, https://doi.org/10.1016/S0048-9697(01)00824-5, 2001.

Smith, A., Welch, C., and Stadnyk, T.: Assessment of a lumped coupled flow-isotope model in data scarce Boreal catchments, Hydrol. Process., 30, 3871–3884, https://doi.org/10.1002/hyp.10835, 2016.

Smith, A. A., Tetzlaff, D., and Soulsby, C.: Using StorAge Selection functions to quantify ecohydrological controls on the time-variant age of evapotranspiration, soil water, and recharge, Hydrol. Earth Syst. Sci. Discuss., 2018, 1–25, https://doi.org/10.5194/hess-2018-57, https://www.hydrol-earth-syst-sci-discuss.net/hess-2018-57/, 2018.

Soderberg, K., Good, S. P., Wang, L., and Caylor, K.: Stable isotopes of water vapor in the vadose zone: A review of measurement and modeling techniques, Vadose Zone Journal, 11, 2012.

Soulsby, C., Tetzlaff, D., Van den Bedem, N., Malcolm, I. A., Bacon, P. J., and Youngson, A. F.: Inferring groundwater influences on surface water in montane catchments from hydrochemical surveys of springs and streamwaters, Journal of Hydrology, 333, 199–213, 2007.

Soulsby, C., Birkel, C., Geris, J., Dick, J., Tunaley, C., and Tetzlaff, D.: Stream water age distributions controlled by storage dynamics and nonlinear hydrologic connectivity: Modeling with high-resolution isotope data, Water Resources Research, 51, 7759–7776, 2015.

Soulsby, C., Bradford, J., Dick, J., McNamara, J. P., Geris, J., Lessels, J., Blumstock, M., and Tetzlaff, D.: Using geophysical surveys to test tracer-based storage estimates in headwater catchments, Hydrological Processes, 30, 4434–4445, 2016.

Soulsby, C., Braun, H., Sprenger, M., Weiler, M., and Tetzlaff, D.: Influence of forest and shrub canopies on precipitation partitioning and isotopic signatures, Hydrological Processes, 2017.

Spence, C. and Woo, M.-k.: Hydrology of subarctic Canadian shield: soil-filled valleys, Journal of Hydrology, 279, 151–166, https://doi.org/10.1016/S0022-1694(03)00175-6, 2003.

Sprenger, M., Herbstritt, B., and Weiler, M.: Established methods and new opportunities for pore water stable isotope analysis, Hydrological Processes, 29, 5174–5192, 2015.

Sprenger, M., Tetzlaff, D., and Soulsby, C.: Soil water stable isotopes reveal evaporation dynamics at the soil–plant–atmosphere interface of the critical zone, Hydrol. Earth Syst. Sci., 21, 3839–3858, https://doi.org/10.5194/hess-21-3839-2017, 2017a.

Sprenger, M., Tetzlaff, D., Tunaley, C., Dick, J., and Soulsby, C.: Evaporation fractionation in a peatland drainage network affects stream water isotope composition, Water Resources Research, 53, 851–866, 2017b.

Sprenger, M., Tetzlaff, D., Buttle, J., Snelgrove, J., Laudon, H., Mitchell, C., Weiler, M., and Soulsby, C.: Measuring and modelling stable isotopes of mobile and bulk soil water, Vadose Zone Journal, https://doi.org/10.2136/vzj2017.08.0149, 2018.

Stadnyk, T. A., Delavau, C., Kouwen, N., and Edwards, T. W. D.: Towards hydrological model calibration and validation: Simulation of stable water isotopes using the isoWATFLOOD model, Hydrological Processes, 27, 3791–3810, 2013.

Stanfield, R. C., Hacke, U. G., and Laur, J.: Are phloem sieve tubes leaky conduits supported by numerous aquaporins?, Am. J. Bot., 104, 719–732, https://doi.org/10.3732/ajb.1600422, 2017.

Stumpp, C. and Maloszewski, P.: Quantification of preferential flow and flow heterogeneities in an unsaturated soil planted with different crops using the environmental isotope δ^{18}O, Journal of Hydrology, 394, 407–415, https://doi.org/10.1016/j.jhydrol.2010.09.014, 2010.

Stumpp, C., Maloszewski, P., Stichler, W., and Maciejewski, S.: Quantification of the heterogeneity of the unsaturated zone based on environmental deuterium observed in lysimeter experiments, Hydrological Sciences Journal, 52, 748–762, https://doi.org/10.1623/hysj.52.4.748, 2007.

Tetzlaff, D., Soulsby, C., Waldron, S., Malcolm, I. A., Bacon, P. J., Dunn, S. M., Lilly, A., and Youngson, A. F.: Conceptualization of runoff processes using a geographical information system and tracers in a nested mesoscale catchment, Hydrological Processes, 21, 1289–1307, 2007.

Tetzlaff, D., Soulsby, C., Buttle, J., Capell, R., Carey, S. K., Laudon, H., McDonnell, J., McGuire, K., Seibert, J., and Shanley, J.: Catchments on the cusp? Structural and functional change in northern ecohydrology, Hydrological Processes, 27, 766–774, 2013.

Tetzlaff, D., Birkel, C., Dick, J., Geris, J., and Soulsby, C.: Storage dynamics in hydropedological units control hillslope connectivity, runoff generation, and the evolution of catchment transit time distributions, Water resources research, 50, 969–985, 2014.

Troy, T. J., Pavao-Zuckerman, M., and Evans, T. P.: Debates—Perspectives on socio-hydrology: Socio-hydrologic modeling: Tradeoffs, hypothesis testing, and validation, Water Resources Research, 51, 4806–4814, https://doi.org/10.1002/2015WR017046, https://agupubs.onlinelibrary.wiley.com/doi/abs/10.1002/2015WR017046, 2015.

Uhlenbrook, S. and Sieber, A.: On the value of experimental data to reduce the prediction uncertainty of a process-oriented catchment model, Environmental Modelling & Software, 20, 19–32, 2005.

van Huijgevoort, M. H. J., Tetzlaff, D., Sutanudjaja, E. H., and Soulsby, C.: Using high resolution tracer data to constrain water storage, flux and age estimates in a spatially distributed rainfall-runoff model, Hydrological Processes, 30, 4761–4778, 2016.

Vargas, A. I., Schaffer, B., Yuhong, L., and Sternberg, L. d. S. L.: Testing plant use of mobile vs immobile soil water sources using stable isotope experiments, New Phytol, 215, 582–594, https://doi.org/10.1111/nph.14616, 2017.

Vogel, T., Sanda, M., Dusek, J., Dohnal, M., and Votrubova, J.: Using Oxygen-18 to Study the Role of Preferential Flow in the Formation of Hillslope Runoff, Vadose Zone Journal, 9, 252–259, https://doi.org/10.2136/vzj2009.0066, 2010.

Vogt, H. J.: Isotopentrennung bei der Verdunstung von Wasser, Staatsexamensarbeit, Institut für Umweltphysik, Heidelberg, Germany, 1976.

Wang, H., Tetzlaff, D., Dick, J. J., and Soulsby, C.: Assessing the environmental controls on Scots pine transpiration and the implications for water partitioning in a boreal headwater catchment, Agricultural and Forest Meteorology, 240, 58–66, 2017a.

Wang, H., Tetzlaff, D., and Soulsby, C.: Testing the maximum entropy production approach for estimating evapotranspiration from closed canopy shrubland in a low-energy humid environment, Hydrological Processes, 31, 4613–4621, 2017b.

Wassenaar, L. I., Hendry, M. J., Chostner, V. L., and Lis, G. P.: High resolution pore water δ^2H and δ^{18}O measurements by H2O (liquid)-H2O (vapor) equilibration laser spectroscopy, Environmental science & technology, 42, 9262–9267, 2008.

Wei, Z., Yoshimura, K., Wang, L., Miralles, D. G., Jasechko, S., and Lee, X.: Revisiting the contribution of transpiration to global terrestrial evapotranspiration, Geophysical Research Letters, 44, 2792–2801, https://doi.org/10.1002/2016GL072235, https://agupubs.onlinelibrary.wiley.com/doi/abs/10.1002/2016GL072235, 2017.

Weiler, M., McGlynn, B. L., McGuire, K. J., and McDonnell, J. J.: How does rainfall become runoff? A combined tracer and runoff transfer function approach, Water Resources Research, 39, 2003.

Welhan, J. A. and Fritz, P.: Evaporation pan isotopic behavior as an index of isotopic evaporation conditions, Geochimica et Cosmochimica Acta, 41, 682–686, https://doi.org/10.1016/0016-7037(77)90306-4, 1977.

Wershaw, R. L., Friedman, I., Heller, S. J., and Frank, P. A.: Hydrogen isotopic fractionation of water passing through trees, Advances in organic geochemistry, p. 55, 1966.

Windhorst, D., Kraft, P., Timbe, E., Frede, H.-G., and Breuer, L.: Stable water isotope tracing through hydrological models for disentangling runoff generation processes at the hillslope scale, Hydrology and Earth System Sciences, 18, 4113–4127, 2014.

Wong, T. E., Nusbaumer, J., and Noone, D. C.: Evaluation of modeled land-atmosphere exchanges with a comprehensive water isotope fractionation scheme in version 4 of the Community Land Model, J. Adv. Model. Earth Syst., 9, 978–1001, https://doi.org/10.1002/2016MS000842, 2017.

Yeh, H.-F., Lee, C.-H., and Hsu, K.-C.: Oxygen and hydrogen isotopes for the characteristics of groundwater recharge: a case study from the Chih-Pen Creek basin, Taiwan, Environmental Earth Sciences, 62, 393–402, 2011.

Zhang, M., Liu, N., Harper, R., Li, Q., Liu, K., Wei, X., Ning, D., Hou, Y., and Liu, S.: A global review on hydrological responses to forest change across multiple spatial scales: Importance of scale, climate, forest type and hydrological regime, Journal of Hydrology, 546, 44–59, https://doi.org/10.1016/j.jhydrol.2016.12.040, https://www.sciencedirect.com/science/article/pii/S0022169416308307, 2017.

Zhao, L., Wang, L., Cernusak, L. A., Liu, X., Xiao, H., Zhou, M., and Zhang, S.: Significant Difference in Hydrogen Isotope Composition Between Xylem and Tissue Water in Populus Euphratica, Plant, Cell & Environment, 39, 1848–1857, https://doi.org/10.1111/pce.12753, 2016.